

UNIVERSITY OF LILLE - COLLEGE OF PHARMACY

INSERM U1008 - Laboratoire de Pharmacotechnie Industrielle

Ecole Doctorale Biologie-Santé

Confidential

**Enzyme-sensitive coatings for colon targeting:
species-independent drug delivery systems**

DOCTORAL THESIS

4 September 2023, Lille

FABIANA FERRARO

Supervised by

Dr. Florence SIEPMANN

Jury President

Dr. Juergen SIEPMANN

UNIVERSITY OF LILLE - COLLEGE OF PHARMACY

INSERM U1008 - Laboratoire de Pharmacotechnie Industrielle

Ecole Doctorale Biologie-Santé

Confidential

**Enzyme-sensitive coatings for colon targeting:
species-independent drug delivery systems**

DOCTORAL THESIS

4 September 2023, Lille

FABIANA FERRARO

Supervised by

Dr. Florence SIEPMANN

Jury composition:

SIEPMANN Juergen

President

ZEITLER Axel

Referee

VERVAET Chris

Referee

BASIT Abdul

Examiner

CORREIA TEIXERA Natalia

Examiner

SIEPMANN Florence

Director

To Christel,

Inspiring woman and passionate scientist.

Table of contents

Table of contents.....	i
Acknowledgments.....	v
Abbreviations.....	vii
Objectives.....	ix
List of figures.....	xi
List of tables.....	xvii
1. Chapter: Introduction.....	2
1.1. Colon targeting.....	2
1.2. The colonic environment.....	5
1.3. Colonic drug delivery strategies.....	7
1.3.1. pH-dependent Drug Delivery Systems.....	8
1.3.1.1. Limitation of pH-sensitive Drug Delivery Systems.....	11
1.3.2. Time-dependent Drug Delivery Systems.....	11
1.3.3. Enzyme-sensitive Drug Delivery Systems.....	13
1.3.3.1. Limitation of enzyme-sensitive Drug Delivery Systems.....	15
1.3.4. Pressure-dependent Drug Delivery Systems.....	17
1.3.5. Hybrid Strategies for Colon Targeting.....	18
1.3.5.1. pH and time triggered combinations.....	18
1.3.5.2. Time and enzymes triggered combinations.....	19
1.3.5.3. pH and enzymes triggered combinations.....	19
2. Chapter: Enzyme sensitive coatings for colon targeting.....	22
2.1. Gut microbiota.....	22
2.2. Animal models for colonic drug delivery.....	23

2.3.	Faecal slurries used to simulate the colonic environment.....	24
2.4.	Materials and methods.....	26
2.4.1.	Materials.....	26
2.4.2.	Inoculation of polysaccharides in culture medium +/- faecal samples.....	27
2.4.3.	Inoculation of Bacteroides and Bifidum bacteria in culture medium +/- DBS	28
2.4.4.	Preparation of drug-loaded starter cores.....	29
2.4.5.	Film coating of drug-loaded pellets.....	29
2.4.6.	Determination of the practical drug loading.....	30
2.4.7.	In vitro drug release measurements.....	30
2.4.8.	Scanning electron microscopy.....	31
2.5.	Results and discussion.....	32
2.5.1.	Polysaccharide degradation in faecal samples from different species.....	32
2.5.2.	Species-dependent drug release from coated pellets.....	37
2.5.3.	Species-independent colon targeting.....	45
2.6.	Conclusions.....	46
3.	Chapter: The SHIME® semi-dynamic gastrointestinal release model for colon-targeting drug delivery systems.....	48
3.1.	Overview.....	48
3.1.1.	The SHIME® (Simulator of the Human Intestinal Microbial Ecosystem). 48	
3.2.	Materials and methods.....	49
3.2.1.	Materials.....	49
3.2.2.	Preparation of drug-loaded starter cores.....	50
3.2.3.	In vitro drug release measurements.....	51
3.2.4.	Film coating of drug-loaded pellets.....	51
3.2.5.	<i>In vitro</i> drug release in SHIME® model.....	51

3.2.6.	Analytical quantification	53
3.3.	Results and discussion.....	54
3.3.1.	Mesalazine release by the six formulations after exposure to the faeces of IBD donor A55	
3.3.2.	Mesalazine release by the six formulations after exposure to the faeces of IBD donor B 59	
3.3.3.	Mesalazine release by the six formulations after exposure to the faeces of IBD donor C 61	
3.3.4.	Impact of the formulations on the metabolic activity of the colonic microbiota	64
3.4.	Conclusion.....	67
4.	Chapter: 3D printing for colonic drug delivery systems	68
4.1.	Overview	68
4.1.1.	Pharmaceutical 3D printing	68
4.1.2.	Selective laser sintering (SLS).....	69
4.1.3.	Direct powder extrusion (DPE)	70
4.1.4.	X-ray computer tomography (CT).....	71
4.2.	Materials and methods.....	73
4.2.1.	Materials.....	73
4.2.2.	Selective laser sintering, (SLS).....	73
4.2.3.	Direct powder extrusion (DPE)	74
4.2.4.	Thermogravimetric analysis (TGA).....	75
4.2.5.	Scanning electron microscopy	76
4.2.6.	X-ray microtomography.....	76
4.3.	Results and discussion.....	77
4.3.1.	Powder characterization.....	77

4.3.1.1.	Scanning electron microscopy	77
4.3.2.	Thermo-gravimetric analysis (TGA)	81
4.3.3.	Printability of the polymers' blends.....	82
4.3.4.	Selective laser sintering (SLS).....	82
4.3.5.	Direct powder extrusion (DPE)	84
4.3.6.	X-ray microtomography.....	95
4.3.7.	Development of a dissolution device	100
4.4.	Conclusion and further perspectives	101
5.	Chapter: Colonic delivery of short chain fatty acid	102
5.1.	Overview	102
5.2.	Materials and methods.....	104
5.2.1.	Materials.....	104
5.2.2.	Preparation of the spray dried formulation	104
5.2.3.	In vitro drug release measurements	105
5.2.4.	Impact of acetate loaded microparticle against IAV infection <i>in vivo</i>	105
5.3.	Results and discussion.....	107
5.3.1.	<i>In vitro</i> drug release	107
5.3.2.	<i>In vivo</i> study in mice model	108
5.4.	Conclusion.....	113
6.	Chapter: Conclusions and future perspectives	114
	References.....	114
	Résumé en Français	138
	Summary in English.....	142
	Publications.....	146

Acknowledgments

This thesis has received fundings from the Interreg 2 Seas programme 2014-2020, co-funded by the European Regional Development Fund under subsidy contract “Site Drug 2S07-033”.

I would like to warmly thank Florence and Juergen Siepmann for welcoming me to their team and offering me the life-changing opportunity to make this Ph.D. under their supervision. Every single day has taught me something and I will always be grateful to you.

A big part of my project was developed in the microbiology laboratory where I was welcomed with open arms by all the team members. A special thank you to Christel Neut, who took me under her wings, sharing her immense knowledge and good humor in any occasion, it has been an honor learning from you. Isabelle and Severine, thank you for your time and patience, you were always there answering my million questions and supporting me in the delicate world of anaerobic bacteria.

My experience abroad has enriched me professionally and personally and it will always be one of the most intense periods of my Ph.D. Thank you Abdul for your inspiring words and for sharing your illimited passion for science. A special thank you to Alvaro and Atheer, I very much enjoyed learning from you about 3D printing and I look forward to following your success. Thank you Alessia and Iria for being part of the best memories I have and thank you Laura for all your support, you are one of the most talented scientists I have ever met.

A warm thank you to Axel, being part of your team made one of my wishes came true and I wish I could spend more time learning from you and your incredibly brilliant students. Thank you, Prince, for your endless availability, your love for science is as contagious as your shiny personality.

I would like to acknowledge particularly Frederic Moens, Seppe De Smet, Cindy Duysburgh, François Trottein, Corinne Grangette and Loic Chollet, it has been a pleasure to collaborate with you.

A very special thanks to Cecile, who works with passion and ethics and showed me the respect in the animal experimentation, you are an example.

Dear U1008 team I don't know how to express you how grateful and lucky I feel for having the chance to work with you during the last 3 years. Every day I was happy to come to work, and this is precious.

Alexandra you are the fastest problem solver and I thank you so much for everything you did for me, you helped me at any moment, in any country. Hugues, I regret I didn't take notes about all your "way of saying", but if my French is quite good today is certainly also thanks to you. Laurence, it is beautiful to work with your always positive and supporting personality, always ready to do everything you can to help others, thank you. Suzie, you bring sparks in the laboratory with your effervescent personality, never change. Dear colleagues and friends, I will be sober and brief because I could write another manuscript to thanks each one of you! Yanis, we definitely shared many moments from the very beginning to the very end, you are incredibly brilliant and smart (although too young) and I wish you the brilliant career you deserve, good luck my friend. Lise-Anne (A-L), you are the most supportive desk neighbor and I already miss having you right next to me. Nina, you sunny girl, I am still doing everything I can to keep you in France. Filipa, it has been clear from the first second there is no chance to keep you here, so I wish you a successful return to Portugal and hope you'll come back here to speak a bit of French. Charline, explosive girl, you definitely made many of my days, thank you. Jeremy, your availability, and kindness are limitless, thank you for teaching me so much, and good luck with your career! Last but not least, thank you Lisa it has been great working with you, and I look forward seeing you in Lille again.

Infine, vorrei ringraziare le persone che ci sono sempre state, supportandomi e sopportandomi in ogni circostanza, la mia famiglia, i miei amici di una vita Giammy, Chiara e Lori e in particolare Felix. MERCI.

Abbreviations

3D	3-Dimensional
3DP	3-Dimensional Printing
4D	4-Dimensional
5-ASA	5-AminoSalicylic Acid
ASTM	American Society for Testing and Materials
BCRP	Breast Cancer Resistant Protein
BMI	Body Mass Indices
CAP	Cellulose Acetate Phthalate
CAS	Cellulose Acetate Succinate
CAT	Cellulose Acetate Trimellitate
CC	Colombia Culture medium
CD	Crohn's Disease
CFU	Colony Forming Unit
CR	Cysteinated Ringer
CT	Computed Tomography
CYPs	Cytochrome P
DBS	DiButyl Sebacate
DDS	Drug Delivery Systems
DNA	DeoxyriboNucleic Acid
DPE	Direct Powder Extrusion
FDA	Dood and Drug Administration
FDM	Fused Deposition Modeling
GI	GastroIntestinal
GIT	GastroIntestinal Tact

GRAS	Generally Recongnized As Safe
HIV	Human Immunodeficiency Virus
HME	Hot Melt Extrusion
HPC	HydroxyPropyl Cellulose
HPMC	HydroxyPropyl MethylCellulose
HPMC-AS	HydroxyPropyl MethylCellulose Acetate Succinate
HPMCP	HydroxyPropyl MethylCellulose Phthalate
IBD	Inflammatory Bowel Disease
ILE	ILEocolonic
MMX	Multi Matrix systems
M-SHIME	Mucosal Simulator of the Human Intestinal Microbial Ecosystem
NHS	National Health Service
PB	Phosphate Buffer
PCDC	Pressure-Controlled Delivery Capsule
PVAP	PolyVinyl Acetate Phthalate
PVAP	PolyVinyl Acetate Phthalate
SCFA	Short Chain Fatty Acids
SEM	Scanning Electron Microscopy
SLS	Selective Laser Sintering
ST	Stomach
TGA	ThermoGravimetric Analysis
TNBS	TriNitroBenzene Sulfonic acid
UC	Ulcerative Colitis

Objectives

The aim of this work was to identify polymeric film coatings allowing for colon targeting in different species, in particular: inflammatory bowel disease model rats (IBD rats), healthy dogs (dogs) and inflammatory bowel disease patients (IBD patients). The film coatings should be poorly permeable for the drug in the upper gastrointestinal tract, but should become permeable as soon as the colon is reached, due to degradation by enzymes secreted by colonic bacteria. These enzymes should be present in the different species in sufficient amounts to reliably trigger the onset of drug release. These key features were to be provided by a suitable polysaccharide. To avoid premature drug release due to the swelling and/or dissolution of the latter, the film coating consisted of a blend of two polymers: (i) the polysaccharide, which is degraded by bacterial enzymes in the colon of the different species, and (ii) ethylcellulose, which is insoluble and non-degradable throughout the gastrointestinal tract. Thus, ethylcellulose traps the release rate triggering polysaccharide to avoid premature release in the stomach and small intestine.

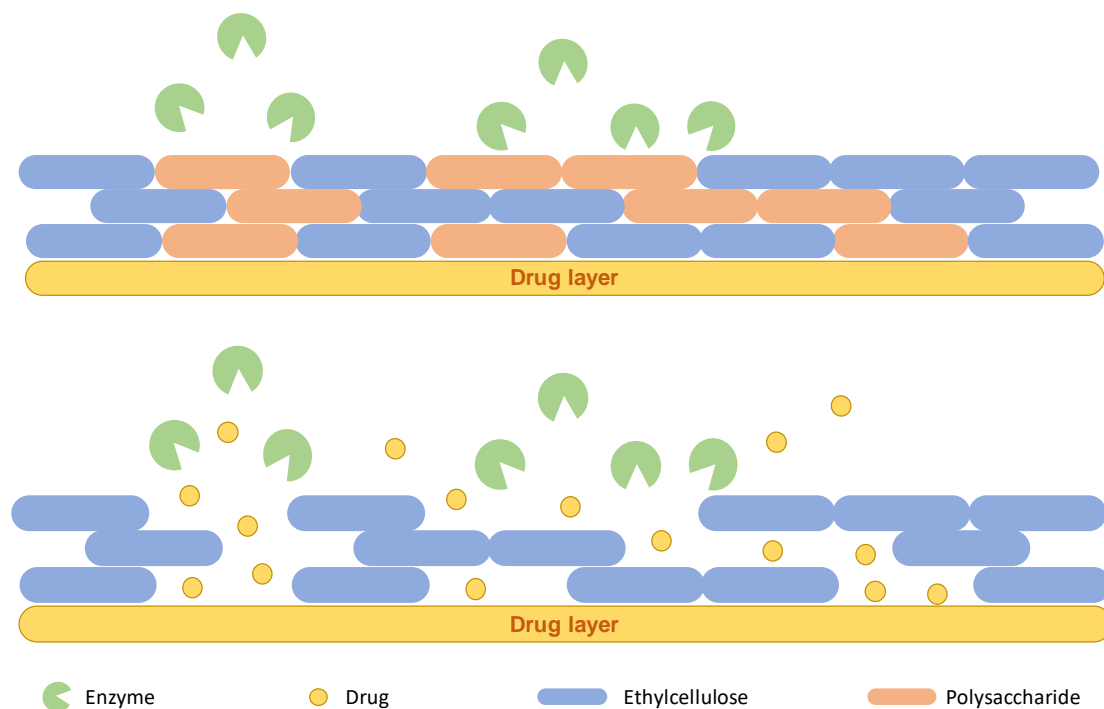


Figure 1 Schematic representation of the drug release mechanism in the colon. The enzymes, produced by the microbial population of the colon, degrade the polysaccharide portion of the coating allowing the drug release.

List of figures

Figure 1 Schematic representation of the drug release mechanism in the colon. The enzymes, produced by the microbial population of the colon, degrade the polysaccharide portion of the coating allowing the drug release.....	ix
Figure 2. Opportunities for the site-specific drug delivery to the colon. IBD, Inflammatory bowel diseases; UC, Ulcerative colitis; CD, Crohn’s disease; HIV, human immunodeficiency virus. Reprinted with permission from (1).	2
Figure 3 Historic evolution of IBD therapies with the key commercial products. Reprinted with permission from (1).....	4
Figure 4. Colon’s physiological properties. SCFA, Short chain fatty acids. Reprinted with permission from (1).	6
Figure 5. Historic evolution of colon targeting technologies with the key commercial products. Reprinted with permission from (1).....	8
Figure 6. Schematic representation of the systems: DuoCoat® and ColoPulse (1).The single-layer technology was improved with the incorporation of a disintegrant (e.g., sodium starch glycolate, croscarmellose sodium, microcrystalline cellulose, or alginic acid) to the enteric coating (30).	10
Figure 7 (A) Mean plasma theophylline levels after administration of uncoated, Eudragit® S coated pellets and amylose/ethyl cellulose coated pellets to eight healthy male subjects. B, C and D show examples of plasma concentration time profiles observed in single subjects: (B) uncoated pellets; (C) Eudragit® S coated pellets and; (D) amylose/ethyl cellulose coated pellets. (1,73).....	15
Figure 8 Schematic representation of the Phloral™ film coat technology (1)	20
Figure 9 pH values of different polysaccharide solutions/dispersions, inoculated with faecal slurries from inflammatory bowel disease patients (IBD patient), inflammatory bowel disease model rats (IBD rat) or healthy dogs (dog) for 8 or 24 h (as indicated). For reasons of comparison, also the pH values at time t = 0 are indicated. Differences in the pH between “t = 0” and “IBD patient 24 h” are important (≥ 2 units).	35

Figure 10 pH values of different polysaccharide solutions/dispersions, inoculated with faecal slurries from inflammatory bowel disease patients (IBD patient), inflammatory bowel disease model rats (IBD rat) or healthy dogs (dog) for 8 or 24 h (as indicated). For reasons of comparison, also the pH values at time $t = 0$ are indicated. Differences in the pH between “ $t = 0$ ” and “IBD patient 24 h” are not very pronounced (< 1.5 units). 36

Figure 11 Growth of Bacteroides and Bifidus bacteria in culture medium in the presence or absence of the plasticizer DBS. 38

Figure 12 SEM pictures of: a) 5-ASA-loaded starter cores, and b) pellets coated with a 2:3 xylan:ethylcellulose blend (20 % coating level)..... 39

Figure 13 5-ASA release from pellets coated with different types of polysaccharides: ethylcellulose blends (2:3 w/w blend ratio; 20 % coating level) in culture medium inoculated with faecal samples from IBD patients, IBD rats or dogs (as indicated). For reasons of comparison, also drug release in pure culture medium is illustrated. 42

Figure 14 5-ASA release from pellets coated with aloe vera extract: ethylcellulose blends or reishi extract: ethylcellulose blends (2:3 w/w blend ratio; 20 % coating level) in culture medium inoculated with faecal samples from IBD patients, IBD rats or dogs (as indicated). For reasons of comparison, also drug release in pure culture medium is illustrated..... 46

Figure 15 Fully automated computer-controlled semi-dynamic SHIME® model for colon-targeted drug delivery system testing. The system harbors nine separated bioreactors allowing to test 3 different conditions in biological triplicate at once. In each bioreactor the passage of the colon-targeted drug delivery system through the complete gastrointestinal tract is simulated by the sequential simulation of the stomach, small intestinal, and colonic phase. 49

Figure 16 5-ASA release from pellets coated with aloe vera extract: ethylcellulose blends or reishi extract: ethylcellulose blends (2:3 w/w blend ratio; 45 % coating level) in HCl (pH=1.2) for 1 h, followed by PB (pH=6.8) for 4 h followed by culture medium inoculated with faecal samples from IBD patients up to 24 h. For reasons of comparison, also drug release in pure culture medium is illustrated. 55

Figure 17 Release of mesalazine (average amount \pm stdev; n = 3) from the six mesalazine-loaded pellet formulations at the end of the stomach incubation (ST end), the start of the ileal incubation (ILE start), the end of the ileal incubation (ILE end) phase and after 0h (Colon 0h), 1h (Colon 1h), 3h (Colon 3h), 16h (Colon 16h), and 24h (Colon 24h) of the colonic incubation phase and the remaining amount of mesalazine present in the undissolved pellets at the end of the colonic incubation phase (A). Normalized time-course analysis of released mesalazine (average amount \pm stdev; n = 3) upon transfer of the six mesalazine-loaded pellet formulations through the complete gastrointestinal tract (B). Results are representative for the experiments performed with the faecal sample of IBD donor A. The red line represents the added dose of mesalazine. 56

Figure 18 Release of mesalazine (average amount \pm stdev; n = 3) from the six mesalazine-loaded pellet formulations at the end of the stomach incubation (ST end), the start of the ileal incubation (ILE start), the end of the ileal incubation (ILE end) phase and after 0h (Colon 0h), 1h (Colon 1h), 3h (Colon 3h), 16h (Colon 16h), and 24h (Colon 24h) of the colonic incubation phase and the remaining amount of mesalazine present in the undissolved pellets at the end of the colonic incubation phase (A). Normalized time-course analysis of released mesalazine (average amount \pm stdev; n = 3) upon transfer of the six mesalazine-loaded pellet formulations through the complete gastrointestinal tract (B). Results are representative for the experiments performed with the faecal sample of IBD donor B. The red line represents the added dose of mesalazine. 60

Figure 19 Release of mesalazine (average amount \pm stdev; n = 3) from the six mesalazine-loaded pellet formulations at the end of the stomach incubation (ST end), the start of the ileal incubation (ILE start), the end of the ileal incubation (ILE end) phase and after 0h (Colon 0h), 1h (Colon 1h), 3h (Colon 3h), 16h (Colon 16h), and 24h (Colon 24h) of the colonic incubation phase and the remaining amount of mesalazine present in the undissolved pellets at the end of the colonic incubation phase (A). Normalized time-course analysis of released mesalazine (average amount \pm stdev; n = 3) upon transfer of the six mesalazine-loaded pellet formulations through the complete gastrointestinal tract (B). Results are representative for the experiments performed with the faecal sample of IBD donor C. The red line represents the added dose of mesalazine. 63

Figure 20 Average increase in concentration (mM) \pm stdev (n = 3) of acetate during the colonic incubations inoculated with the faecal inoculum of IBD donor A, B, or C upon dosing of the six different formulations. Statistically significant differences (Student's T-test; p < 0.05) in between formulations are highlighted with different letters above the different bars.	65
Figure 21 Average increase in concentration (mM) \pm stdev (n = 3) of ammonium during the colonic incubations inoculated with the faecal inoculum of IBD donor A, B, or C upon dosing of the six different formulations. Statistically significant differences (Student's T-test; p < 0.05) in between formulations are highlighted with different letters above the different bars.....	66
Figure 22 X-ray computed tomography configuration. Cone beam system typical of laboratory system (216)	72
Figure 23 Graphical illustration of an SLS 3D printer, highlighting its major components (227).....	74
Figure 24 Design of the nozzle of the direct single-screw powder extruder FabRx 3D printer. The blue arrows indicate the site of addition of the powder (228).	75
Figure 25 SEM picture of corn maltodextrin (Glucidex® 17D) as provided by the supplier.....	77
Figure 26 SEM picture of pregelatinized starch (Starch 1500®) as provided by the supplier.....	78
Figure 27 SEM picture of xylan as provided by the supplier	78
Figure 28 SEM picture of aloe vera extract powder as provided by the supplier.	79
Figure 29 SEM picture of Reishi extract powder as provided by the supplier.....	79
Figure 30 SEM picture of inulin (Orafti® HSI) as provided by the supplier.....	80
Figure 31 TGA thermal traces for the individual polymers' raw material.	81
Figure 32 picture of 3D printed object produced with SLS technology with the blend of maltodextrin: a) capsule b) disc.	83
Figure 33 picture of 3D printed object produced with DPE technology with the blend of aloe vera.	84
Figure 34 picture of several 3D printed capsules produced with DPE technology with the blend of aloe vera.	85

Figure 35 SEM images of the surface of the capsule printed with DPE technology of aloe vera, at different scales.....	86
Figure 36 SEM images of the surface of the disc printed with DPE technology of aloe vera at different scales.	87
Figure 37 picture of 3D printed object produced with DPE technology using the blend of reishi extract.	88
Figure 38 SEM images of the surface of the capsule printed with DPE technology of ReiSHIELD at different scales.....	89
Figure 39 SEM images of the surface of the disc printed with DPE technology of reishi extract at different scales.	90
Figure 40 picture of discs produced with DPE technology using the blend of xylan. .	91
Figure 41 SEM images of the surface of the disc printed with DPE technology of xylan at different scales	92
Figure 42 picture of 3D printed disc produced with DPE technology using the blend of starch.	93
Figure 44 SEM images of the surface of the disc printed with DPE technology of starch at different scales	94
Figure 45 μ CT images of cross-sections of aloe vera blend capsule printed with DPE technology: a) base of the body b) intermediate portion of the body, c) and d) cartoons of the planes of the cross-sections. The capsule body external diameter was 0.5 m....	96
Figure 46 μ CT images of cross-sections of aloe vera blend capsule printed with DPE technology: a) base of the cap b) intermediate portion of the cap, c) and d) cartoons of the planes of the cross-sections of a) and b) respectively. The capsule cap external diameter was 0.5 mm.	97
Figure 47 μ CT images of cross-sections of aloe vera blend capsule printed with DPE technology: a) intermediate portion of the capsule 1, b) intermediate portion of the capsule 2, c) cartoons of the plane of the cross-sections	98
Figure 48 μ CT images of cross-sections of aloe vera blend capsule printed with DPE technology: a) intermediate portion of the capsule 1, b) intermediate portion of the capsule 2, c) cartoon of the plane of the cross-sections.....	99

Figure 49 Pictures of the dissolution device designed for the study of 3D printed films release behaviours after exposure to conditions simulating the colonic environment. 100

Figure 50 Dietary fiber protection effects against Flu mechanisms (235) 103

Figure 51 Na-acetate release from the investigated microparticles in HCl pH=1.2 (dashed curves) or phosphate buffer pH=6.8 (solid curves). The drug loading was varied as indicated..... 108

Figure 52 Protective effect of acetate against IAV infection. Weight loss A) during infection and B) at 7DPI and C) impact on colon length and D) viral load measured in the lung by specific qRT-PCR (Taq man). Results are expressed as mean \pm SEM. # corresponds to impact of IAV infection (IAV/Veh vs MOCK), * corresponds to treatment effect (IAV/Acetate vs IAV/ Veh); # p < 0.05; ## p < 0.01 110

Figure 53 Impact of acetate supplementation on the expression of A) genes encoding interferons, B) interferon-stimulated genes and C) pro-inflammatory genes in the lung. Results are expressed as mean \pm SEM. # corresponds to impact of IAV infection (IAV/Veh vs MOCK), * corresponds to treatment effect (IAV/Acetate4 vs IAV/ Veh); # or * p < 0.05; ## p < 0.01, ### p < 0.001. 111

Figure 54 Impact of acetate supplementation on the expression of A) interferon-stimulated genes, B) inflammatory genes and C) genes encoding Clnd22 (Tight junction); GJA3 (gap junction) and Camp (cathelicidin antimicrobial peptide) in the colon. Results are expressed as mean \pm SEM. # corresponds to impact of IAV infection (IAV/Veh vs MOCK), # or * p < 0.05; ## p < 0.01. 112

List of tables

Table 1 Coating composition, drug loading, and added dose of pellets of the six different formulations tested.....	50
--	----

1.1. Colon targeting

Colonic drug delivery has traditionally been used for the local treatment of inflammatory bowel disease (IBD), to administer mesalazine (5-aminosalicylic acid, 5-ASA) and corticosteroids as first-choice therapy. Scientific advances in site-specific drug delivery to the colon proved the possibility to treat systemic disease as well as local ones (Figure 2).

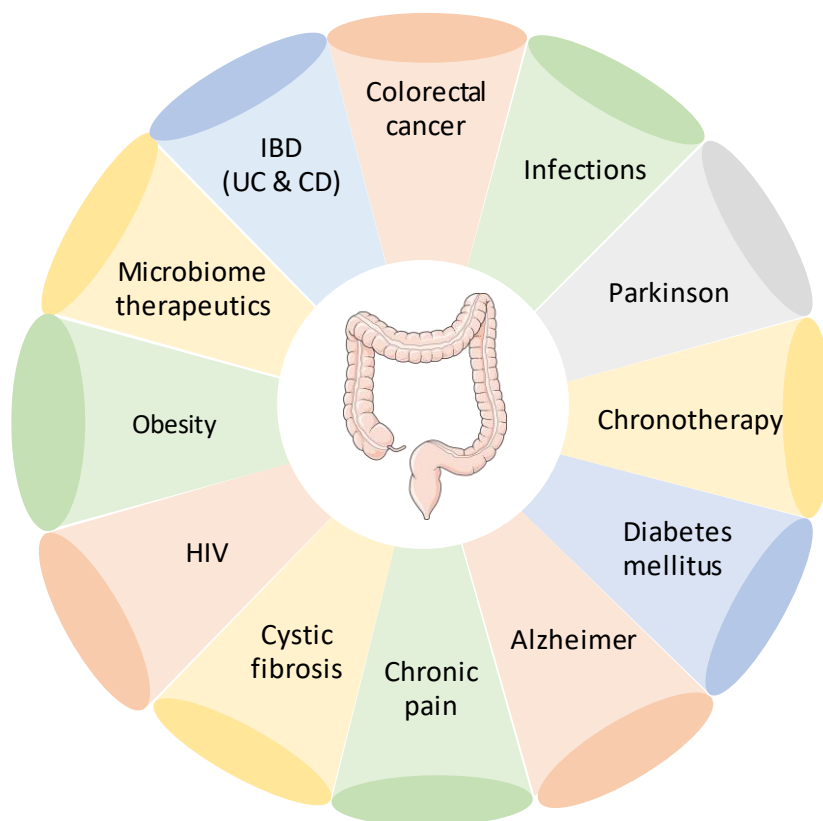


Figure 2. Opportunities for site-specific drug delivery to the colon. IBD, Inflammatory bowel diseases; UC, Ulcerative colitis; CD, Crohn's disease; HIV, human immunodeficiency virus. Reprinted with permission from (1).

In the last decades, researchers focused on the importance of the colonic microbiome, revealing its influence and role played in several diseases both local and systemic (2–4). For this reason, the human microbiome can be targeted and used to improve and preserve human health.

The colonic microbiota consists of trillions of microorganisms and interindividual differences are observed between healthy individuals as well as in patients (5). This complex system is actively involved in absorption of nutrients and immune protection from pathogenic bacteria and viruses as well as metabolization of drugs. The microbiome could influence the efficacy of a therapy by enhancing or inhibiting clinical response, for example for treatment of systemic diseases such heart failure, Parkinson's disease, cancer, and type 2 diabetes mellitus (6–12). Furthermore, it could potentially offer opportunities for the delivery of biologics (13).

Colonic physiology offers several advantages to improve drug absorption and bioavailability of oral drug delivery. Drug absorption in the small intestine is limited by cytochrome P450 enzymes (CYPs) (14), efflux pumps (e.g., P-glycoprotein (P-gp) and breast cancer resistant protein (BCRP)) (15). Thanks to medical imaging it was shown that the lower GI tract has lower levels of luminal and mucosal metabolic enzymes and transporters compared to the upper GI, resulting in therapeutic advantages. An example is represented by simvastatin (a CYP3A4 substrate), that showed greater bioavailability when delivered to the distal ileum compared with an immediate release formulation delivered in the small intestine (16).

Another advantage of delayed-release systems is related to the drug protection in the acidic gastric environment and, following the same principle, the stomach protection from irritant compounds. The macromolecules, such as peptides, proteins or antibodies can be achieved, thanks to the lower proteolytic activity in the colon compared to the upper GIT (13,17,18).

Although the colon might be a favourable environment for drug absorption, the complexities of the entire GI tract must be considered for efficient colonic drug delivery. In summary, changes between healthy and disease states can cause inter-individual variability across the GI tract. For example, IBD patients have lower colonic pH;

colorectal cancer patients have alterations to the epithelium and its transporters; and a variety of disorders affect colonic transit time (6,19,20). GI infections, colorectal tumours, and chirurgical interventions can all have an impact on colonic physiology and function, affecting drug absorption and efficacy (21–25). The pH value in the ascending colon is more acidic in ulcerative colitis (UC) patients than in healthy individuals (26). Furthermore, IBD patients have up to 20% longer small intestine transit times (27), different fluid volumes and composition, an increased epithelial permeability due to damages at the cell junction level (28), inflammation state (29) and a decreased mucus production Systemic disorders that are not directly related to the GI tract, such as cystic fibrosis, Parkinson's disease, diabetes mellitus, human immunodeficiency virus (HIV), and chronic pain, can also have an impact on gut function (21–25). Variations in the gut-brain axis and the gut flora are frequently observed in the disease state and can affect pharmaceutical pharmacokinetics (30,31). Colonic drug delivery systems should then be developed considering physiological and functional variations.

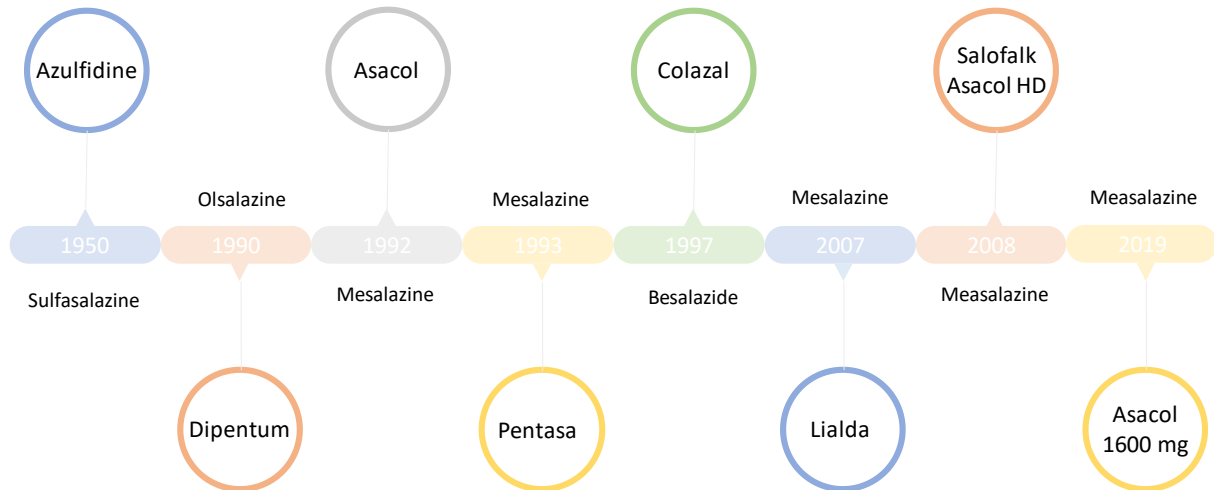


Figure 3 Historic evolution of IBD therapies with the key commercial products. Reprinted with permission from (1).

Sulfasalazine, first introduced in the 1950s was the first colonic prodrug to be approved for the treatment of rheumatoid arthritis and, later, inflammatory bowel disease (IBD).

It is a pro-drug constituted of a 5-aminosalicylic acid (5-ASA) moiety coupled to a carrier molecule, sulfapyridine, by an azo bond(32,33). Following oral administration, the colonic microbiome cleaves the azo-bond, releasing the active 5-ASA to the site of inflammation. Although beneficial therapeutic results were observed for the remission in most of patients affected by mild to moderate UC, allergic reactions to the inactive moiety of the molecule were registered in almost 50 % of patients. (34,35).

Other prodrugs were developed and approved in an attempt to avoid such unfavourable outcomes. Olsalazine is one such example, in which 5-ASA is azo linked to another 5-ASA molecule (36); and Basalzine, in which 5-ASA is azo linked to an 4-aminobenzoyl-beta-alanine (37). The focus was then placed on developing new formulations rather than new drugs Several successful modified release formulations of 5-ASA have been created and marketed as first-line therapies for IBD. (Figure 3) (38).

1.2. The colonic environment

In order to be able to design a colonic drug delivery system it is essential to know and exploit the physiology of the gastrointestinal tract both in healthy individuals and in the disease state. Several parameters have to be taken into account, the anatomical environment such as surface, length and diameter or the gastrointestinal (GI) motility on which the transit time depends. A major role is played by GI content such as bacteria population, responsible for the short chain fatty acid production and concentration. Some of the most important features to consider in developing a site-specific drug delivery system to the colon are reported in Figure 4 (6,39).

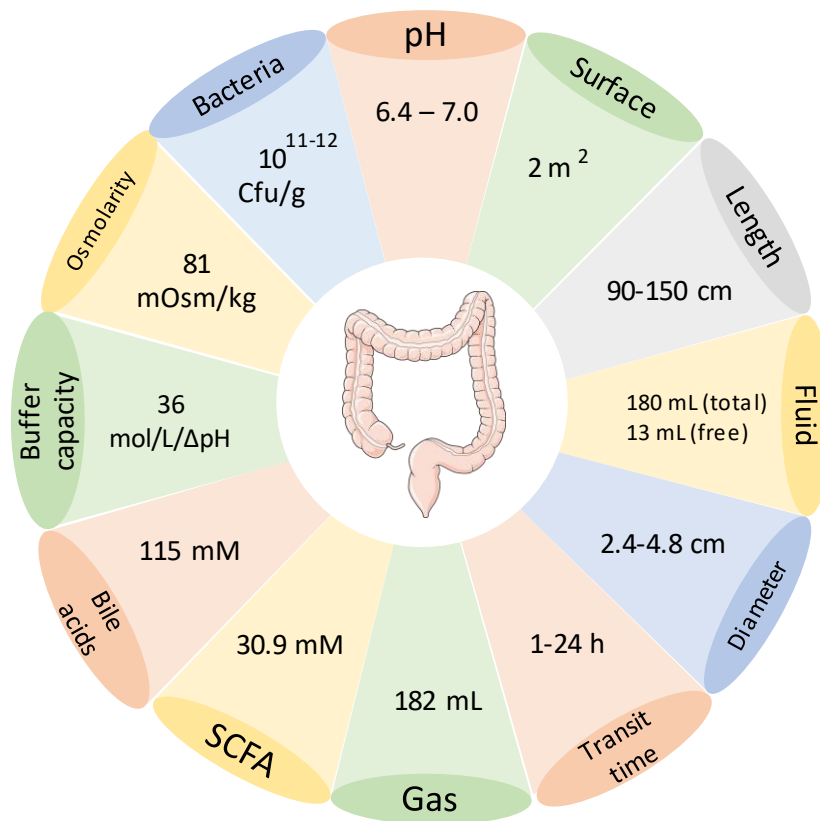


Figure 4. Colon's physiological properties. SCFA, Short chain fatty acids. Reprinted with permission from (1).

The administration of drugs through the oral route must consider the transit along the upper and lower gastrointestinal tract (GIT). To achieve colon specific drug delivery, the oral dosage forms must prevent the drug release through the stomach and small intestine, protecting its cargo from the acidic environment of the stomach and the enzymatic degradation in the small intestine.

The colon has a total length of 90-150 cm and it constitutes ~6% of mucosal area of the GI tract (40,41). Unlike the small intestine, the colon there are no villi and its epithelium is coated with two layers of mucus composed of water, lipids, electrolytes, and glycoproteins with an average thickness of 400-600 μm depending on the colonic regions (42).

The disintegration of a dosage form, dissolution and absorption of drugs closely depend on the intra-luminal fluid or its lack. The amount and composition of GI fluid

dynamically change and fluctuate within an individual depending on several factors: fasted or fed state, fluid intake, lifestyle, and pathological conditions. In particular with respect to the concentration of acid, bicarbonate, bile salts, chyme, electrolytes, bacteria, and gases (39).

It was estimated that the colonic fluid volume slightly decreases in the ascending, transverse, and descending colon (as water is absorbed from faeces), and it amounts to ~372 mL in fasting healthy individuals (43). It must be pointed out that most of the water in the colon is associated with biomass or bacteria, and therefore is not freely available to interact and disaggregate dosage forms (44). The free water available in the colon is located in fluid pockets, rather than being homogeneously distributed in the lumen (45). These fluid pockets are generally grouped in a single region of the colon and each of them carries < 0.5 mL of water (44). Considering that the disintegration and dissolution of oral forms depend on the contact with water, the higher free water content of the small intestine could partially explain why the drug absorption is often faster in the upper GIT compared to the colon (46).

Once dissolved, drugs absorption into the systemic circulation depends on their physiochemistry. Most of the drugs are lipophilic and they diffuse transcellularly across the epithelium, whereas hydrophilic drugs permeate paracellularly (42,47).

1.3. Colonic drug delivery strategies

Given the physiology of the colon, efficient drug delivery systems must be designed to assure successful delivery (42). To ensure complete and site-specific drug release in the colon, the technologies shifted away from a single drug delivery mechanism toward a mix of stimuli based on numerous colon-targeting technologies. Figure 5 depicts a history of the historical progression of colonic drug delivery system design, including major technological examples.

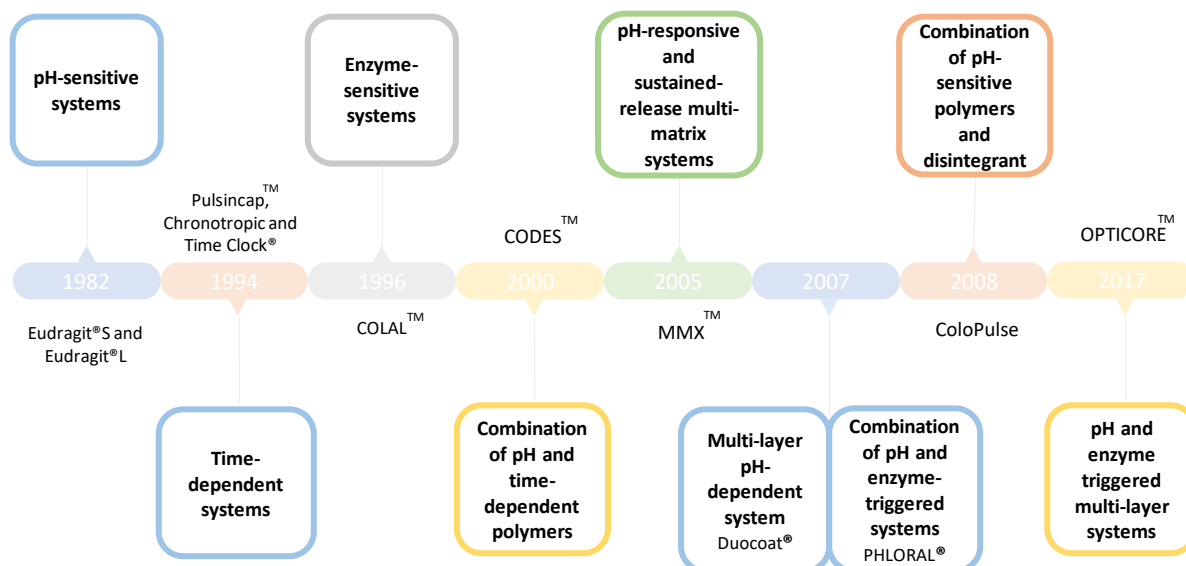


Figure 5. Historic evolution of colon targeting technologies with the key commercial products. Reprinted with permission from (1).

1.3.1. pH-dependent Drug Delivery Systems

The GIT pH variability, both between subjects (intersubject variability) and within subjects (intrasubject variability), depend on several factors such as pathological conditions, absence or presence of intraluminal food. The lowest pH value is registered in the stomach (pH 2.0 – 4.5 in the fed state and pH 0.4 – 4.0 in the fasted) (48,49) and it raises in the proximal section of the duodenum pH 5.0 – 7.0) (50), reaching the jejunum (pH 6.6 ± 0.5) followed by the ileum (7.5 ± 0.5) (51). The pH in the colon drops to lower values 6.4 ± 0.6 in the cecum and raises gradually along the ascending, transvers and descending colon, reaching 7.0 ± 0.7 in the rectum.

The colonic bacteria play an important role in the regulation of the pH values in the colon, the carbohydrate substrates indigestible to human enzymes are converted by the bacterial enzymes in short chain fatty acid (SCFAs), which can lower the pH in the proximal colon (52). The reduced production of SCFA in distal regions of the colon explains the raising of the pH.

Considering these range values, it is possible to exploit the pH variations in the GIT for the site-specific delivery of drugs in different regions. A solution is represented by the coating of solid formulations with an enteric polymer that disintegrates or dissolves at certain specific pH values. The ideal polymeric coating for the colon targeting should be insoluble under the acidic condition of the stomach and proximal regions of the small intestine and start dissolving at pH about 6 to 7. Furthermore, it should be thick enough to ensure that the drug release is delayed until the colonic region is reached. Considering that most pH-dependent systems release the drug from the terminal ileum to the colon, it would be more appropriate to talk about ileo-colonic delivery (53).

Methacrylic acid and methyl methacrylate anionic co-polymers are the most commonly used pH-sensitive polymers (54), cellulose derivatives [e.g., hydroxypropyl methylcellulose acetate succinate (HPMC-AS); hydroxypropyl methylcellulose phthalate (HPMCP); cellulose acetate phthalate (CAP); cellulose acetate succinate (CAS); cellulose acetate trimellitate (CAT)]; polyvinyl acetate phthalate (PVAP); and shellac (55,56). In general, the free carboxylic acid groups in these polymers are un-ionised in acid conditions, rendering the molecules insoluble in acid. Once exposed to a neutral environment it becomes deprotonated, increasing the hydrophilicity of the molecules and triggering their dissolution (57,58). Consequently, the pH threshold values and dissolution rate of the different polymers depend on the number of carboxylic acid moieties available: the higher is this number, the lower the pH threshold and the faster the dissolution rate (59–61).

The first attempt to utilise pH-sensitive polymers for the site-specific delivery of drugs to the ileo-colonic region dates back to 1982 (62). Eudragit[®] S (solubility threshold pH 7) was employed as capsules coating and studied *in vivo* in humans. X-ray imaging showed that most of the capsules were disintegrated in the ileo-colonic region (63).

Currently, several commercialised products use Eudragit[®] as enteric polymer, including Asacol[®] MR, Mesren[®] MR, and Ipocol[®] (Eudragit[®] S - solubility threshold pH 7) and Salofalk[®] (Eudragit[®] L - solubility threshold pH 6) (64).

The single-layer pH-dependent polymer coating was developed to double-layer systems, incorporating two different coating layers; the inner made of partially neutralized

Eudragit® S combined with a buffer agent and the outer of Eudragit® S alone (57,65). DuoCoat® is a commercialised product which exemplifies this drug delivery technology (Figure 6).

The advantage of the double-layer technology on the single one is the shorter dissolution lag time and higher drug release rate once the polymer solubility pH threshold is reached (62,66).

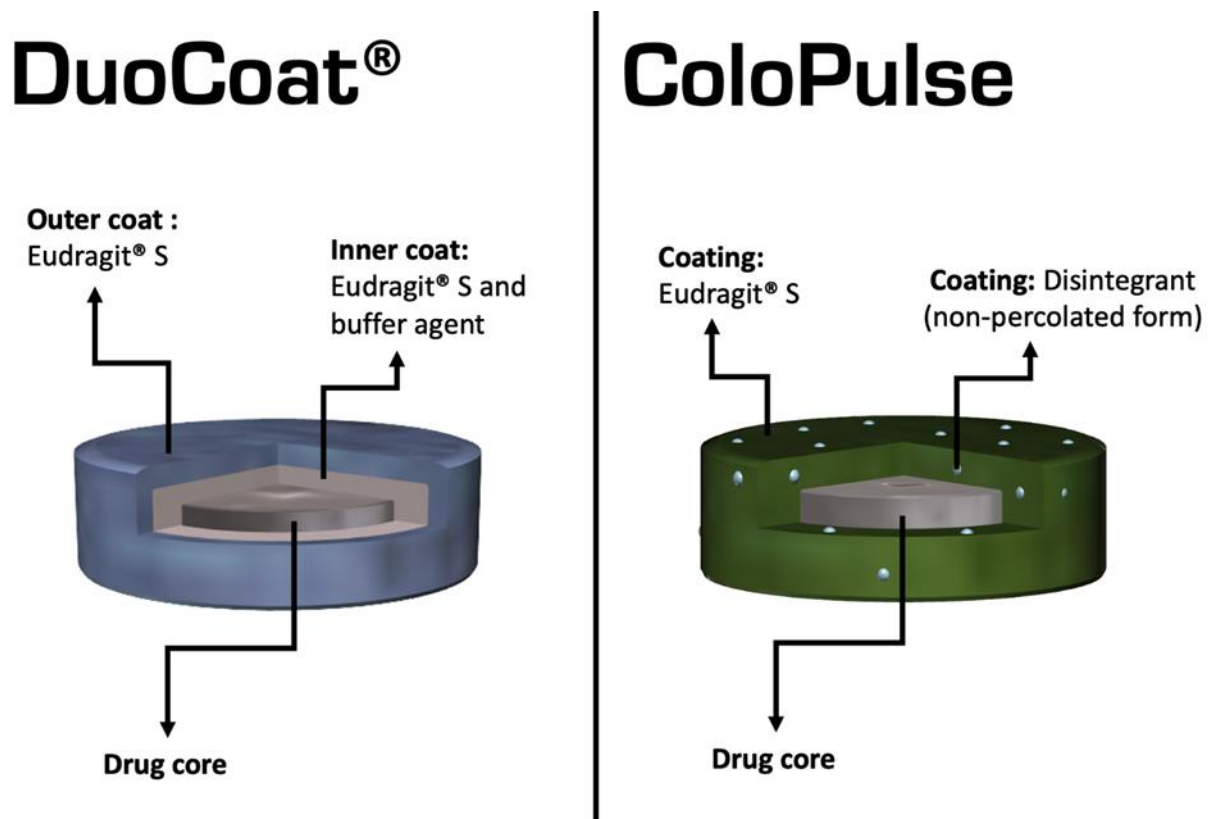


Figure 6. Schematic representation of the systems: DuoCoat® and ColoPulse (1).The single-layer technology was improved with the incorporation of a disintegrant (e.g., sodium starch glycolate, croscarmellose sodium, microcrystalline cellulose, or alginic acid) to the enteric coating (30).

In the ColoPulse system, the coating layer is made of a matrix of Eudragit® S in which a disintegrant is dispersed in a non-percolating form (no continuous network between particles is created). Once the pH threshold is reached, the fluids penetrate into the coating and the hydrophilic disintegrant accelerates the disruption of the latter, leading to a pulsatile drug release. The drawback of this system is the need of an organic-based coating to prevent the premature swelling of the superdisgregant, leading to the drug release in the upper GIT (68).

1.3.1.1. Limitation of pH-sensitive Drug Delivery Systems

The clinical success of commercialised pH-dependent drug delivery systems (DDS) has been proved during the clinical trials. Nevertheless, the unreliability of Eudragit S® coated formulation to disintegrate in the colonic regions has been reported by several studies (53,69,70). The reasons behind the coating failure can be attributed to a myriad of physiological factors, including gut motility, fluid volumes, feed status, buffer capacity (71) which might lead to a premature drug release in the upper GIT or an insufficient coating degradation, resulting in the expulsion of the tablets in patients' stools.

The market offers a wide choice of formulation for the therapy of inflammatory bowel disease, such as Lialda®, Asacol®, Octasa®, Pentasa® and Salofalk® each of them with a different drug release profile (72). This allows the patients to benefit from switching to a different type of formulation after an inadequate therapeutic response to a specific treatment (73).

1.3.2. Time-dependent Drug Delivery Systems

Time-dependent drug delivery systems are designed to delay the release of their drug cargo after a reasonably predictable time lapse. For colonic delivery, it corresponds to the transit along the small intestine, from the pylorus down to the ileo-caecal valve.

Historical data reported that the whole gut transit time is on average 27.4 hours, with a minimum of 5.1 and a maximum of 58.3 hours (74). These values have been recently confirmed by a study in which electromagnetic capsules were used to measure the transit time across the different regions on the GI tract in humans (75). The study was performed on 111 healthy volunteers, selected in order to cover a large variability of age, sex and body mass indices (BMI). The data reported similar results compared to the historical values: a mean GI transit time of 28.52 hours, with a minimum of 14.10 and a maximum of 57.49 hours.

The age plays an important role on GI motility and transit, elder volunteers were associated with longer colon transit time (75,76) as well as to decreased colonic motor activity (77). Advanced age has been also linked to risk factors associated with the slow colonic transit, such as multitherapy, decreased fibre intake, and reduced physical activity (78).

Biological sex clearly has a significant effect on gut motility. Men are reported to have shorter gastric emptying compared to females (79,80). The hormonal regulation has been considered the cause of these differences, however further studies are required to validate this hypothesis (81).

In order to achieve colonic drug delivery, time-dependent systems should remain intact upon contact with the acidic environment of the stomach and prevent premature drug release in the small intestine. Once in the duodenum, a triggering signal should initiate the drug release in a controlled manner (82). In order to insure this result, polymer coatings or sealing plugs of swellable and erodible polymers are often used (82–84). Time-sensitive systems are conventionally classified as reservoir, capsular, and osmotic devices.

Reservoir systems represent the first attempt and several references date back to the late 1990s (85–87). Such systems were coated with an external layer of rupturable, erodible, or diffusive polymer that upon contact with the body fluids, slowly starts to disintegrate exposing the drug reservoir (88,89). The progenitor capsular system is PulsincupTM, which consisted of a rigid insoluble body encapsulating the drug, closed with a hydrogel PEG8000 plug and a water-soluble cup (90). Upon contact with gastrointestinal fluids,

the water-soluble cap dissolves exposing the hydrogel plug. The latter absorbs the external fluid and starts to swell, the resulting increase of its dimension ejects the plug, exposing the drug cargo to the colon environment.

Most recently, a double-layer coating was proposed for 5-aminosalicylic acid (5-ASA)-loaded tablets: an inner layer of HPMC, and an outer layer based on Eudragit® L30D (91). The imaging study on 6 healthy volunteers showed that disintegration of the administered units was in no cases observed prior to colon arrival.

1.3.3. Enzyme-sensitive Drug Delivery Systems

It is now common knowledge that bacteria largely contribute towards human health and disease (5,92). Human body hosts about 100 trillion microbial cells and the great majority of them reside in the gut, with the highest concentration registered in the colon (1012 bacteria per gram of tissue)(93,94).

The bacterial metabolic power can be exploited for drug delivery. The enzymatic degradation of specific chemical bonds can be used to activate prodrugs; Sulfasalazine represent one of the first example of prodrug used in the treatment of IBD, where the active moiety, 5-aminosalicylic acid is released after the enzymatical cleavage (95).

The metabolic activity of colonic microbiota can be also used to degrade enzyme-sensitive materials used for the coating of the dosage forms, facilitating the drug release. Such materials include different types of polysaccharides, which serve the bacteria as a substrate for the production of SCFAs (96).

Each person has a different microbiome composition, depending on the age, sex, nutritional habits and lifestyle. Although these differences create a unique environment inside the individual gut, there is substantial functional redundancy amongst microbiota. Polysaccharide digestion is performed in most of the population, making these materials reliable for colonic drug delivery (97).

On the other hand, microbial activity can lead to undesirable effects such as the reduction of bioavailability (98) following an extensive metabolism or the production of toxic metabolites (99).

In the last 20 years enzymes-sensitive polymers have been widely explored for the site-specific delivery of drugs in the colon (100).

There are two main classes of polymers exploited for the colonic drug delivery: azo-polymers and polysaccharides (101). The latter are generally recognised as safe (GRAS) by the United States (U.S.) Food and Drug Administration (FDA) which means non-toxic, slightly immunogenetic and highly biocompatible (102), which favours their use in the pharmaceutical field. Furthermore they are available at large scale and have relatively low cost (103). Synthetic azo-polymers present possible safety issues due to their chemistry and the need for organic solvents in their preparation, which represents a limitation for their use (104).

The wide variety of examples of natural polysaccharides employed for the colon targeting includes pectin, starch, alginate, gums, amylose, chitosan, dextran, chondroitin sulphate, inulin, β -cyclodextrin and galactomannan (51–57).

An *in vivo* study in humans compared a pH-sensitive coating to an enzyme-sensitive one in order to analyse the ability of the different materials to target the drug release to the colon (71). For this purpose, theophylline loaded pellets were coated with either Eudragit[®] S or amylose-ethyl cellulose blend; uncoated pellets acted as control. The results showed a more specific colonic release of the systems coated with amylose/ethylcellulose blend compared to the pH-sensitive systems. Theophylline earlier peaks in drug plasma concentration might suggest a premature release of the drug in the small intestine. Furthermore, no drug release at all was observed in one of the patients to whom it was administered the Eudragit[®] S coated pellets, suggesting the elimination of intact formulations in the stools (Figure 7).

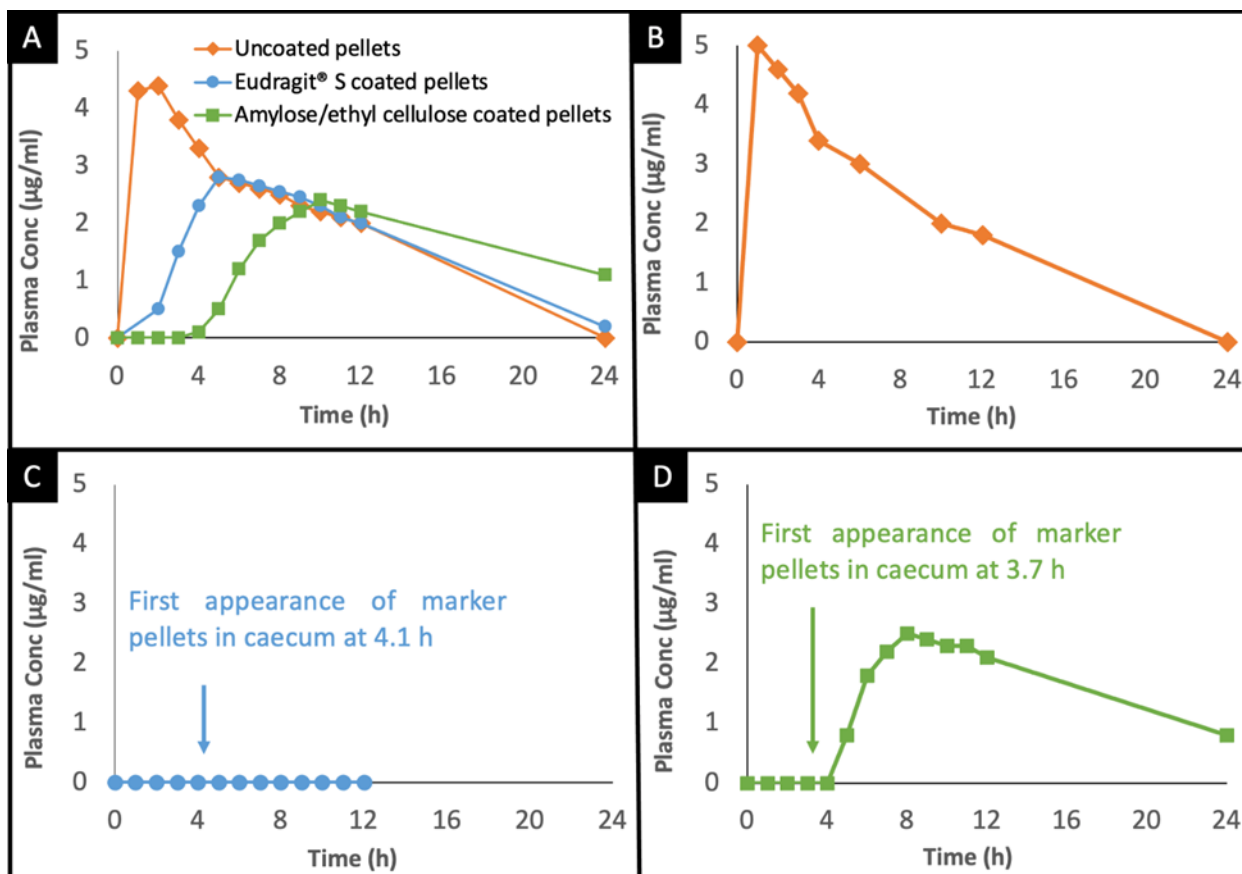


Figure 7 (A) Mean plasma theophylline levels after administration of uncoated, Eudragit® S coated pellets and amylose/ethyl cellulose coated pellets to eight healthy male subjects. B, C and D show examples of plasma concentration time profiles observed in single subjects: (B) uncoated pellets; (C) Eudragit® S coated pellets and; (D) amylose/ethyl cellulose coated pellets. (1,71).

1.3.3.1. Limitation of enzyme-sensitive Drug Delivery Systems

When formulating polysaccharides as colonic targeting coatings, it must be considered their relatively high hydrophilicity. Depending on their chemical properties, polysaccharides can swell following the absorption of fluid. The use of these polymers alone might then result in premature release of the drug cargo in the upper GIT due to disintegration of the coating upon contact with intestine luminal fluids. Different

strategies are reported in the literature to overcome this drawback, such as the chemical modification of the polysaccharide structure, to reduce its hydrophilicity, or the combination with water insoluble or hydrophobic polymers (e.g., ethyl cellulose or cellulose acetate). The polysaccharide/polymer blend will be partially degraded by the colonic bacteria triggering the drug release (105–107)

Another challenge using bacteria-sensitive colonic delivery systems is the enzymatic activity of colonic microflora. Although the enzymatic degradation of the coating is essential to trigger the drug release, the bacterial metabolic power could affect pharmacokinetics and pharmacodynamics (108). Chemical modifications of drugs might render them inactive, toxic or even more active (13,98,109).

Despite the substantial functional redundancy amongst microbiota, inter-individual unique microflora can have an impact on the success or failure of a therapy. Microbiome dysbiosis might induce failure in the degradation of polysaccharides coating, preventing the drug of being released (110). Such dysbiosis can be directly associated with a pathological state (e.g., Cystic fibrosis, Parkinson's disease, HIV infection, obesity, metabolic syndrome, intestinal cancer, and diabetes) (6,111) as well as a pharmacological treatment. Antibacterial drugs are known to have a relevant impact on the microbiome composition, with possible long-term effects up to 4 years after administration (112).

1.3.4. Pressure-dependent Drug Delivery Systems

As a solid dosage form transits via the GI tract, it is subjected to pressure generated by muscular contractions. On this basis, pressure-controlled drug delivery systems exploit the luminal pressure as a triggering event to release their drug cargo as the external coating breakdowns. Interestingly, whilst the coating layer must resist pressure conditions in the upper GI tract, it should be susceptible to contraction forces in the distal gut (113). The peristaltic movements result from muscular contractions that take place mainly in the digestive tract, pushing the ingested food from the stomach to the anus (114). Compared to the small intestine, the luminal pressure in the large intestine is higher due to the reabsorption of water, which increases the viscosity of its content (90). An example of such includes a gelatine capsule that is internally covered by an insoluble polymer layer (e.g., ethyl cellulose), whose thickness determines the disintegration of the capsule (e.g., varies from 40 to 220 μm). Following its administration, the body temperature causes the base to melt and subsequently leads to the absorption of body fluids, which in turn results in the increase of viscosity and pressure inside the system, expelling the drug from the device (115,116). The system can be improved by drilling micropores into the bottom of the ethyl cellulose layer and by adding a highly swellable excipient (e.g., low-substituted HPC). This has shown to promote the drug release after *in vitro* and *in vivo* lag phases (117).

More recently, a pressure-controlled colon delivery capsule (PCDC) based on a hard gelatine core and Eudragit® S 100 was proposed (118). Herein, theophylline was dispersed in a lipid matrix then coated and encapsulated. The system was subsequently coated with Eudragit® S 100 and studied for the treatment of nocturnal asthma. *In vivo* evaluation revealed that a longer lag time occurs prior to the sudden rise in theophylline blood levels. Following the disintegration of the PCDCs in the GI tract, the drug is promptly released.

1.3.5. Hybrid Strategies for Colon Targeting

The colonic release strategies that include a single-triggered mechanism have their limitations, due to interindividual differences in the gastrointestinal physiology. To overcome the therapeutic failure, it is possible to combine more technologies, ideally in a way that each mechanism works independently to the other/s. This backup strategy would improve the reliability of the system, increasing the probability of success in drug release.

1.3.5.1. pH and time triggered combinations

Systems that combine time-controlled mechanisms along with pH-triggered strategy are named Multi Matrix System® (or MMX™) (119). Commercial examples of MMX™ are Lialda® (Mezavant® XL) and Cortiment® (UCERIS®), loaded respectively with mesalazine and budesonide. These systems have a double matrix: an internal lipophilic portion, encapsulating the drug, is imbedded in a hydrophilic matrix. This double system is enclosed in an enteric film coating. Contradictory results are found in the literature concerning the drug release profiles of these systems, experiments performed in phosphate buffer showed a sustained drug release for more than 8 h. On the contrary, experiments performed in a bicarbonate buffer showed a more instantaneous drug release, similar to the profiles observed with conventional pH-sensitive colon targeting systems (e.g., Asacol® and Ostasa®) (72,120). An *in vivo* experiment performed on 189 patients with ulcerative colitis (UC) and 23 patients with Crohn's disease showed a better correlation between bicarbonate buffer and *in vivo* pharmacokinetics (121). Similarly, Budenofalk® presents a complex double layer coating consisting of an inner mix of polymers: Eudragit® RS, Eudragit® L100 and Eudragit® S and an external layer of Eudragit® RL (68).

Another example is Entocort™ EC, a multi-particule dosage product designed for local delivery of budesonide in the colon to treat ulcerative colitis and Crohn disease

(122,123). The system consists in a hard gelatine capsule, loaded with 3 mg of drug and coated with an inner layer of ethylcellulose and an outer layer of Eudragit® L100-55 (pH threshold = 5.5) (124).

Promising *in vivo* results were obtained with Eudratec® COL, a multi-unit system composed of an outer layer of Eudragit® FS 30D coating and an inner layer of Eudragit® RL or Eudragit® RS. A study demonstrates a better control of the drug release compared to pH-dependent systems alone (125).

1.3.5.2. Time and enzymes triggered combinations

The combination of time and enzyme sensitive mechanisms has been recently explored, developing paracetamol loaded capsules coated with a blend of high amylose starch and HPMC (126). Different HPMC molecular weights were tested, in order to evaluate the swelling and degradation of the polymer once in contact with the GI fluid. HPMC degradation takes place in the upper GIT, offering a sufficient lag-time to the formulation to reach the colon without releasing the drug cargo. Once in the colon, the enzymes produced by the microbiota digest the polysaccharide portion, leading to fast and complete drug release.

1.3.5.3. pH and enzymes triggered combinations

CODES™ is an example of pH and bacteria-sensitive systems (127). It is a multilayer formulation consisting of a lactulose core coated with an internal layer of Eudragit® E and a second layer of Eudragit® L. The outermost polymer has gastroprotective function and start to dissolve in the upper GIT. The fermentation of the lactulose core by the colonic bacteria will lead to the production of SFCA. The consequent acidification of the media dissolves the acid-soluble polymer Eudragit® E, leading to an immediate release of the drug (128,129).

Although the formulation combines two different release mechanisms, the risk of failure is not necessarily eliminated. The first mechanism will always be the limiting factor; a failure in the degradation of the outermost layer will result in the impossibility for the microbiome to access and ferment the polysaccharide core resulting in no drug release.

A way to overcome the risk of failure or patient variability is to use different triggering mechanisms that work in parallel. Phloral™ represents the first commercialised technology combining pH and enzyme sensitive polymers in a single layer (figure 8) (130,131). Eudragit® S is directly blended to resistant starch, providing a fail-safe colonic drug release (132).

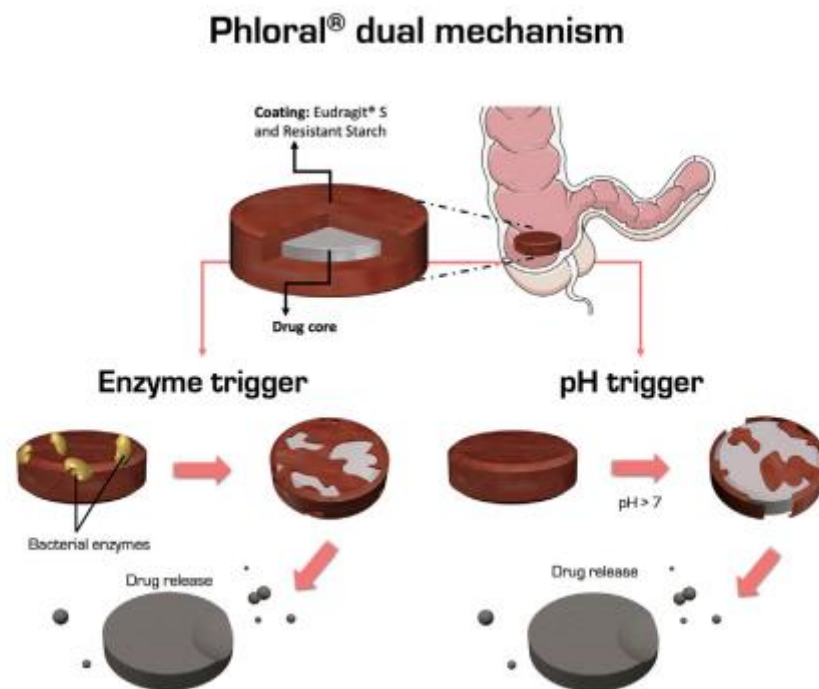


Figure 8 Schematic representation of the Phloral™ film coat technology (1) .

OPTICORE™, a dual-triggered device used to successfully administer 5-ASA to the colon for the treatment of IBD (133), is a more recently marketed technology. The word OPTICORE™ refers to OPTImised COLonic RElease, which explains the formulation's aim.

To ensure optimal colonic drug administration, OPTICORE™ blends an inner alkaline coat (containing a neutral enteric polymer, such as Eudragit S, and a buffering salt) with an exterior Phloral™ coating.

The pH, buffer capacity, buffer salt concentration, ionic strength, and viscosity of the colonic fluid all influence drug release in the OPTICORE™ system. The coating promotes early and rapid drug release in the ileo-colonic region, where fluid is more abundant compared to colon's distal regions. As the outer coat dissolves or is fermented by bacterial enzymes, fluid enters the formulation through the pores formed in the coating, causing the inner coat to dissolve. At the inner surface of the Phloral™ coating layer, this creates an environment with higher pH, buffer capacity, and ionic strength.

As a result, the Eudragit S in the Phloral™ coat ionises and dissolves quickly, accelerating drug release (65,134,135). OPTICORE™ was studied in a recent phase I clinical trial to deliver metronidazole benzoate to the colon to treat localised Clostridioides (previously Clostridium difficile) infection. When compared to immediate-release findings, accurate ileo-colonic targeting was accomplished with lower systemic concentrations (136). Furthermore, Asacol™ 1600 mg, a 5-ASA medication based on OPTICORE™ technology, has completed Phase III clinical studies and is now available in Europe (137). This dual-trigger technique allows the inclusion of up to 1.6 g of 5-ASA due to its excellent colonic specificity and dependability; significant doses of 5-ASA (up to 4.8 g daily) are necessary to attain the prescribed levels in mild to moderate UC cases.

This capacity to deliver a significant dose in a once-daily formulation decreases the number of doses patients must take, enhancing patient compliance and acceptability.

While they were initially designed to treat local colonic disorders, the clinical success of the dual trigger of the Phloral™ and OPTICORE™ systems has transformed them into universal delivery systems capable of transporting almost any product to the colon. This provides the path for their application in diseases other than IBD and local disorders of the colon (1).

2. Chapter: Enzyme sensitive coatings for colon targeting

2.1. Gut microbiota

Colonic microbiota is experiencing a renaissance due to the multitude of associated benefits and opportunities and it is now becoming an emerging therapeutic target (108,138,139).

It was demonstrated that the highest concentration of microorganism of the entire body is hosted in the colon, with 10^{10} - 10^{12} cells per mL, including more than 1000 different species (78,79). This diversity includes not only bacteria but also fungi, viruses, archaea, free DNA, and many associated enzymes and metabolites (94). Bacteroidetes, Firmicutes, Proteobacteria, and Actinobacteria are the most common bacteria inhabiting the colon (142) and their distribution varies through the different sections of the colon. Generally bacteria concentration increases between the proximal and distal colon and gradually decreases in the rectum (143), the species responsible for the fermentation of complex polysaccharides are generally located within the proximal colon (140).

It is important to know that the microbiome composition varies between individuals and within the same individual, it varies naturally during the life-time due to age, lifestyle, disease state and alimentation habits. Despite these variations, the general functions, such as fibre fermentation, is similar in healthy adults (97).

Microbiome composition and functionality are closely linked to several disease states, being the cause or the consequences of health problems. These effects can be local, related for example to inflammatory bowel diseases (144) or systemic. Recent studies proved the relation between microbiome dysbiosis and systemic disorders such as dyslipidaemia, urinary tract infections, and neurological conditions, such as Alzheimer's and Parkinson's disease (145–149).

The effects of the microbiome activity are not only limited to the body physiology but extended to drug modification, accumulation or inactivation (79,90,91,92), having

important consequences on the therapeutic and side effects. For these reasons it is essential to take into account the microbiome activity while aiming local drug delivery to the colon (151,153).

There exists a plethora of molecules whose administration significantly impacts the intestinal microbiome. Antibiotics are the most known drugs to have effects on bacteria composition and activity that can last for months or even years (112,154,155). Other drugs and excipients that do not directly target the microbiome have been identified as causing dysbiosis, 27 % of non-antibiotics inhibited the growth of at least one species (156,157).

2.2. Animal models for colonic drug delivery

It is critical to choose *in vivo* animal models that best resemble the physiology of the human GI tract for developing innovative colon targeted formulations. Price, availability, and convenience of handling are frequently more influential than physiological similarities in the selection of animal models (158).

Animals show significant interspecies differences in GI anatomy and physiology, resulting in a wide range of drug bioavailability and absorption (159). Unfortunately, no single animal can exactly mimic the human GI tract. Because of this variability, researchers studying colonic site-specific delivery technologies frequently employ a variety of animal models, including small rodents such as mice, rats, rabbits, guinea pigs, and larger animals such as dogs, pigs, and non-human primates (159). Recognizing the usefulness of animal models for evaluating colon-targeted drug delivery in humans is critical for optimising pre-clinical development efficacy. The most appropriate animal model is likely to be determined by dosage form features, parameters to be investigated, and the indication to be treated.

Furthermore, for formulations intended to treat both sexes of humans, equitable representation of female and male animals during pre-clinical testing is critical (80). Although the mouse/rat microbiome differs from the human colon in composition, rat

caecal material shows similar concentration of Bifidobacteria and Bacteroides (160). Variability amongst animals can also be reduced by standardising their living habitat and diet.

2.3. Faecal slurries used to simulate the colonic environment

While performing *in vitro* drug release of formulation aiming colon targeting, it is important to simulate as much as possible the colonic environment. One possibility is the use of faecal material dispersed in an appropriate release media (faecal slurries). This media inoculated with colonic bacteria will mimic the microbial composition and diversity, supporting the microbial growth during the experiment and enabling the prediction of drug release, solubility and stability (161,162).

Depending on the aim of the experiment, donors with different characteristics can be used (healthy individuals, patients, animal models etc.) and several parameters such as media pH, faecal material concentration and type of growth media can be modified. Healthy humans have an average pH of 6.64 and contain between 25-54 % of solid material. The concentration of undigested polysaccharides, proteins and lipids varies according to the eating habits and it is generally around 25 % (163). In order to allow an effective homogenization of the faecal material and to guarantee a continuous bacterial growth, a concentration between 10-25 % is commonly used (109,162,164).

One of the main advantages in using patients' faeces or animal models is the possibility to reproduce *in vitro* the disease state that it is aimed to target (165). Inflammatory bowel diseases play an important role in the microbiome dysbiosis; therefore, it is recommended to test drugs/formulations in a disease simulated environment (144).

It must be taken into account that the parameters set at the beginning might vary during the experiment due to the production of short chain fatty acids resulting in a decrease in pH (166). The acidification of the media will eventually lead to bacterial stasis/death (167).

In this work, a setup known as “static batch culture” was used to analyse drug dissolution, stability, and solubility. In this type of setup, the drugs/formulation are incubated in faecal slurry for short timeframes (≤ 24 hours) with regular samples withdrawal (168).

More complex systems are available to simulate several regions of the gastrointestinal tract, they normally consist in multiple compartments connected to each other and which allow the fine settings of parameters such transit time, pH, fasted or fed state (169,170).

The Mucosal Simulator of the Human Intestinal Microbial Ecosystem (M-SHIME[®]) is one of the most advanced systems, which includes vessels representative of the stomach, small intestine, and ascending, transverse, and descending colon (171). One of the main advantages of this system is the presence of a simulated mucus layer, able to foster the growth of both mucosal and luminal microbiota (172). The most promising candidates selected during the first phase of the project were tested with the M-SHIME system (Chapter 3).

Faecal slurries cannot fully represent the colonic microbiome composition, but they offer an easy and effective method to reproduce formulation behaviour *in vivo*, in a controlled and reproducible manner (171,173,174).

2.4. Materials and methods

2.4.1. Materials

5-aminosalicylic acid (5-ASA, Alfa Aesar, Kendel, Germany); Bacto™ Tryptone, Bacto™ desiccated Beef extract (Becton, Dickinson and Co., Le Pont de Claix, France); Sodium chloride 99.5 % (Acros organics, Geel, Belgium); Yeast Extract (Oxoid, Dardilly Cedex, France); L-Cysteine hydrochloride (Sigma-Aldrich Co., Steinheim, Germany). Anerogen™ 3.5 L/2.5 L (ThermoScientific, Basingstoke, UK), pH-Fix (Macherey-Nagel, Düren, Germany).

Aqueous ethylcellulose dispersion (Aquacoat ECD, Colorcon, Kent, England); dibutyl sebacate (Acros organics, France); hydroxypropyl methylcellulose (HPMC, Methocel K3 premium LV, Colorcon, Kent, England).

Suglets® (sucrose/starch starter cores, mesh 30/35, 500-600 µm, Colorcon, Dartford, England); Starch 1500® (pregelatinized maize starch, Colorcon, Kent, England); Glucidex® 17 (corn maltodextrin, Roquette Freres, Lestrem, France); Glycolys® Sodium Starch Glycolate (Roquette Freres, Lestrem, France); SweetPearl® P300 DC Maltitol (D-Maltitol, Roquette Freres, Lestrem, France); Cleargum® (octenyl succinate starch, Roquette Freres, Lestrem, France); Clearam® (cook-up starch, Roquette Freres, Lestrem, France); Wheat starch (Roquette Freres, Lestrem, France); aloe vera extract powder, Reishield (Specialty Natural Products Co., Ltd, Thailand); Goji Berry Extract Powder (Specialty Natural Products Co., Ltd, Thailand); Reishi Extract Powder (Specialty Natural Products Co., Ltd, Thailand); Coix lacryma Extract powder (Centella asiatica Extract powder, (Specialty Natural Products Co., Ltd, Thailand); Abelmoscus esculentus extract powder (Specialty Natural Products Co., Ltd, Thailand); Orafti®Synergy1 (Inulin, BENE0-Orafti S.A. plant, Oreye, Belgium); Orafti®HIS (Inulin, BENE0-Orafti S.A. plant, Oreye, Belgium); Orafti®ST-Gel (Inulin, BENE0-Orafti S.A. plant, Oreye, Belgium); Orafti®HP (Inulin, BENE0-Orafti S.A. plant, Oreye, Belgium); Orafti®P95 (oligofructose, BENE0-Orafti S.A. plant, Oreye, Belgium); Remypro® N80+ (rice protein, BENE0-Orafti S.A. plant, Oreye, Belgium);

Palatinose™ (Isomaltulose, BENEIO-Orafti S.A. plant, Oreya, Belgium); pectin from apple and pectin from citrus (Sigma Chemical Co., St. Louis, USA); Locust bean gum powder, Gellan Gum High Acyl, Konjac Gum Powder (Special Ingredients Ltd, Chesterfield, UK); Spray dried Gum Acacia and Gum Karaya Powder (Alland & Robert, Saint-Aubin sur Gaillon, France); 1500® (pregelatinized maize starch) (Colorcon, Kent, UK); Xylan from corn core (Tokyo Chemical industry, Zwijndrecht, Belgium); Genu Pectin citrus (Hercules, Atlanta, Georgia); ChitoClear® (Chitosan, Melun cedex x EHF, Iceland); Novelose® 240 and Novelose® 330 (starch, Ingredion Germany GmbH, Hamburg, Germany); Marine Colloids™ (Carrageenan, France); rice starch (Cooper, Melun cedex, France); EMCOSOY® (soy polysaccharides, JRS Pharma GmbH & Co. KG, Rosenberg, Germany).

Hydrochloric acid S.G. (FisherScientific, Loughborough, UK); PB-buffer pH 6.8 made of: Potassium dihydrogenphosphat (Acros organics, Geel, Belgium), Sodiumhydroxide White Pellets (FisherScientific, Loughborough, UK). Methanol (Carlo Erba Reagents, Val de Reuil Cedex, France); Acetic acid glacial (Fisher Scientific, Loughborough, UK).

2.4.2. Inoculation of polysaccharides in culture medium +/- faecal samples

Culture medium was prepared by dissolving 1.5 g beef extract, 3 g yeast extract, 5 g tryptone, 2.5 g NaCl and 0.3 g L-cysteine hydrochloride in 1 L distilled water under heating. The pH was adjusted to 7.0 ± 0.2 with HCl or NaOH. The culture medium was sterilised in an autoclave at 115 °C for 20 min, and stored at 4 °C until use. Prior to inoculation with bacteria, the medium was heated to 100 °C for 20 min to reduce the amount of oxygen and cooled to room temperature.

Two g polysaccharide were dissolved/dispersed in 100 mL culture medium, followed by sterilization in an autoclave at 115 °C for 20 min. Eight mL of the solution/dispersion were inoculated in a glass tube with 2.0 mL faecal slurry (10⁶ CFU/mL bacteria) from inflammatory bowel disease patients, healthy dogs, or inflammatory bowel disease model rats. In the latter rat model, the disease was induced as follows: The animals were

anesthetized for 90–120 min using pentobarbital (40 mg/kg) and received an intrarectal administration of TNBS (trinitrobenzene sulfonic acid, 250 μ L, 20 mg/rat), dissolved in a 1:1 mixture of an aqueous 0.9 % NaCl solution and ethanol. The rat faeces were collected 1 d after TNBS administration. The tubes were incubated at 37 °C under anaerobic conditions (5 % CO₂, 10 % H₂, 85 % N₂). The pH value of the bulk fluid was measured using pH indicator paper (Macherey-Nagel, Duren, Germany): immediately after faecal slurry addition, as well as after 8 and 24 h incubation. All experiments were performed in triplicate. Mean values +/- standard deviations are reported.

2.4.3. Inoculation of Bacteroides and Bifidum bacteria in culture medium +/- DBS

The kill-time test was applied to evaluate the antimicrobial activity of the plasticizer DBS by determining the reduction of the bacterial (Bacteroides Vulgatus and Bifidobacterium) population in terms of the exposure time to the plasticizers.

0.38 mg of plasticizer were added to 10.0 mL of bacteria suspension (1×10^5 CFU mL⁻¹) and the tubes were incubated at 37 °C under anaerobic atmosphere. At predetermined time (0, 2, 6 and 24 h) 0.1 mL sample was collected and diluted to 10 mL of Cysteinated Ringer solution (CR). Successive 1/10 dilutions in (CR) were made up to 10⁻⁶ from the recovered bacterial suspension and 0.1 mL of each dilution was seeded onto Colombia Culture medium (CC). The plates are then incubated for 4 days at 37 °C. The number of viable bacteria (colony forming unit, CFU) was counted and expressed in Log CFU·mL⁻¹ using the following formula: Viable bacteria (Log CFU·mL⁻¹) = $\log(1 + n \cdot 0.1 \cdot d)$, 1 d where n represents the counted number of outgrown colonies and d represents the dilution.

2.4.4. Preparation of drug-loaded starter cores

5-aminosalicylic acid (5-ASA)-loaded starter cores were prepared by layering an aqueous drug-binder solution (18.2 % w/w 5-ASA, 0.9 % w/w HPMC) onto drug-free sucrose starter cores in a fluidized bed coater (Solidlab 1, Bosch, Schopfheim, Germany). The process parameters were as follows: inlet temperature = 50 °C, product temperature = 39 ± 2 °C, spray rate = 0.3 g/min, atomization pressure = 0.6 bar, air flow rate = 25 % (10 m³/h), batch size = 100 g, internal nozzle diameter = 0.8 mm, external nozzle diameter = 1.7 mm. The coating was performed until a drug loading of 6 % (w/w) was obtained.

2.4.5. Film coating of drug-loaded pellets

Three (3.0) g plasticizer (DBS) were dispersed in 40.0 g aqueous ethylcellulose dispersion (Aquacoat ECD). The formulation was stirred at room temperature for 24 h (magnetic stirrer, Heidolph, Schwabach, Germany).

A solution/dispersion of a second polysaccharide was prepared by dispersing 8.0 g of that compound in water, followed by stirring at room temperature for 3 h. The amount of water was adapted to the type of polysaccharide, assuring an appropriate viscosity of the liquid formulation for spraying: Twenty mL water were used in the case of Orafti Synergy 1, Orafti HSI, Orafti P95, Orafti HP, xylan from corn core, aloe vera extract powder, Novelose 240, Glucidex[®] 17 D, SweetPearl P300 DC, LAB 4118, Palatinose PST-N, Cleargum, rice starch, abelmoscus esculentus extract powder, Clearam and raffinose. Forty mL water were used in the case of reishi extract, goji berry extract powder and coix lacryma extract powder. Sixty mL water were used in the case of Starch 1500 and spray dried acacia gum.

The polysaccharide solution/dispersion was blended with the plasticized aqueous ethylcellulose dispersion. The final ratio of the 2nd polysaccharide: ethylcellulose (dry

masses) was 2:3 (w/w). The blends were stirred for 1 h prior to coating. The drug-loaded starter cores were coated in a fluidized bed coater (Solidlab 1). The process parameters were as follows: inlet temperature = 50 °C, product temperature = 39 ± 2 °C, spray rate = 0.3 g/min, atomization pressure = 0.6 bar, air flow rate = 25 % (10 m³/h), batch size = 70 g, internal nozzle diameter = 0.8 mm, external nozzle diameter = 1.7 mm. The weight gain was 20 % (w/w). After coating, the pellets were further fluidized for 10 min without spraying of liquid, and subsequently cured in an oven for 24 h at 60 °C.

2.4.6. Determination of the practical drug loading

Eighty mg pellets were manually ground for 5 min in a mortar with a pestle. The powder was dispersed in 50.0 mL deionized water, followed by stirring for 30 min at room temperature (magnetic stirrer, Heidolph, Schwabach, Germany). One (1.0) mL sample were withdrawn, filtered (0.2 µm) and their drug content determined by HPLC-UV analysis as follows: An UltiMate3000 HPLC apparatus (Thermo Fisher Scientific, Waltham, USA), equipped with a reversed-phase column [Gemini®, 5 µm C18, 150 x 4.6 mm (Phenomenex, Le Pecq, France)] was used. The mobile phase consisted of 10.0 % methanol and 90.0 % of an aqueous acetic acid solution (1.0 %). The flow rate was set to 1.0 mL/min, the column temperature to 25 °C. The drug was detected at 330 nm. All experiments were performed in triplicate. Mean values +/- standard deviations are reported.

2.4.7. *In vitro* drug release measurements

Eighty mg pellets were placed into 50 mL falcon tubes, filled with: (i) 42.5 mL culture medium inoculated with 2.5 mL faecal slurry (10⁶ CFU/mL bacteria) from inflammatory bowel disease patients, inflammatory bowel disease model (TNBS) rats or healthy dogs; or (ii) 45.0 mL culture medium free of faeces, for reasons of

comparison. The samples were incubated at 37 °C under horizontal agitation (80 rpm, mini orbital shaker; Stuart, Staffordshire, UK) and anaerobic conditions (5 % CO₂, 10 % H₂, 85 % N₂). At predetermined time points, 3.0 mL samples were withdrawn, congealed and stored at -25 °C until further analysis. The samples were de-congealed at room temperature during 2 h, followed by centrifugation at 15,000 rpm for 10 min (Hettich fixed angle rotor, Tuttlingen, Germany) and filtration (0.2 µm PTFE mesh filter; Agilent Captiva Econofilters, Santa Clara, USA). The drug content was determined by HPLC-UV analysis, as described in section 2.6.

The stability of 5-ASA in the different release media was evaluated as follows: Five mg drugs were dissolved in 50 mL culture medium free of faeces or culture medium inoculated with faecal slurries. At pre-determined time points, 1.5 mL samples were withdrawn, filtered (0.2 µm) and their drug content was determined by HPLC-UV analysis, as described in section 2.6.

All experiments were performed in triplicate. Mean values +/- standard deviations are reported.

2.4.8. Scanning electron microscopy

The morphology of drug layered started cores and polymer coated pellets was observed using a JEOL field emission SEM (JSM-7800F, Tokyo, Japan). Samples were fixed on the sample holder with a ribbon carbon double-sided adhesive and covered with a fine carbon layer.

2.5. Results and discussion

Novel colon targeting systems have been prepared based on polymers, which are degraded by bacterial enzymes, which are present in the colon of the patient, and which show similar performance upon exposure to faecal samples from rats, dogs and IBD patients.

Drug loaded cores are coated with innovative polymer blends. The film coatings minimize drug release in the upper gastrointestinal tract. Once the colon is reached, the bacterial enzymes present in rat, dog and IBD patient faeces degrade the film coatings, and drug release sets on.

2.5.1. Polysaccharide degradation in faecal samples from different species

To identify a suitable release rate triggering polysaccharide, a variety of polymeric candidates was exposed to culture medium inoculated with faecal samples from the different species. Bacterial proliferation was monitored via dynamic changes in the pH of the medium. Figures 9 and 10 show the pH values of culture medium inoculated with faecal samples from IBD patients, IBD rats and healthy dogs after 8 and 24 h. For reasons of comparison, also the pH values at $t = 0$ (right after the addition of the polysaccharide to the medium) are illustrated. If the polysaccharide serves as a substrate for the bacteria present in these samples, the latter proliferate, and in case their amount is high, the pH rapidly drops due to the generation of short chain fatty acids (175). Thus, steep pH drops can serve as an indication for substantial polysaccharide degradation. A suitable polysaccharide candidate for species-independent colon targeting should show steep pH drops in IBD rats, healthy dogs and IBD patients. As it can be seen, a variety of behaviours were observed, differing in the importance of the pH drop and degree of dependence on the species.

From a practical point of view, the capacity of the film coating to allow for colon targeting in IBD patients is most important. This is why the investigated polymers were divided into two groups: (i) Polysaccharides showing an important decrease in pH upon 24 h incubation with faecal slurries from IBD patients (the difference in pH “t = 0” versus “IBD patient 24 h” was equal or larger than 2 units). (ii) Polysaccharides showing a less pronounced difference (< 1.5 pH units) under these conditions. The first type of compounds is potentially promising for colon targeting (illustrated in Figure 9), the second type of polysaccharides exhibits a less promising potential (shown in Figure 10).

The order of the polysaccharides in Figure 9 and 10 corresponds to the importance of the decrease in pH (“t = 0” versus “IBD patients 24 h”). The first compounds show the highest pH drop and can be considered as the “most promising” polysaccharides in the light of these results. However, it has to be pointed out that the polymers exhibiting promising potential for colon targeting in IBD patients did not necessarily lead to steep and rapid decreases in the pH upon incubation with faecal slurries from IBD rats and/or healthy dogs (Figure 9). This can probably be attributed to the fact that in the colon of IBD patients, IBD rats and healthy dogs the types and amounts of bacteria secreting enzymes (which are able to degrade the polysaccharides) substantially differ. This can be expected to cause highly species-dependent colon targeting performance. For instance, a dosage form coated with a polymeric film containing a polysaccharide, which exhibits a steep pH drop in IBD patients, but not in healthy dogs, likely fails in the preclinical phase of product development, although it has an interesting potential to treat patients.

The polysaccharides shown in Figure 10 are “less promising candidates” in the light of the pH drops observed upon incubation with faecal slurries from IBD patients, IBD rats and healthy dogs in this study. The differences in pH at “t = 0” and after 24 h incubation with faeces from IBD patients are inferior to 1.5 units. Again, the order of the compounds in the figure corresponds to the importance of the difference in pH (highest differences are shown at the beginning). However, great caution must be paid in the case of polysaccharides, which acidify the culture medium themselves, for example pectin

from apple and citrus: In these cases, the pH is about 4 right from the beginning and none of the conditions shows a pH drop.

It is worth noting that certain polysaccharides (e.g., chitosan) showed a relatively pronounced decrease in pH of the culture medium after inoculation with faecal samples from healthy dogs. Thus, film coatings based on these compounds might allow for colon targeting in these animals. However, the pH drop was not very pronounced upon incubation with faecal samples from IBD patients. Consequently, the systems might show promising results in the preclinical phase, but fail in subsequent clinical trials.

Due to the less promising results obtained with the polysaccharides shown in Figure 10 in terms of potential clinical performance, they were not further investigated in this study. Instead, the more promising compounds shown in Figure 9 were used to coat 5-ASA-loaded starter cores and the resulting drug release kinetics were measured in culture medium inoculated with faecal samples from IBD rats, healthy dogs and IBD patients.

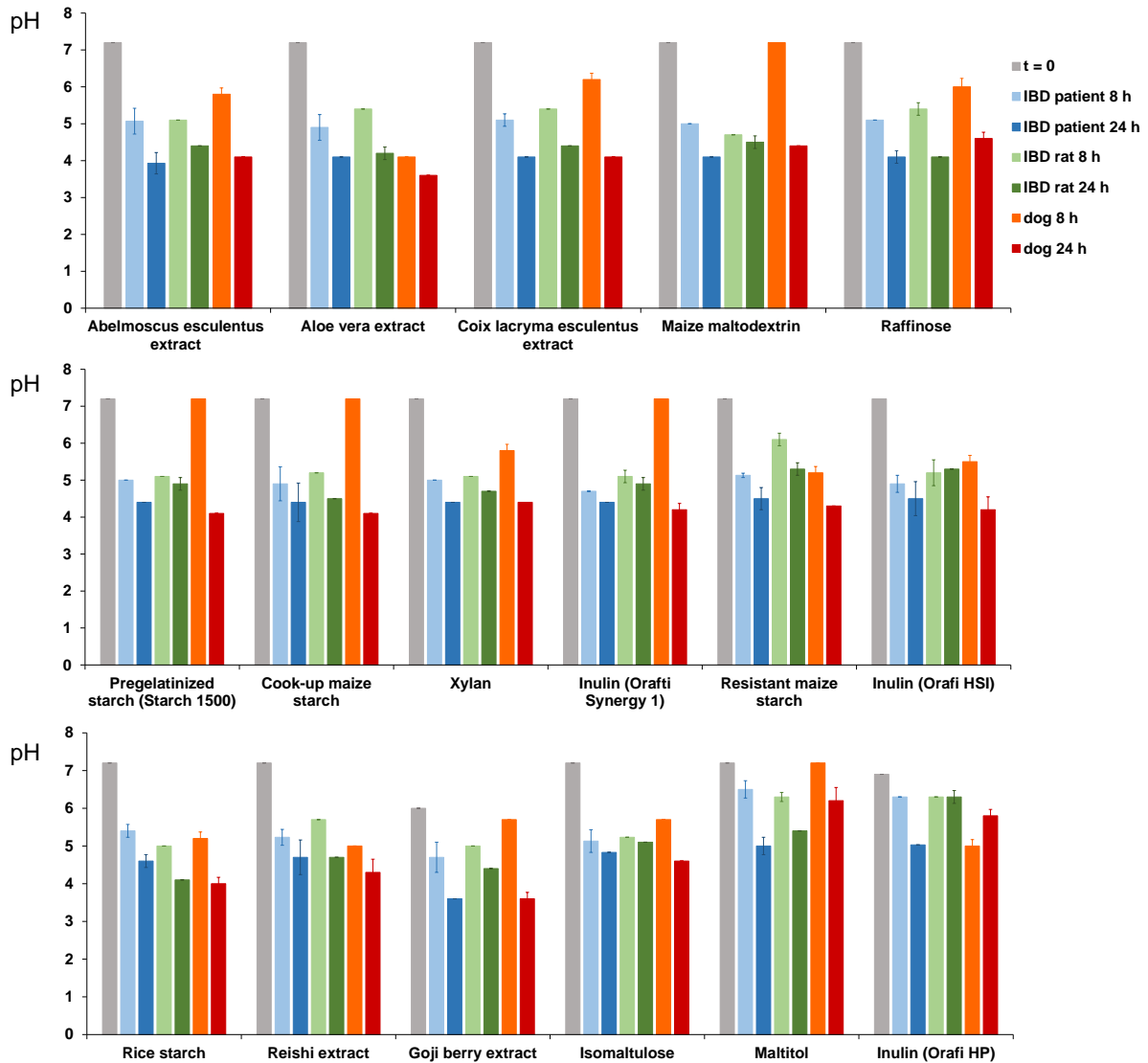


Figure 9 pH values of different polysaccharide solutions/dispersions, inoculated with faecal slurries from inflammatory bowel disease patients (IBD patient), inflammatory bowel disease model rats (IBD rat) or healthy dogs (dog) for 8 or 24 h (as indicated). For reasons of comparison, also the pH values at time $t = 0$ are indicated. Differences in the pH between “ $t = 0$ ” and “IBD patient 24 h” are important (≥ 2 units).

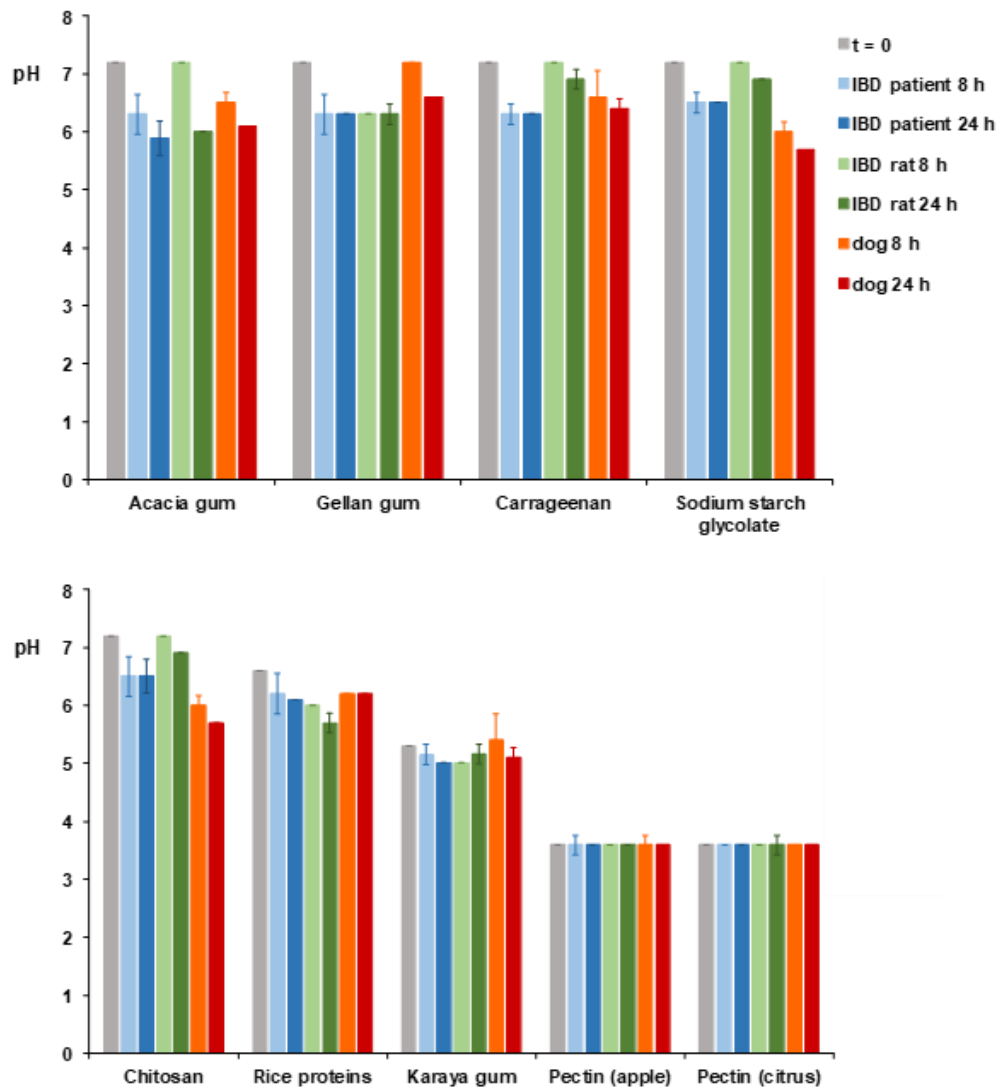


Figure 10 pH values of different polysaccharide solutions/dispersions, inoculated with faecal slurries from inflammatory bowel disease patients (IBD patient), inflammatory bowel disease model rats (IBD rat) or healthy dogs (dog) for 8 or 24 h (as indicated). For reasons of comparison, also the pH values at time $t = 0$ are indicated. Differences in the pH between “ $t = 0$ ” and “IBD patient 24 h” are not very pronounced (< 1.5 units).

2.5.2. Species-dependent drug release from coated pellets

5-ASA-loaded starter cores were prepared by layering an aqueous drug-binder (hydroxypropyl methylcellulose) solution onto sucrose starter cores in a fluidized bed (6 % drug loading). These starter cores were coated with 20 % of a blend of “colon targeting polysaccharide”: ethylcellulose (2:3, w/w, based on dry polymer masses). The ethylcellulose trapped the “colon targeting polysaccharide” to limit premature swelling and/or dissolution of the film coating in the upper gastrointestinal tract. An aqueous ethylcellulose dispersion was used for this purpose. Thus, a plasticizer was added to facilitate polymer particle coalescence: dibutyl sebacate (DBS). It has to be pointed out that certain plasticizers have been reported to inhibit specific bacterial enzymes (176–178). Thus, it was important to evaluate the potential impact of the presence of this plasticizer on the growth of the bacteria in faecal samples from IBD patients. Figure 11 shows the growth of *Bacteroides* and *Bifidus* species in culture medium in the presence and absence of 38 mg/L DBS (dashed and solid curves, respectively). As it can be seen, no inhibitory effect of DBS was observed on the growth of these bacteria under these conditions. Thus, the capacity to allow for colon targeting in IBD patients using the investigated polymeric film coatings is probably not affected by the presence of this plasticizer.

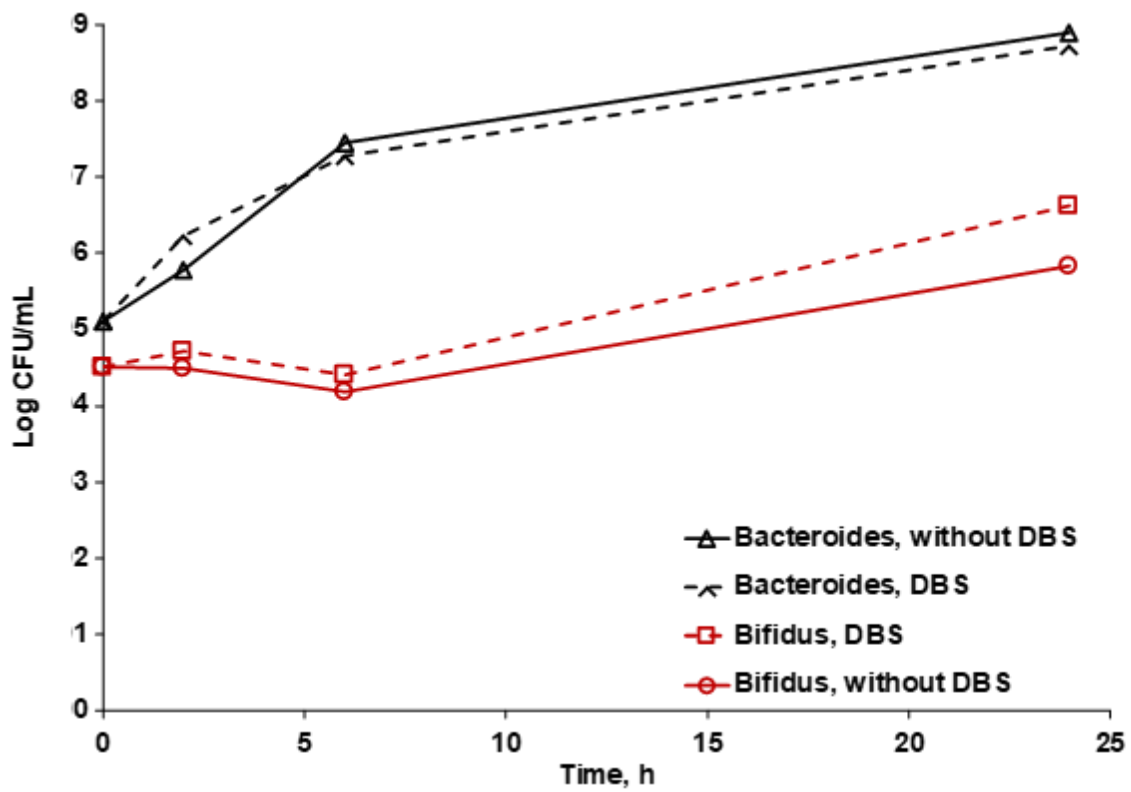


Figure 11 Growth of Bacteroides and Bifidus bacteria in culture medium in the presence or absence of the plasticizer DBS.

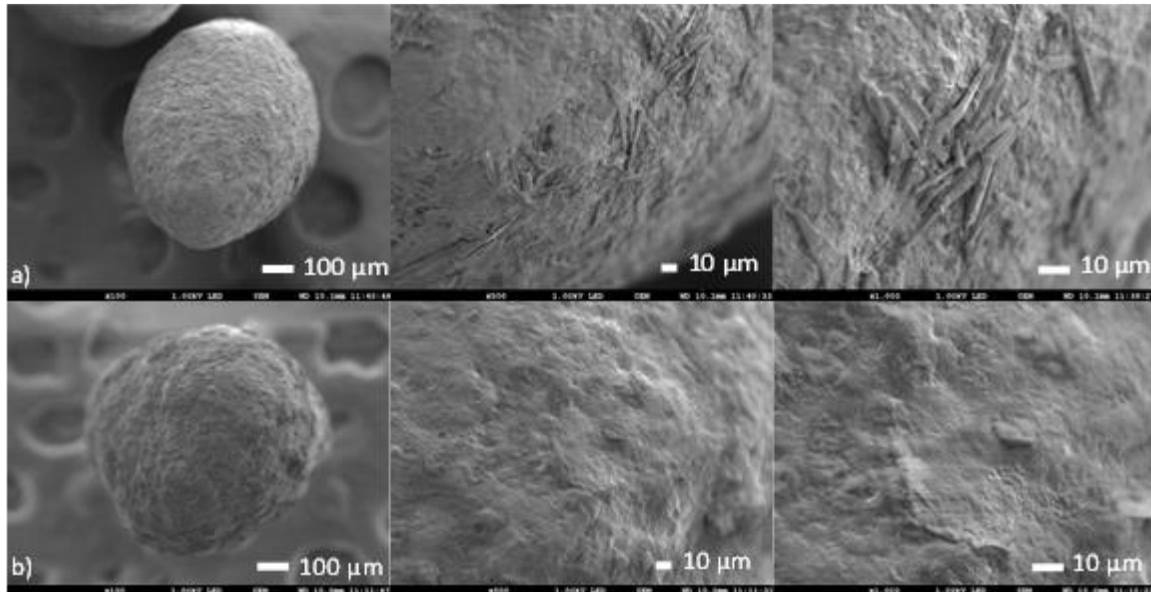


Figure 12 SEM pictures of: a) 5-ASA-loaded starter cores, and b) pellets coated with a 2:3 xylan:ethylcellulose blend (20 % coating level).

Figure 12 shows examples of SEM pictures of surfaces of 5-ASA loaded starter cores and xylan: ethylcellulose coated beads (20 % coating level), respectively. As it can be seen, the drug-binder as well as the polysaccharide: ethylcellulose layers completely cover the surfaces of the spheres and have a homogeneous appearance. At higher magnification, needle-shaped 5-ASA crystals are visible in the case of the drug-layered starter cores, but not in the case of the xylan:ethylcellulose coated beads. This can serve as an indication for the fact that the drug layer is fully surrounded by the outer “colon targeting layer”.

Drug release from the polymer-coated beads was measured in culture medium inoculated with faecal samples from IBD rats, healthy dogs and IBD patients under anaerobic conditions. For reasons of comparison, 5-ASA release was also monitored in pure culture medium. Importantly, the drug was stable during the observation period in all types of media, irrespective of the presence or absence of faecal slurries: Not more than 5 % 5-ASA was degraded after 48 h (at 0.1 mg/mL). Thus, the enzymes present in the faecal samples do not chemically attack the drug to an important extent.

The green and blue curves in Figure 13 show the observed 5-ASA release kinetics from pellets coated with different polysaccharide: ethylcellulose blends in culture medium inoculated with faecal samples from IBD rats, healthy dogs and IBD patients. The black curves illustrate drug release in the absence of faecal slurries. A promising colon targeting system should show clear differences in the release rates in the presence versus absence of faecal samples: The presence of the colonic bacteria should trigger film coating degradation and result in faster drug release. Hence, promising film coating candidates show important differences between the colored and the black curves. The black curves should show limited 5-ASA release during the observation period. As it can be seen in Figure 13, this is the case for all formulations. Unfortunately, several film coatings do not show very pronounced differences in the release rates in the presence of faecal slurries. For example, in the case of *Abelmoschus esculentus* extract even after 24 h, the difference of drug release in the presence versus absence of faecal samples from IBD patients, IBD rats and healthy dogs was less than 30 %. Please note that this polysaccharide showed the most promising results with respect to the steepness in the pH drop upon incubation of the pure compound in culture medium with or without faecal slurries (Figure 9). The structure of the polymeric film coating (containing also water-insoluble ethylcellulose) might at least in part explain this observation: Eventually, the enzymes cannot freely attack the polysaccharide in the film coating, because it is too effectively trapped in the ethylcellulose matrix. The inner film coating structure depends on a variety of parameters, including the miscibility of the two polymers and their behavior during film formation (e.g., precipitation rate of dissolved polymer chains and phase separation).

Furthermore, ideal film coatings allowing for colon targeting should be species-independent and exhibit similar drug release kinetics upon incubation in culture medium containing faecal samples from IBD rats, healthy dogs and IBD patients. As it can be seen in Figure 13, this was not the case for the illustrated polysaccharide: ethylcellulose blends. In certain cases, drug release was much faster in the presence of faeces from IBD rats compared to IBD patients (e.g., isomaltulose and rice starch). In many cases, drug release was slower in the presence of faecal samples from healthy dogs compared to faecal samples from IBD rats or IBD patients (e.g., raffinose, xylan, resistant maize starch). This is consistent with the observation that the pH drop upon incubation of several pure polysaccharides with faecal slurries from healthy dogs was limited after 8 h compared to the other species (Figure 9). So, it seems that the colon of a dog does not contain the same types and amounts of enzymes needed to rapidly degrade these compounds.

Thus, film coatings based on these polysaccharides: ethylcellulose blends might lead to erroneous decisions during the preclinical development phase of novel colon targeting products, or show only limited colon targeting potential in IBD patients.

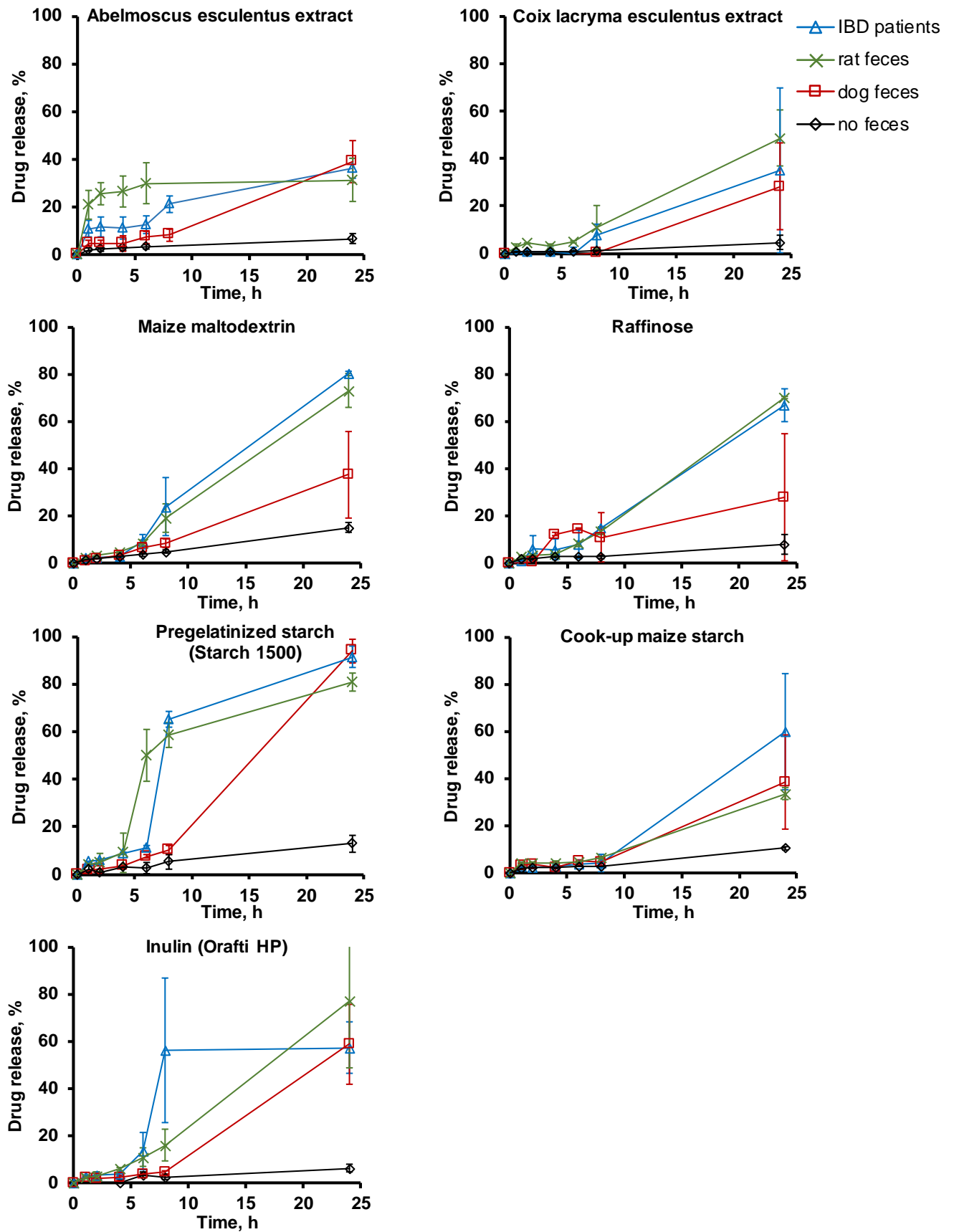


Figure 13 5-ASA release from pellets coated with different types of polysaccharides: ethylcellulose blends (2:3 w/w blend ratio; 20 % coating level) in culture medium

inoculated with faecal samples from IBD patients, IBD rats or dogs (as indicated). For reasons of comparison, also drug release in pure culture medium is illustrated.

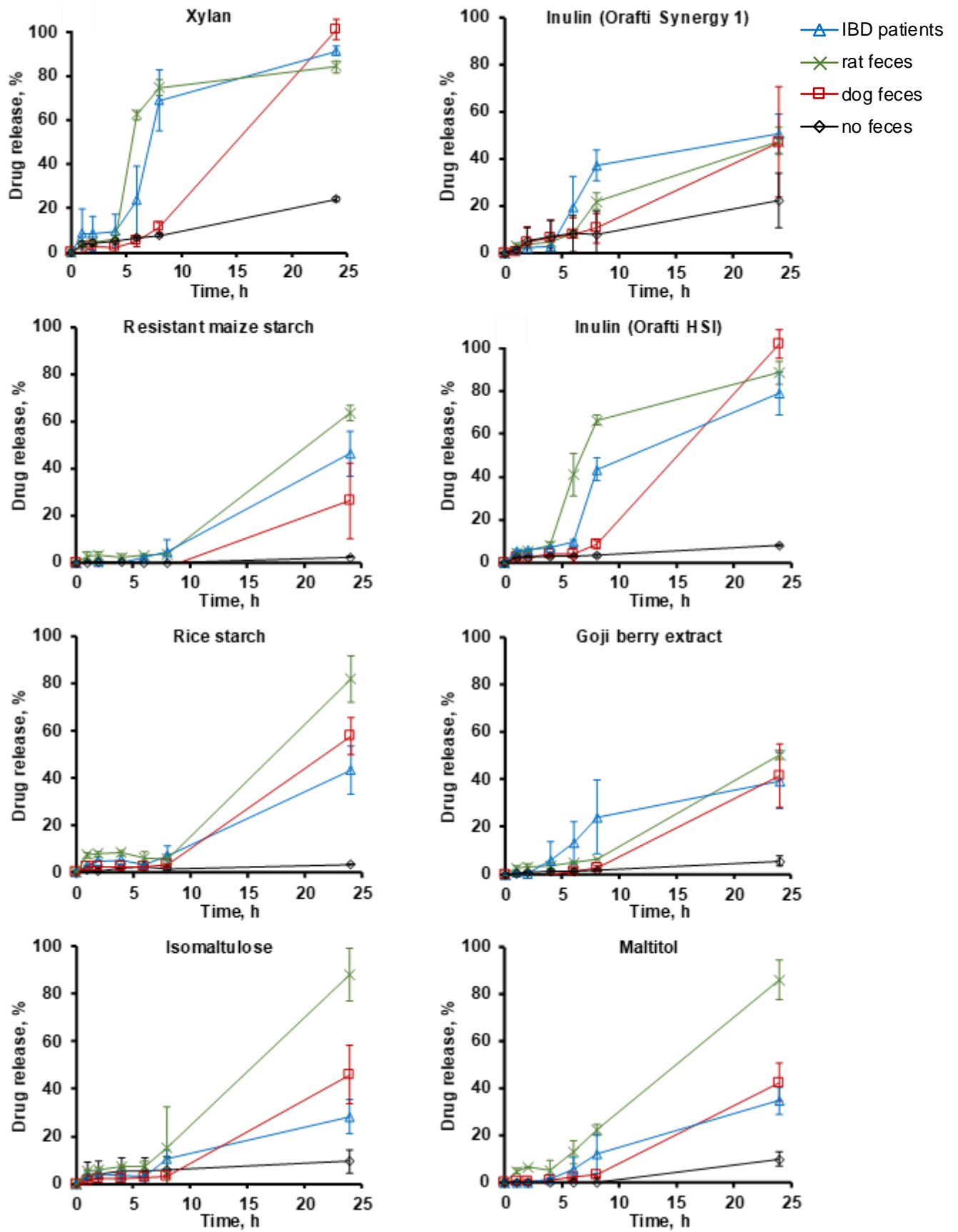


Figure 13 (continue)

2.5.3. Species-independent colon targeting

Interestingly, two of the investigated film coatings showed a highly promising potential to allow for colon targeting in IBD patients and exhibit only limited species dependence: Figure 14 illustrate the release of 5-ASA from pellets coated with aloe vera extract: ethylcellulose (2:3 w/w) and reishi extract: ethylcellulose (2:3 w/w) blends (20 % coating level in both cases). Again, the green, red and blue curves show drug release in the presence of faecal samples from IBD rats, healthy dogs and IBD patients, while the black curves illustrate 5-ASA release in culture medium free of faeces. Reishi extract is obtained from the fruiting body of a mushroom: *Ganoderma lucidum*, Ganodermataceae. Clearly, for both types of extracts (aloe vera and reishi) drug release was much faster in the presence of faecal slurries compared to pure culture medium. Thus, these film coatings offer an interesting potential to allow for colon targeting. Importantly, the observed release kinetics were rather similar for all types of investigated faecal samples: from IBD rats, healthy dogs and IBD patients. Thus, results observed in the preclinical development phase of a new drug product aiming at colon targeting are likely predictive for the performance of the system in subsequent clinical trials, in terms of drug release. This is very important from a practical point of view, to minimize the risk of erroneous decisions at this early stage of product development. In addition, these film coatings also offer an interesting potential to allow for colon targeting in dogs as advanced veterinary medicines. The reason for the promising performance of these film coatings is probably the fact that the enzymes, which are required to degrade the compounds in aloe vera extract and reishi extract, are present in sufficient quantities in the colon of IBD rats, healthy dogs and IBD patients.

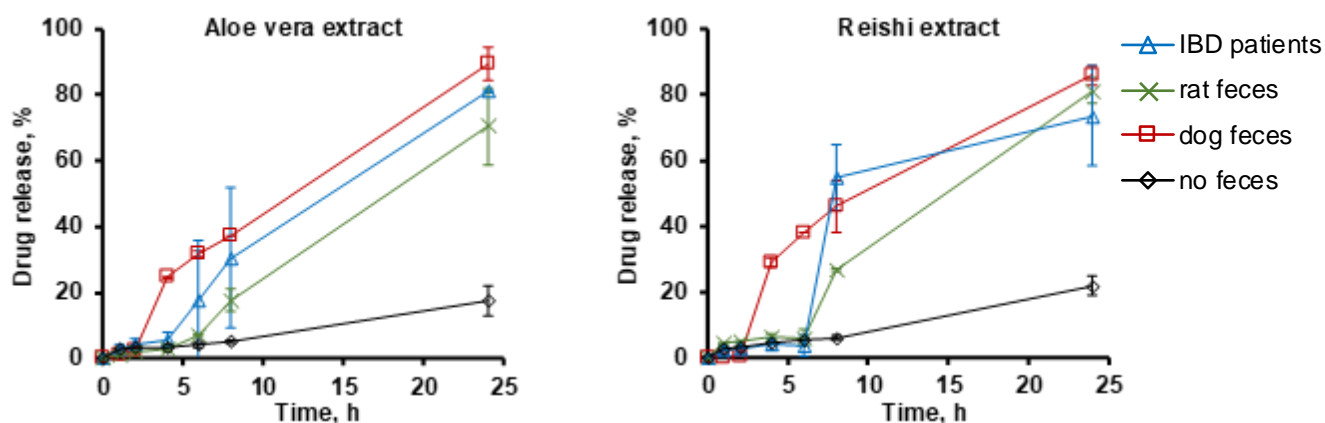


Figure 14 5-ASA release from pellets coated with aloe vera extract: ethylcellulose blends or reishi extract: ethylcellulose blends (2:3 w/w blend ratio; 20 % coating level) in culture medium inoculated with faecal samples from IBD patients, IBD rats or dogs (as indicated). For reasons of comparison, also drug release in pure culture medium is illustrated.

2.6. Conclusions

Great caution must be paid when studying the performance of bacteria-sensitive film coatings aiming at colonic drug delivery in animals in order to predict their performance in human patients. The types and amounts of bacteria substantially differ between species and erroneous conclusions during the preclinical development phase can easily be made. Interestingly, film coatings containing aloe vera extract or reishi extract show a promising potential for colon targeting in IBD patients and exhibit similar release patterns in IBD rats and healthy dogs.

3. Chapter: The SHIME[®] semi-dynamic gastrointestinal release model for colon-targeting drug delivery systems.

The *in vitro* measurements reported in this chapter were performed by ProDigest B.V. (Technologiepark-Zwijnaarde 73, 9052 Gent, Belgium).

3.1. Overview

3.1.1. The SHIME[®] (Simulator of the Human Intestinal Microbial Ecosystem).

The SHIME[®] semi-dynamic gastrointestinal release model is a fully automated computer-controlled system allowing to test 3 conditions in biological triplicate per experimental run (Figure 15). Each bioreactor consists of a double jacket custom-made (ProDigest B.V.) glass reactor that allows the control of the temperature of the bioreactor through a circulating water bath. Each reactor is sealed at the top with a custom-made lid (ProDigest B.V.) harbouring multiple passage ways for inserting a pH electrode, tubing for active pH control, and sampling ports. The sampling ports are surrounded at the bottom by a mesh that prevents the removal of pellets from the bioreactor during sampling of the aqueous phase. Anaerobic conditions can be maintained by active flushing of the vessels with nitrogen. The pH of the bioreactors is actively controlled by the software at a dedicated setpoint by the addition of 2 M NaOH and 0.5 M HCl. All automated pump actions are controlled by the software and executed with peristaltic precision pumps. Each vessel is put on top of a magnetic stirrer that drives a stirrer bar inside the vessel. In each bioreactor, the transit of oral dosage forms through the complete gastrointestinal tract is studied by sequentially simulating the passage through the stomach, small intestine, and colon (Figure 15).



Figure 15 Fully automated computer-controlled semi-dynamic SHIME[®] model for colon-targeted drug delivery system testing. The system harbors nine separated bioreactors allowing to test 3 different conditions in biological triplicate at once. In each bioreactor the passage of the colon-targeted drug delivery system through the complete gastrointestinal tract is simulated by the sequential simulation of the stomach, small intestinal, and colonic phase.

3.2. Materials and methods

3.2.1. Materials

The study performed on film coated 5-ASA-loaded pellets presented in Chapter 2 (Figures 13 and 14), lead to the selection of six formulations, considered the most promising of the research project. The formulations were tested *in vitro* using the SHIME[®] model. Each of the formulations had a specific drug loading. Based on this drug loading a pre-determined amount of pellets was added to the bioreactors to end up

with a final dose of 1500 mg mesalazine, corresponding to the drug loading presents in commercial products (Table 1).

Table 1 Coating composition, drug loading, and added dose of pellets of the six different formulations tested.

Formulation	Coating composition (6:4)	Coating level (%)	Drug loading (%)	Dose (g)
A	Ethylcellulose: Aloe vera extract	45	15.5	9.7
B	Ethylcellulose: Pregelatinized starch (Starch 1500)	45	17	8.8
C	Ethylcellulose: Reishi extract	45	15.5	9.7
D	Ethylcellulose: Maize maltodextrin	45	15.5	9.7
E	Ethylcellulose: Xylan	45	15.5	9.7
F	Ethylcellulose: Inulin (Orafti HSI)	45	15.5	9.7

Pepsin, NaCl, K₂HPO₄, KH₂PO₄, NaHCO₃ and MgSO₄.7H₂O (ChemLab, Zedelgem, Belgium); yeast extract and pepton (Oxoid, Basingstoke, GB); starch (Sourby, Roeselare, Belgium); phosphatidylcholine (Carl Roth GmbH + Co. KG, Karlsruhe, Germany); oxgall (Becton-Dickinson (BD), Erembodegem, Belgium); pancreatin, L-Cystein HCl, Tween 80, ZnSO₄.7H₂O, FeSO₄.7H₂O, Menadione stock solution and Hemin stock solution (Merck Life Science, Hoeilaart, Belgium); MeOH, CaCl₂.2H₂O and MnCl₂.4H₂O (VWR, Leuven, Belgium)

3.2.2. Preparation of drug-loaded starter cores

5-aminosalicylic acid (5-ASA)-loaded starter cores were prepared by layering an aqueous drug-binder solution (18.2 % w/w 5-ASA, 0.9 % w/w HPMC) onto drug-free sucrose starter cores in a fluidized bed coater (Solidlab 1, Bosch, Schopfheim, Germany). The process parameters were as follows: inlet temperature = 50 °C, product temperature = 39 ± 2 °C, spray rate = 0.3 g/min, atomization pressure = 0.6 bar, air flow

rate = 25 % (10 m³/h), batch size = 500 g, internal nozzle diameter = 0.8 mm, external nozzle diameter = 1.7 mm. The coating was performed until a drug loading of 15% (w/w) was obtained.

3.2.3. *In vitro* drug release measurements

Twenty-five mg pellets were placed into 50 mL falcon tubes, filled with: (i) 33.5 mL HCl (pH=1.2) to simulate the stomach. After 1 h, 11.5 mL of 0.20 M solution of trisodium phosphate dodecahydrate were added to simulate the small intestine (pH=6.8) during 4 h, then the formulations were transferred in 45 mL of culture medium inoculated with 2.5 mL faecal slurry (106 CFU/mL bacteria) from inflammatory bowel disease patients; or (ii) 45.0 mL culture medium free of faeces, for reasons of comparison. The samples were incubated at 37 °C under horizontal agitation (80 rpm, mini orbital shaker; Stuart, Staffordshire, UK) and anaerobic conditions (5 % CO₂, 10 % H₂, 85 % N₂). At predetermined time points, 3.0 mL samples were withdrawn, congealed and stored at -25 °C until further analysis. The samples were stocked, de-congealed and analysed as reported in Chapter 2.

All experiments were performed in triplicate. Mean values +/- standard deviations are reported.

3.2.4. Film coating of drug-loaded pellets

The drug-loaded pellets were coated with a blend of ethylcellulose: polysaccharide as reported in Chapter 2. The weight gain was 45 % (w/w). After coating, the pellets were further fluidized for 10 min without spraying of liquid, and subsequently cured in an oven for 24 h at 60 °C.

3.2.5. *In vitro* drug release in SHIME[®] model

At the start of the experiment 55 mL of simulated gastric juice were added to the reactors together with 250 mL of water simulating the ingestion of a dose under fasted state conditions. A pre-determined amount of pellets was added to the reactor to end up with a final dose of 1500 mg mesalazine. The stomach phase lasted for 45 min. Throughout the stomach phase the pH of the vessel was automatically controlled at 1.6 (pH interval 1.45-1.65). At the end of the stomach phase all liquid was removed from the bioreactor and 53.3 mL of simulated duodenal juice was added to the system. The pH of the duodenum was kept at a value of 6.5. After 20 min, 46.7 mL of simulated jejunal juice was added to the reactor. Under IBD conditions the jejunal pH linearly increased from a value of 6.5 to a value of 6.9 over a period of 2h. After 140 min of small intestinal incubation 46.7 mL of jejunal juice was removed from the system and 146.7 mL of ileum juice was added to the reactor. The pH was kept constant at 6.9 (pH interval 6.6-6.9) throughout the 100 min of ileal incubation. In total the small intestinal transit time under IBD conditions was 240 min. The bioreactors were maintained anaerobic through flushing with nitrogen and the temperature was controlled at 37°C. The content of the bioreactors was mixed through stirring at 450 rpm. Samples for determination of the amount of released mesalazine by UHPLC-PDA were taken at dedicated time points namely at the end of the stomach phase, at the start of the ileal phase, and at the end of the ileal phase.

At the end of the ileal incubation phase the colonic phase was initiated by adding 332 mL of simulated colonic medium to the reactors together with 28 mL of resuspended faecal inoculum. For the simulation of IBD conditions three separate faecal samples obtained from three IBD donors were used as a source of inoculum. The initial pH of the colon was at a low value of 5.0 (pH interval 4.9-5.1) for the first 7h of the colonic phase simulating the transit of the dosage form through the proximal colon. In between 7h and 9h of colonic incubation the pH increased till a value of 6.3 (pH interval 6.2-6.45) and was maintained for 4 hours simulating the passage through the transversal colon. Finally, the pH linearly increased till 6.8 (pH interval 6.7-6.9) in between 13h and 14h of colonic incubation and was maintained constant till the end of the colonic phase (24h). This pH profile was implemented to simulate the transfer of a dosage form through the colon of people suffering from IBD. The bioreactors were maintained

anaerobic through flushing with nitrogen and the temperature was controlled at 37°C. The content of the bioreactors was mixed through stirring at 450 rpm. Samples were taken at the start (0h) and after 1h, 3h, 16h, and 24h of colonic incubation for the quantification of the amount of mesalazine released during colonic transfer. Furthermore, concentrations of short-chain fatty acids (SCFA), lactate, branched short-chain fatty acids (B-SCFA) and ammonium were determined to study the impact of the different formulations on the colonic microbiota activity of the different IBD donor faecal samples. At the end of the colonic incubations the remaining undissolved pellets were harvested from the bioreactors in order to quantify the fraction of mesalazine that was not released throughout the complete gastrointestinal transfer.

3.2.6. Analytical quantification

Determination of SCFA concentrations, including acetate, propionate, butyrate and branched chain fatty acids (bcFA; sum of isobutyrate, isovalerate and isocaproate) was executed as previously described by De Weirdt et al..(179) Lactate levels were determined using a commercially available enzymatic assay kit (R-Biopharm, Darmstadt, Germany) according to manufacturer's instructions and measured on an iCubio iMagic-M9 (Shenzhen iCubio Biomedical Technology Co. Ltd., Shenzhen, China). Ammonium analysis was run on an AQ300 Discrete Analyzer (Seal-Analytical, Rijen, The Netherlands) using the indophenol blue spectrophotometric method according to manufacturer's instructions.

3.3. Results and discussion

The preliminary study performed on drug-layered coated pellets reported in Chapter 2 allowed the selection of 6 polymers considered the most promising candidates for a functional coating aiming colon targeting.

The screening phase was performed on pellets coated with 20 % weight gain coating. The following study focused on the optimization of the coating characteristics as well as the increasing of the drug loading. For this reason, smaller starter cores (250 – 355 μm) were coated with a higher amount of drug (20 %) and a thicker functional coating (45 % coating level).

The formulations were tested *in vitro*, simulating the different sections of the GIT. The dissolution study was performed in a 50 mL falcon changing the release media during time, in order to simulate consequently: stomach, small intestine and colon. The coated pellets were exposed for 1 h to pH =1.2 and once a 3 mL sample was taken, the release medium was carefully replaced with PB pH=6.8 with the help of a syringe. After 4 h exposure to pH=6.8 the release medium was replaced with culture medium inoculated with faeces from IBD patients. For comparison, the test was also performed in a culture medium free of faeces. Figure 16 shows the release profiles of mesalazine from formulations coated with a blend of alternatively aloe vera or reishi extract and ethylcellulose. In both cases the coating prevents the release in the acidic environment. Aloe vera coating is able to prevent the release in the simulated small intestine and a burst effect is observed after one 1 h exposure to the simulated colonic environment in the presence of bacteria. In the control medium (free of bacteria) the drug release is moderated and only after 8 h exposure to the medium most of the drug is released (Figure 16 A). The formulation coated with the blend of reishi extract and ethylcellulose is able to prevent the drug release at pH=1.2 but showed a similar release behaviour in the absence and presence of colonic bacteria, with important standard deviation in the latest case (Figure 16 B).

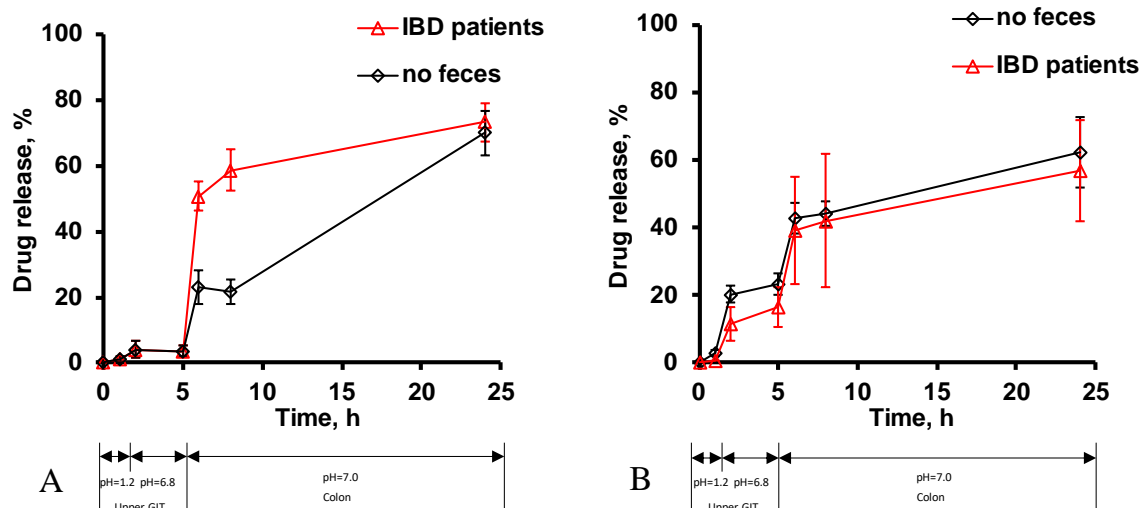


Figure 16 5-ASA release from pellets coated with aloe vera extract: ethylcellulose blends (A) or reishi extract: ethylcellulose blends (B) (2:3 w/w blend ratio; 45 % coating level) in HCl (pH=1.2) for 1 h, followed by PB (pH=6.8) for 4 h followed by culture medium inoculated with faecal samples from IBD patients up to 24 h. For reasons of comparison, also drug release in pure culture medium is illustrated.

3.3.1. Mesalazine release by the six formulations after exposure to the faeces of IBD donor A

During the semi-dynamic SHIME[®] experiments using the faecal inoculum of IBD donor A all formulations started to release mesalazine during passage of the pellets through the upper gastrointestinal tract. Whereas the release of mesalazine from the six different formulations was similar at the end of the stomach incubation phase, differences in release characteristics started to appear during passage of the formulations through the small intestine. Indeed, formulations B (pregelatinized starch (starch 1500)), E (xylan), and F (inulin (Orafti HSI)) demonstrated a high release of mesalazine at the start of the ileal incubation phase which continued towards the end of the ileal incubation phase releasing $53 \pm 3 \%$, $61 \pm 20 \%$, and $64 \pm 2 \%$ of the total released mesalazine throughout the upper gastrointestinal tract, respectively (Figure 17).

the undissolved pellets at the end of the colonic incubation phase (A). Normalized time-course analysis of released mesalazine (average amount \pm stdev; n = 3) upon transfer of the six mesalazine-loaded pellet formulations through the complete gastrointestinal tract (B). Results are representative for the experiments performed with the faecal sample of IBD donor A. The red line represents the added dose of mesalazine.

On the contrary, formulations A (Aloe Vera), C (Reishi extract), and D (maize maltodextrin) resulted in a more moderate release of mesalazine during passage of the pellets through the small intestine thereby only releasing 27 ± 2 %, 31 ± 2 %, and 39 ± 22 % of the total released mesalazine, respectively (Figure 17). During the colonic incubation phase a different release mechanism was observed. In general, all six formulations did not release a substantial amount of mesalazine during the initial 3h of colonic incubation. In between 3h and 16h of colonic incubation an increase in the amount of released mesalazine was observed for all formulations and this presumably due to the activity of the colonic microbiota which degraded the polysaccharide constituent of the coating of the formulations. Due to the prior release from the formulations during passage through the upper gastrointestinal tract differences were observed in mesalazine release during passage through the colon. Formulations B (pregelatinized starch), E (xylan), and F (inulin) resulted in the lowest amounts of mesalazine released during transfer through the colon with 33 ± 9 %, 34 ± 22 %, and 23 ± 3 % of total mesalazine released, respectively. This was due to the fact that these formulations already released a substantial amount of mesalazine during passage through the small intestine. Whereas formulations A (Aloe Vera), C (Reishi extract), and D (maize maltodextrin), resulted in a small release of mesalazine during passage through the small intestine, the degradation of the polysaccharide portion of the coating by the colonic microbiota of IBD donor A resulted in a substantial release of mesalazine after 24h of colonic incubation with 54 ± 9 %, 54 ± 9 %, and 34 ± 23 % of the total fraction released, respectively. Formulation D (maize maltodextrin) resulted in the lowest total release after passage through the complete gastrointestinal tract (Figure 17).

Overall formulation A (Aloe Vera) resulted in the highest release of mesalazine during passage through the colon.

3.3.2. Mesalazine release by the six formulations after exposure to the faeces of IBD donor B

During the experiments using the faecal inoculum of IBD donor B similar mesalazine release characteristics were observed for the different formulations as compared to those observed during the experiments with the faecal inoculum of IBD donor A. Formulations B (pregelatinized starch), E (xylan), and F (inulin) demonstrated a comparable and high release of mesalazine at the start of the ileal incubation phase which continued towards the end of the ileal incubation phase resulting in $60 \pm 15 \%$, $61 \pm 17 \%$, and $59 \pm 18 \%$ of the total amount of mesalazine released throughout the complete experiment, respectively. Mesalazine release from formulation C (Reishi extract) was lower ($56 \pm 12 \%$ of total amount released) as these formulations but higher as compared to formulations A (Aloe Vera) and D (Maize maltodextrin) which only released minor amounts of mesalazine during passage through the upper gastrointestinal tract, namely $37 \pm 6 \%$ and $35 \pm 19 \%$ of total fraction released throughout the experiment (Figure 18). Upon entering the colon, all six formulations did not release any substantial amounts of mesalazine during the initial 3h of incubation. However, after 16h of colonic incubation the degradation of the polysaccharide fraction of the coating by the colonic microbiota resulted in an additional release of mesalazine by all formulations. The highest colonic release of mesalazine was observed for formulations A (Aloe Vera) and D (Maize maltodextrin) with $54 \pm 7 \%$ and $34 \pm 22 \%$ of the total fraction released during this period. Comparison of both formulations revealed that lower amounts of mesalazine were release from formulation D (maize maltodextrin) as compared to formulation A (Aloe Vera) during passage through the colon thereby demonstrating the superior colon-targeting release characteristics of this formulation (Figure 18).

the undissolved pellets at the end of the colonic incubation phase (A). Normalized time-course analysis of released mesalazine (average amount \pm stdev; n = 3) upon transfer of the six mesalazine-loaded pellet formulations through the complete gastrointestinal tract (B). Results are representative for the experiments performed with the faecal sample of IBD donor B. The red line represents the added dose of mesalazine.

3.3.3. Mesalazine release by the six formulations after exposure to the faeces of IBD donor C

During the experiments using the faecal inoculum of IBD donor C, formulation B (pregelatinized starch) resulted in the highest release of mesalazine (67 ± 15 % of total fraction released throughout the experiment) during passage through the upper gastrointestinal tract. Formulations C (Reishi extract), E (xylan), and F (inulin) resulted in high and similar amounts of released mesalazine during passage through the upper gastrointestinal tract with 52 ± 7 %, 44 ± 15 %, and 47 ± 14 % of total fraction released, respectively (Figure 4). As was observed during the experiments with faecal inoculum of IBD donor A and B, formulations A (Aloe Vera) and D (maize maltodextrin) resulted in a low release of mesalazine in the upper gastrointestinal tract with only 33 ± 2 % and 19 ± 8 % of the total mesalazine fraction released throughout this experimental phase. As was observed during the previous experiments none of the six formulations released any substantial amounts of mesalazine during the initial 3h of the colonic incubation (Figure 19). Degradation of the polysaccharide portion of the coating by the colonic microbiota resulted in a further release of mesalazine after 16h of colonic incubation.

Considering the fact that both formulations B (partially pregelatinized starch), C (Reishi extract), E (xylan), and F (inulin) already released a great portion of its mesalazine drug load during passage through the upper gastrointestinal tract only moderate amounts of mesalazine were released upon passage of these formulations through the colon. On the contrary, formulations A (Aloe Vera) and D (maize maltodextrin) released the major portion of its drug load during passage through the colon, namely 53 ± 2 % and 38 ± 19 %

%, thereby implicating the necessity of the microbial trigger for the release of mesalazine. As was observed during the previous experiments formulation A (Aloe Vera) gave a near complete release of mesalazine during passage through the colon whereas microbial degradation of formulation D (maize maltodextrin) was incomplete resulting in the release of the lowest overall total amounts of mesalazine during the complete passage of the gastrointestinal tract. As such, these data indicated that formulation A (Aloe Vera) had promising colon-targeting release characteristics which were superior as compared to the other formulations tested (Figure 19).

course analysis of released mesalazine (average amount \pm stdev; $n = 3$) upon transfer of the six mesalazine-loaded pellet formulations through the complete gastrointestinal tract (B). Results are representative for the experiments performed with the faecal sample of IBD donor C. The red line represents the added dose of mesalazine.

3.3.4. Impact of the formulations on the metabolic activity of the colonic microbiota

Quantification of the concentration of acetate revealed that inter-individual differences existed in between the colonic microbiota activity of the three IBD donors. The highest concentration of acetate was produced by the colonic microbiota of donor A whereas the colonic microbiota of IBD donor B and C produced lower concentrations (Figure 20). Time-course analyses of acetate production clearly demonstrated that acetate was not produced during the initial 3h of colonic incubation, namely the colonic phase during which no substantial colonic release of mesalazine occurred. The highest production of acetate occurred in between 3h and 16h of colonic incubation (Figure 20). Hence, this demonstrated that the colonic microbiota was metabolically active during this period which could explain the efficient degradation of the polysaccharides contained in the coating and the associated increased release of mesalazine by the different formulations during this period of colonic incubation. All six formulations resulted in similar concentrations of acetate produced thereby indicating that none of the polysaccharides more selectively stimulated acetate-producing bacteria as compared to the other formulations (Figure 20).

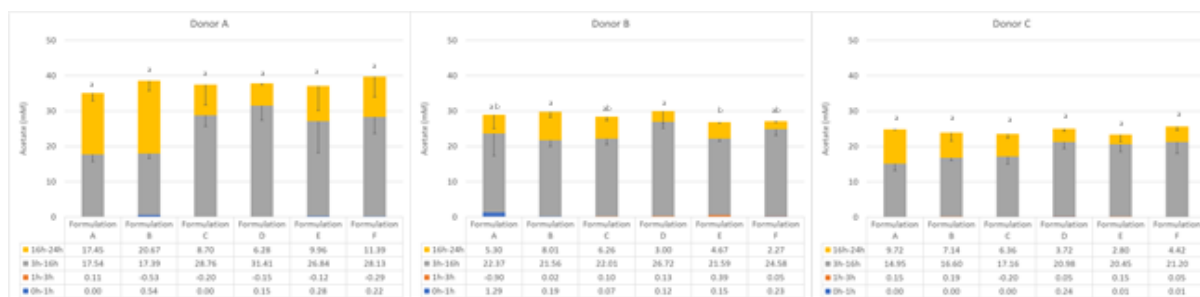


Figure 20 Average increase in concentration (mM) \pm stdev (n = 3) of acetate during the colonic incubations inoculated with the faecal inoculum of IBD donor A, B, or C upon dosing of the six different formulations. Statistically significant differences (Student's T-test; $p < 0.05$) in between formulations are highlighted with different letters above the different bars.

Quantification of the concentrations of propionate and butyrate demonstrated that the colonic microbiota of the IBD donors were not capable of producing these short-chain fatty acids to a substantial extent which is typically associated with people suffering from IBD. However, IBD donor B had a tendency towards higher propionate production as compared to the other donors whereas donor A had a slight tendency towards more butyrate production. Propionate and butyrate were generally produced in between 16h and 24h of colonic incubation. Considering the low concentrations of these metabolites produced no clear impact was observed for any of the formulations on the production of propionate and butyrate (data not shown). Next to this, only minor amounts of lactate and branched short-chain fatty acids were produced by the colonic microbiota of the three donors tested with no substantial impact of any formulation type on the production of these metabolites (data not shown). On the contrary, substantial concentrations of ammonium were produced by the colonic microbiota of the three donors tested. Interestingly, formulation A, containing Aloe Vera, consistently resulted in a higher ammonium production as compared to the other formulations and this for all IBD donors tested (Figure 21).

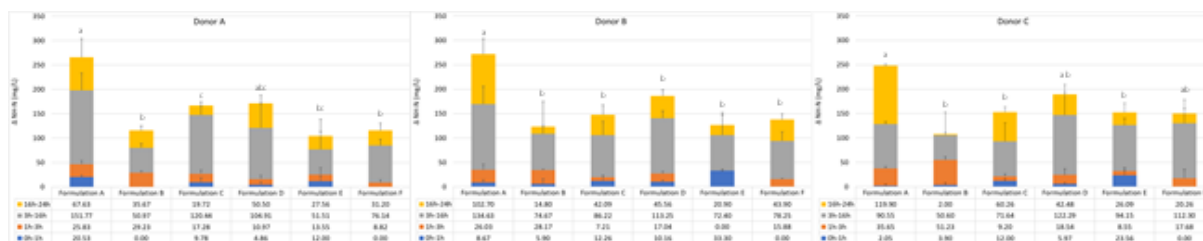


Figure 21 Average increase in concentration (mM) \pm stdev (n = 3) of ammonium during the colonic incubations inoculated with the faecal inoculum of IBD donor A, B, or C upon dosing of the six different formulations. Statistically significant differences (Student's T-test; $p < 0.05$) in between formulations are highlighted with different letters above the different bars.

3.4. Conclusion

In vitro tools should accurately simulate the gastrointestinal physiology and colonic microbiota composition and metabolic activity of the target patient population. This is essential when the disease itself can have a substantial impact on the gastrointestinal physiology and colon. Mesalazine is a model drug that is used to decrease the symptoms associated with IBD. As such, a semi-dynamic SHIME[®] model that simulates the physiology and colonic microbiota of patients suffering from IBD was used to study the colon-targeting release characteristics of six different formulations, containing mesalazine, and the final impact of these formulations on the colonic microbiota activity of three IBD donors. All formulations resulted in a partial release of mesalazine during passage through the upper gastrointestinal tract. The formulations containing partially pregelatinized starch, xylan, inulin and to a lesser extent Reishi extract resulted in a high release of mesalazine during passage through the upper gastrointestinal tract. The formulations containing Aloe Vera or maize maltodextrin were successful in lowering the amount of mesalazine released in the upper gastrointestinal tract and this across all donors. Upon entering the colon, none of the formulations released an additional amount of mesalazine during the initial phase of the colonic incubations whereas the degradation of the polysaccharide fraction of the coating by the colonic microbiota in between 3h and 16h of colonic incubation resulted in a substantial increase in mesalazine release. Overall, the formulation containing Aloe Vera demonstrated superior colon-targeting release characteristics by limiting mesalazine release in the upper gastrointestinal tract followed by a colonic microbiota-triggered substantial release during passage through the colon. Furthermore, this formulation resulted in increased ammonium production by the colonic microbiota as compared to the other formulations and this effect was observed across all donors.

4. Chapter: 3D printing for colonic drug delivery systems

4.1. Overview

4.1.1. Pharmaceutical 3D printing

The pharmaceutical industry is quickly evolving, with old 'one-size-fits-all' treatment techniques becoming obsolete. According to a National Health Service (NHS) England assessment, this traditional therapy method including mass manufacturing of pharmaceuticals is unsuccessful in up to 70% of patients, highlighting the urgent need for innovative tailored therapeutics (180). Traditional manufacturing procedures, which are fundamentally labor-intensive, dose-inflexible, and time-consuming, are inappropriate for the development of customised drug delivery solutions. As a result, the healthcare business must adapt and embrace new platforms for personalised therapeutic medicines.

Structures may be easily manufactured from a digital 3D file utilizing 3D image software, resonance imaging (MRI) or computed tomography (CT) analysis (181). 3D printing processes differ in terms of the material used (e.g., plastics, ceramics, metals, resins), deposition technology, layer formation mechanism, or product characteristics.

3D printing technologies are divided by the American Society for Testing and Materials (ASTM) into seven main categories: material jetting, powder bed fusion, material extrusion, binder jetting, sheet lamination, vat photopolymerization, and directed energy deposition. Invented more than three decades ago, 3D printing has altered manufacturing in an infinite number of applications. It appears that the possibilities of 3D printing are barely restricted by the imagination, with stories of 3D printed automobile components, bespoke fashion items, organs, and even houses (182,183). The possibilities for 3D printing are endless.

Various structures in the field of drug delivery have previously been constructed utilizing 3D printing, including drug-eluting implants, medical devices, and tailored solid oral dosage forms (184–190). As a result, this technique has been investigated as a possible tool for customizing medications and therapies, with the goal of eventually expanding into quick throughput screening of novel drug candidates on 3D-printed biological tissues to find intra-individual therapeutic responses (191). 3D printing is cost-effective for small-scale manufacture of medical equipment and medication items that require customisation and regular dose changes, as well as products with complicated geometries. Such personalization is not possible with traditional mass production procedures and has been found to improve patient compliance and provide personalized medication release patterns (192,193).

4.1.2. Selective laser sintering (SLS)

The energy source in the SLS 3D printing is a laser beam used to fuse the surfaces of the powder particles together, a process called ‘sintering’ (194). Invented in 1984 by Carl Deckard, SLS printers employ today a variety of laser types, including diode, fiber and carbon dioxide (CO₂) lasers (195). Recent studies demonstrated that it is possible to modify and control the porosity of a 3D printed object modifying the laser speed and intensity; the faster is the laser and the higher is the porosity of the system (196). Several studies evaluated the effect of the printing settings on the drug release, producing complex structures made with different laser speed and materials blend. The pharmaceutical field is exploring this technology for the production of advanced formulations, focusing on controlled drug release systems (196), the use of biodegradable polymers (197) and, more recently, evaluating the drug stability after exposure to the laser beam energy (198).

The mechanism driving the fusion process is the energy absorption of the particles’ surface. Most of the pharmaceutical powders are white in colour, therefore no absorption

from the laser occurs. The solution to this problem, is the addition of a pharmaceutical grade colorant to the powder blend, in low concentration (3 %) (199).

4.1.3. Direct powder extrusion (DPE)

Within the 7 groups of different 3D printing technologies, material extrusion (particularly fused deposition modeling; FDM) is the most often utilized in the pharmaceutical field owing to the printers' wide availability and inexpensive cost (191,200). *In vivo* investigations on FDM 3D printed medicines in animal models (188,201,202) and humans have already highlighted the potential use of 3D printing in the healthcare industry (202,203).

The FDM 3DP technology required a drug-loaded polymer filament, usually produced by hot melt extrusion (HME). The filament is heated and extruded via a nozzle tip, whose movement on a support plate determines the construction of the object in a 3-dimensional way through the cooling-solidification of the melted material (204).

FDM 3DP enables the creation of solid dispersions and solutions by drug dispersion or dissolution (205) into a polymer making it particularly well suited to medicines with limited water solubility and high heat stability.

Many polymers have been investigated in HME + FDM 3DP (206), the most commonly used is hydroxypropyl cellulose (HPC), thanks to its good mechanical properties and ease of extrusion through the nozzle (192,207,208).

One of the main drawbacks of the FDM technology is the necessity for the drug-loaded filaments, which need to be consistent in shape and guarantee the protection of the drug from degradation (209,210). In fact, the use of HME prior to 3D printing raises the possibility of medication degradation due to the heat impact. The limitation in the use of excipients and pharmaceuticals to generate filaments with the right mechanical and physical properties for 3D printing is the most significant drawback (211,212). Nowadays, a large portion of the effort in all pharmaceutical publications relevant to

FDM 3DP is centered on excipient selection and optimization to develop filaments appropriate for 3D printing, and there are usually constraints in the drug loading capacity of the chosen polymers.

Direct pellet extrusion, a novel material extrusion 3DP technique, has recently been launched in the plastics sector as a viable alternative to FDM printing (213). This approach entails the ejection of material via the printer's nozzle in the form of pellets/powder (rather than filaments), which is directly produced using a single screw extruder. This approach does not need the creation of filaments using HME and may allow the extrusion of combinations that would not be able to be printed by traditional FDM due to the filaments' insufficient mechanical properties, such as being too brittle or too flexible.

4.1.4. X-ray computer tomography (CT)

X-ray computer tomography (CT) is a technique that can reveal in a non-destructive way, the internal details of objects in three dimensions, up to the nanometers length scale. More recently, it can also provide 4D information following the structural evolution of materials in time, for example to monitor the growth of a tumour under treatment (214). The results are reported in a digital 3D grayscale representation, referred to as a tomogram. Commonly used CT scanners consist of three basic physical components: X-ray source, X-ray detector and the sample holder (Figure 22).

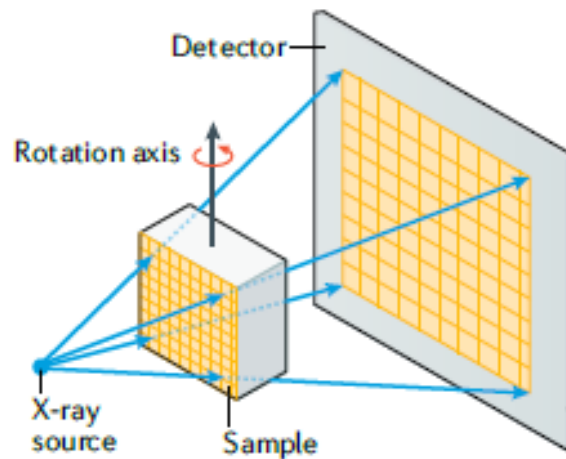


Figure 22 X-ray computed tomography configuration. Cone beam system typical of laboratory system (215)

In this project, the X-ray source used was an X-ray tube where the X-ray is produced by the acceleration of electrons (216). It is possible to modulate the magnification of the image by moving the sample stage; the closer the sample is to the source; the bigger will be the projection of the image on the detector and the higher will be the resolution (214). In order to have a better representation of the object, it is common practice to select the magnification ratio that guarantees the full width of the sample lies within the cone beam during all the analysis (217). The X-ray, emitted by the source, pass through the samples, while the latest is rotating, and it propagates in the space before being projected and recorded by the detector. The contrast obtained in each projection of the object is related to the attenuation of the laser beam. Materials with different density and molecular weight will interact with the laser in different ways, generating a different X-ray phase contrast (218). The X-ray are then converted by the detector in visible light with a scintillator and then, via an array of complementary metal- oxide semiconductor or other devices, to electrons for digital processing (219).

X-ray CT provide information for a wide range of applications including industrial metrology and manufacturing (220), material science (221), food science (222),

biomedical and life science for the *ex vivo*, *in situ* or *in vivo* examination of biological samples or entire animals (223,224).

4.2. Materials and methods

4.2.1. Materials

Aloe vera extract powder, Reishi extract (Specialty Natural Products, Bangkok, Thailand); Glucidex® 17 (corn maltodextrin, Roquette Freres, Lestrem, France); Starch 1500® (pregelatinized maize starch, Colorcon, Kent, England); Orafti® HSI (Inulin, BENEIO-Orafti S.A. plant, Oreye, Belgium); Xylan from corn core (Tokyo Chemical industry, Zwijndrecht, Belgium); Candurin® Sheen (Merck KGaA, Darmstadt, Germany); Magnesium stearate, tech. (Aldrich, Gillingham, England); Aqualon™ EC-N7 PHARM (ethylcellulose, Ashland, Schaffhausen, Switzerland); Methylparaben (VWR Life Science, Radnor, Pennsylvania, USA).

4.2.2. Selective laser sintering, (SLS)

All the powders were sieved using a 180 µm sieve prior to their use to permit a better flow of particles in the chamber, resulting in a better printing procedure (225). For all the formulations, 20 g of polymer mixture were blended using a mortar and pestle. 3 % Candurin Gold Sheen was added to the formulations to enhance energy absorption from the laser and aid printability. Powder mixtures were transferred to a desktop SLS printer, in the reservoir platform (Figure 23) (Sintratec Kit, AG, Brugg, Switzerland) to fabricate the oral dosage formulations. The chamber temperature was kept at 100 °C while the powder's surface temperature was 120 °C. The laser speed was 75 mm/s. 123D Design (Version 14.2.2, Autodesk Inc., San Rafael, CA, USA) was used to design the templates of the capsule's shapes, (body and cap printed separately using as a size reference the 00 capsule) and of the circular discs (2 cm diameter and 0.1 mm thickness).

The 3D models were exported as a stereolithography (.stl) file into the 3D printer Sintratec central software (Version 1.1.13, Sintratec, AG, Brugg, Switzerland). The capsules were fabricated in a vertical configuration.

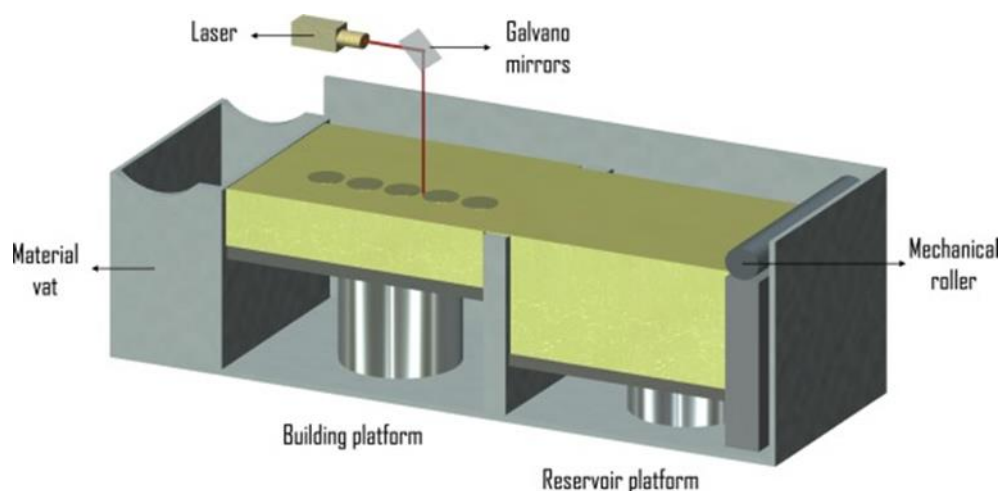


Figure 23 Graphical illustration of an SLS 3D printer, highlighting its major components (226).

4.2.3. Direct powder extrusion (DPE)

For each batch, 15 g of a polymers blend were manually mixed using a mortar and pestle until no agglomerated particles of polymers were observed. The prepared mixture was then added to the hopper of the 3D printer extruder. The 3D printer (FabRx, UK) is specifically designed to prepare pharmaceutical products and it can incorporate different exchangeable tools. The selected tool was a direct single-screw powder extruder (FabRx, UK) with a nozzle diameter of 0.8 mm (Figure 24). The design is based on a single-screw HME however the rotation speed (and hence the extrusion) is controlled by the software of the 3D printer. Furthermore, the extruder nozzle moves in 3 dimensions to create the objects in a layer-by-layer fashion. 123D Design (Version 14.2.2, Autodesk Inc., San Rafael, CA, USA) was used to design the templates of the capsules' shapes or the discs shape, exported as a stereolithography (.stl) file into 3D

printer software (Repetier host v. 2.1.3, Germany). The .stl format contains only the object surface data, and all the other parameters need to be defined from the Repetier Host software in order to print the desired object. The printer settings of the software were as follows: feed 2100 steps/mm, infill 100%, high resolution with brim, without raft and an extrusion temperature of 140 °C, speed while extruding (5 mm/s for the discs and 2 mm/s for the capsules), speed while travelling (90 mm/s), number of shells (30) and layer height (0.2 mm).

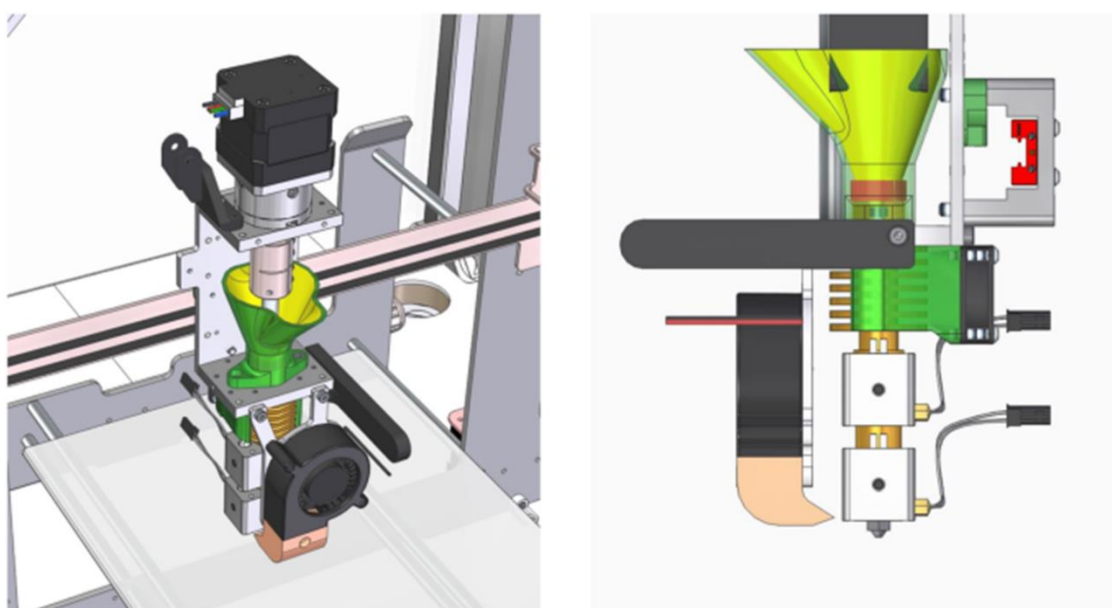


Figure 24 Design of the nozzle of the direct single-screw powder extruder FabRx 3D printer. The blue arrows indicate the site of addition of the powder (227).

4.2.4. Thermogravimetric analysis (TGA)

TGA analysis, samples were heated at 10 °C/min in open aluminum pans with a Discovery TGA (TA Instruments, Waters, LLC, U.S.A.). Nitrogen was used as a purge gas with a flow rate of 25 mL/min. Data collection and analysis were performed using

TA Instruments Trios software and percent mass loss or onset temperature were calculated.

4.2.5. Scanning electron microscopy

Morphology of the printed capsules and discs were evaluated by scanning electron microscopy (SEM) using a Philips XL30 FEG SEM, operating at 20 kV. Samples were placed on double-sided carbon tape, mounted on stubs and sputter coated using a Polaron E5000 machine with Au/Pd. Samples were coated for 1 min prior to imaging.

4.2.6. X-ray microtomography

X-ray microcomputed tomography (X μ CT) measurements were conducted using a Skyscan 1172 scanner (Bruker, Antwerp, Belgium) to investigate the presence of pores in the 3D printed objects. The capsule was fixed on the sample holder using a double-sided sticky tape and then placed in the X μ CT instrument. Shadow projection images were collected with a resolution of 2.95 μ m at an angular step, i.e. rotation increment, of 0.25° over 180° without any filter. 10 frames were averaged per position with an exposure time of 4.5s. The projected images were then reconstructed using NRecon software (Bruker, Version: 1.7.4.2) to obtain cross-sections of the sample. DataViewer software (Bruker, Version: 1.5.3.4) was then utilised to visualize the cross-sectional images of the sample.

4.3. Results and discussion

4.3.1. Powder characterization

4.3.1.1. Scanning electron microscopy

Scanning electron microscopy (SEM) was performed on the pure polysaccharide powders in order to evaluate the initial particle size and shape. Considering that the 3D printing technologies selected for the study (SLS and DPE) include the melting of the powders, the particle size can play an important role in the process.

Different shapes were selected for the printing process:

- A disc, one-layer object printed directly on the plate support.
- A capsule, a more complex multi-layer object printed in the vertical orientation.

Between the six polymers selected for the printing it was possible to obtain 3D printed capsules only with aloe vera and reishi extract. Interestingly, these polymers showed the smallest size and regular shape (spherical) (Figure 28 and 29).

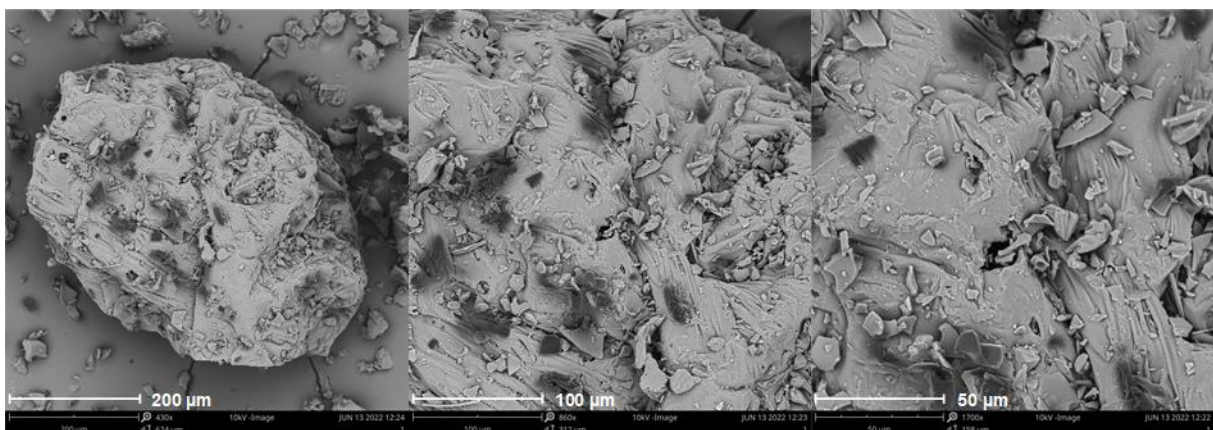


Figure 25 SEM picture of corn maltodextrin (Glucidex® 17D) as provided by the supplier.

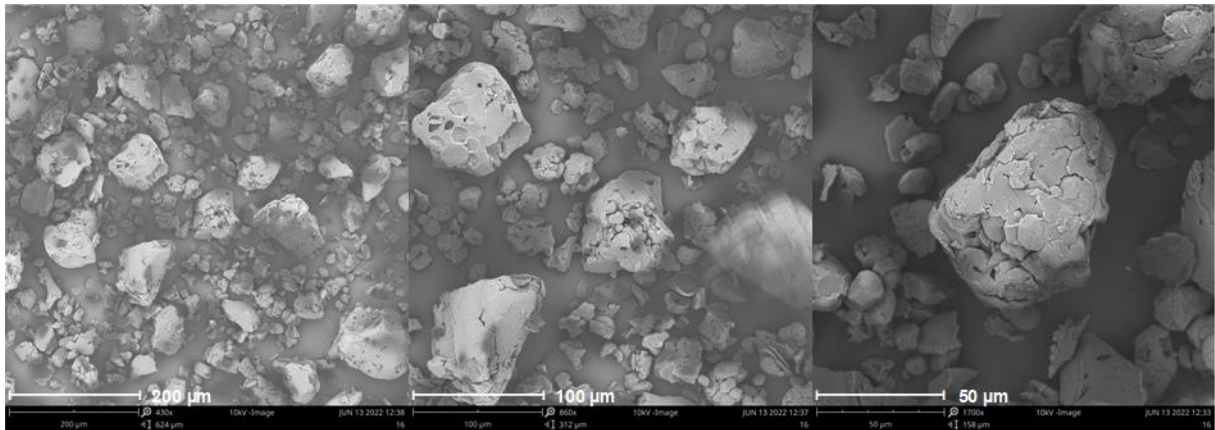


Figure 26 SEM picture of pregelatinized starch (Starch 1500®) as provided by the supplier

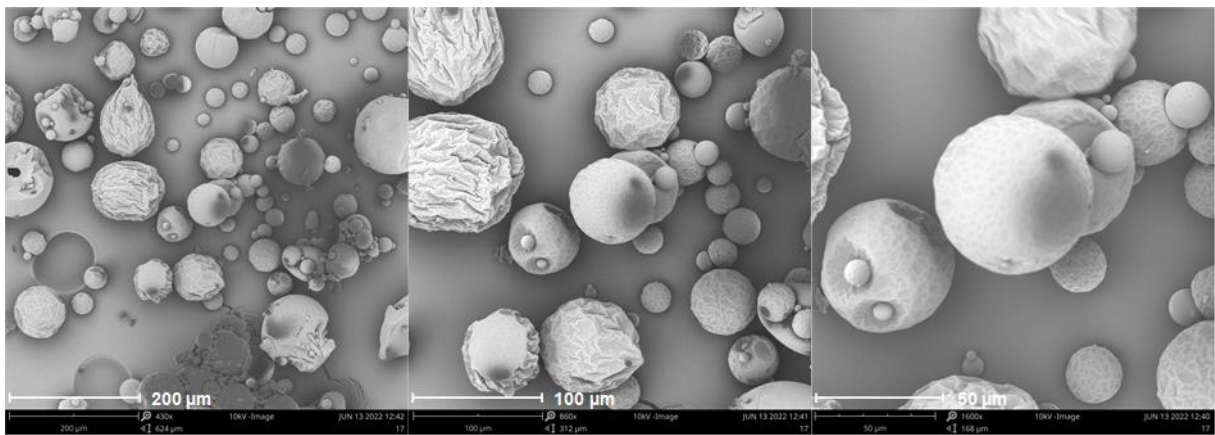


Figure 27 SEM picture of xylan as provided by the supplier

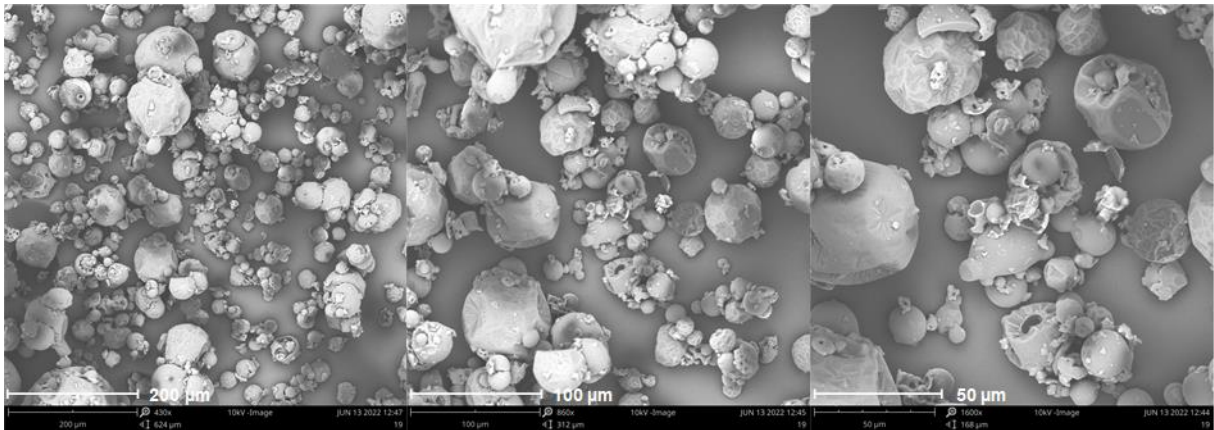


Figure 28 SEM picture of aloe vera extract powder as provided by the supplier.

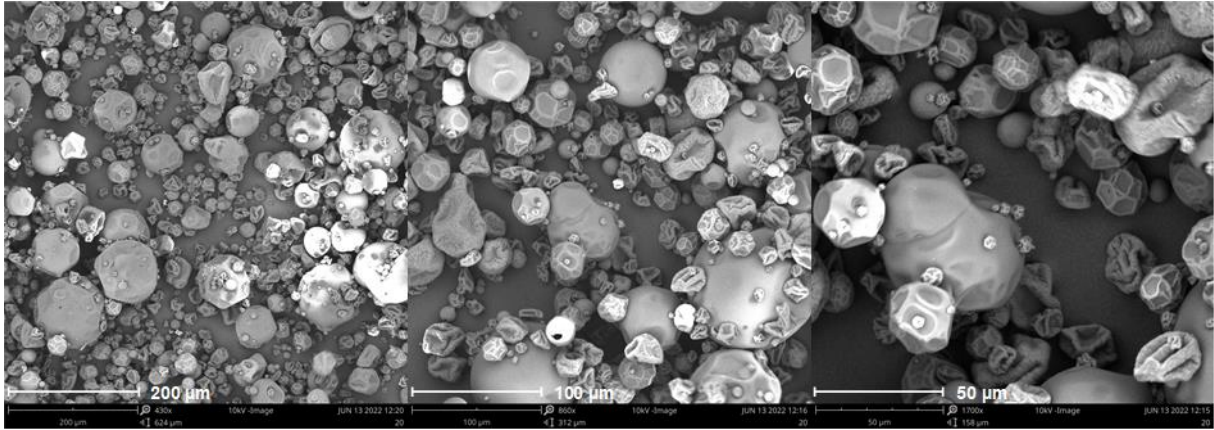


Figure 29 SEM picture of Reishi extract powder as provided by the supplier.

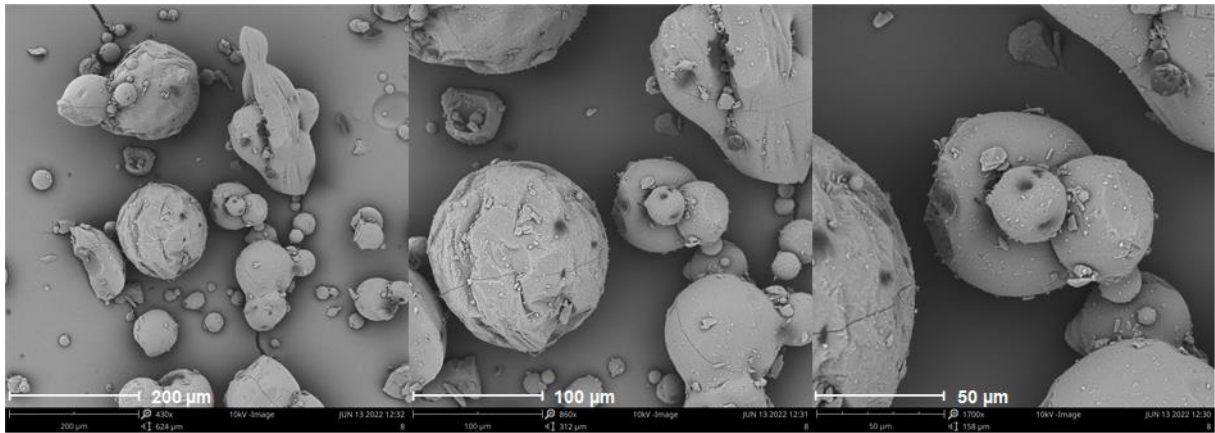


Figure 30 SEM picture of inulin (Orafti® HSI) as provided by the supplier.

4.3.1.2. Thermo-gravimetric analysis (TGA)

Thermo-gravimetric analysis (TGA) was performed on the polysaccharide powders to determine the degradation temperature of the polymers and evaluate the temperature to select for the melting during the printing process. It must be taken into account that the degradation occurring during the printing does not depend exclusively on the temperature. Shear stress and frictions are phenomena that also occur in the screw, while the material is pushed through the nozzle. These parameters, together with the heat, play an important role in the degradation of the material during the printing process.

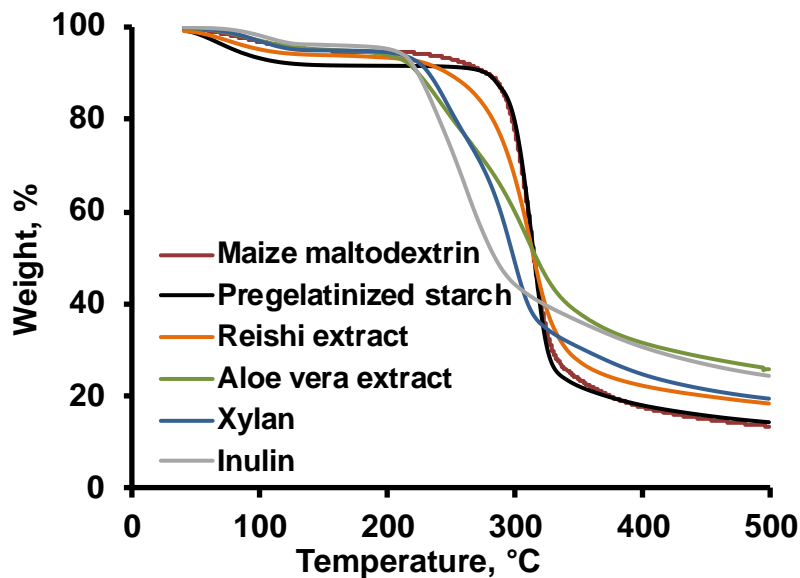


Figure 31 TGA thermal traces for the individual polymers' raw material.

Considering that the highest temperature used in the DPE 3D printing is 140 °C, a maximum degradation < 10% is observed below this temperature (Figure 31).

4.3.2. Printability of the polymers' blends

In vitro drug release studies performed in chapter 2 allowed the selection of the 6 most promising candidates for the colonic delivery of drugs. The selection was made based on the differences between the drug released in the presence of IBD patients' bacteria and the control, the higher the difference the more promising is considered the polymer.

The aim of this study is to evaluate the printability of the polymer blend used in the coating of the pellets in order to produce capsules shape 3D printed objects and be able to load them with a higher amount of drug. Two different technologies were selected: selective laser sintering (SLS) and direct powder extrusion (DPE).

As a reminder, for the coating of the 5-ASA loaded pellets, the polysaccharides were blended with ethylcellulose in order to prevent the drug release in the upper GIT and a plasticizer was used to guarantee optimal mechanical properties of the film. For this reason, maize maltodextrin, inulin (Orafti HSI), pregelatinized starch (Starch 1500), xylan, aloe vera extract and reishi extract were blended with ethylcellulose using the same proportion of the pellets coating (polysaccharide: ethylcellulose; 2:3).

4.3.3. Selective laser sintering (SLS)

123D Design (Version 14.2.2, Autodesk Inc., San Rafael, CA, USA) was used to design the templates of the capsule's shapes, (body and cap printed separately using as a size reference the 00 capsule) and of the circular discs (2 cm diameter and 0.1 mm thickness). It is important to underline that the thickness of a gelatine capsule (used as a template for this study) is about 100 μm and that the sensibility of the laser is 800 μm . This is due to the fact that once the laser hits the powder bed, the particle surface melts and fuses with the particles around. Furthermore, the powders were sieved using a 180 μm sieve prior to their use to permit a better flow of particles in the chamber.

For this reason, it has been necessary to adapt the 3D designed template to the experimental sizes.

Maltodextrin was the first polymer printed with SLS technology and as shown in Figure 32 the resolution is insufficient for the printing of a homogeneous and symmetric capsule. The cause of the irregular shape is the shifting of the powder surface in the reservoir platform while the mechanical roller deposits the follower layer of powder. In order to avoid this event, it would be necessary to increase the temperature of the chamber, due the thermos-sensitivity of the polymers used, this shrewdness could not be applied.

The first test revealed that it is possible to print 3D objects with SLS but the limitation is the complexity of the shape. For this reason, circular films were designed for printing. Although it was possible to obtain the 3D printed discs, the experimental thickness was different from the 3D designed model. Considering the friability of the material, thinner films would be impossible to manipulate.



Figure 32 picture of 3D printed object produced with SLS technology with the blend of maltodextrin: a) capsule b) disc.

4.3.4. Direct powder extrusion (DPE)

The second technique explored was the Direct Powder Extrusion (DPE) technology which allows the production of 3D printed objects starting from a blend of powders.

Maltodextrin: ethylcellulose blend could not be printed with this technology. It was difficult to obtain a consistent filament and the material stocked in the nozzle.

Between the 6 polymers selected it was possible to print 4 of them in the simple shape (disc) and only two of them in a more complex shape (capsule).

The printing parameters were adapted to each polymer and the different printed shapes required different settings.



Figure 33 picture of 3D printed object produced with DPE technology with the blend of aloe vera.

With the blend of aloe vera it was possible to obtain both capsule and disc shapes. Figure 33 shows the disc and the capsule printed with the aloe vera: ethylcellulose blend. The figure shows how the same polymer blend reacts to different printing parameters. The

disc's colour is lighter compared to the capsule's colour. The reason behind this difference is related to the time exposure to heat as a consequence of the different printing speed. It was possible to print discs at a speed of 5 mm/s while for the printing of the capsule it was necessary to decrease the printer speed to 2 mm/s. The degree of polymer degradation needs to be evaluated for both the printed objects.

The nozzle diameter was 0.8 mm and the capsule's shell thickness reflects this size. Albeit the 3D design was adapted to the 0.8 mm thickness, there was no direct correlation between the theoretical design and the printed object. For this reason, several trials were needed to find the good design to be able to fit the body of the capsule in the cap. These tests were performed with the blend of aloe vera, printing different body and cap diameters, as represented in Figure 34.



Figure 34 picture of several 3D printed capsules produced with DPE technology with the blend of aloe vera.

SEM pictures were collected in order to evaluate the deposition of the melted material during the production of the 3D object. In Figure 35 and 36 are shown the surfaces of the capsule and the disc respectively, printed with the blend of aloe vera. The comparison underlines the fact that bigger void spaces are present between the layers of the capsule, while the layers constituting the discs are closer one to each other. This is

probably due to the fact that the capsules are printed in the vertical orientation, while the discs are directly printed on the printer support and the nozzle itself pushes the material on the surface while moving.

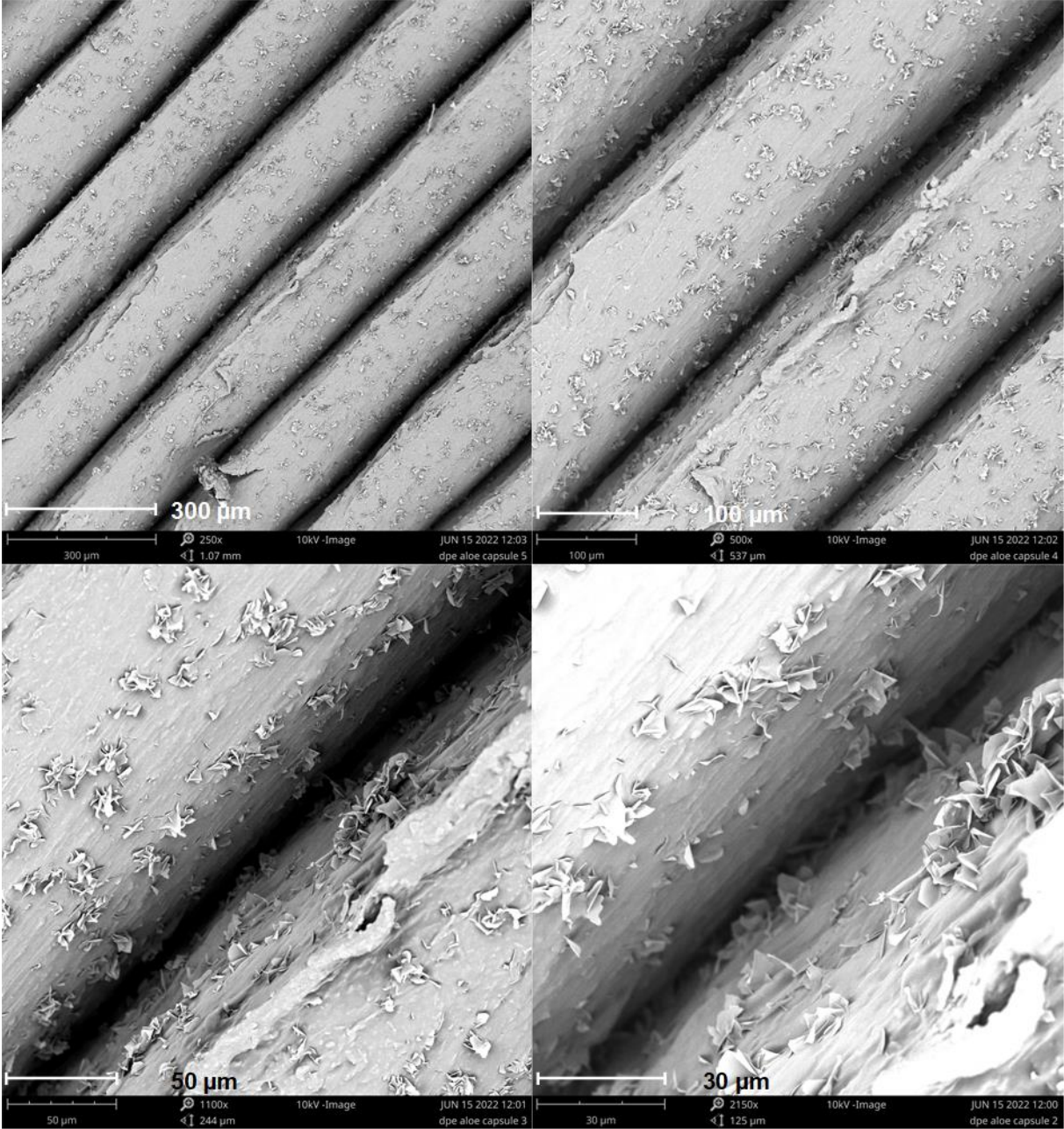


Figure 35 SEM images of the surface of the capsule printed with DPE technology of aloe vera, at different scales.

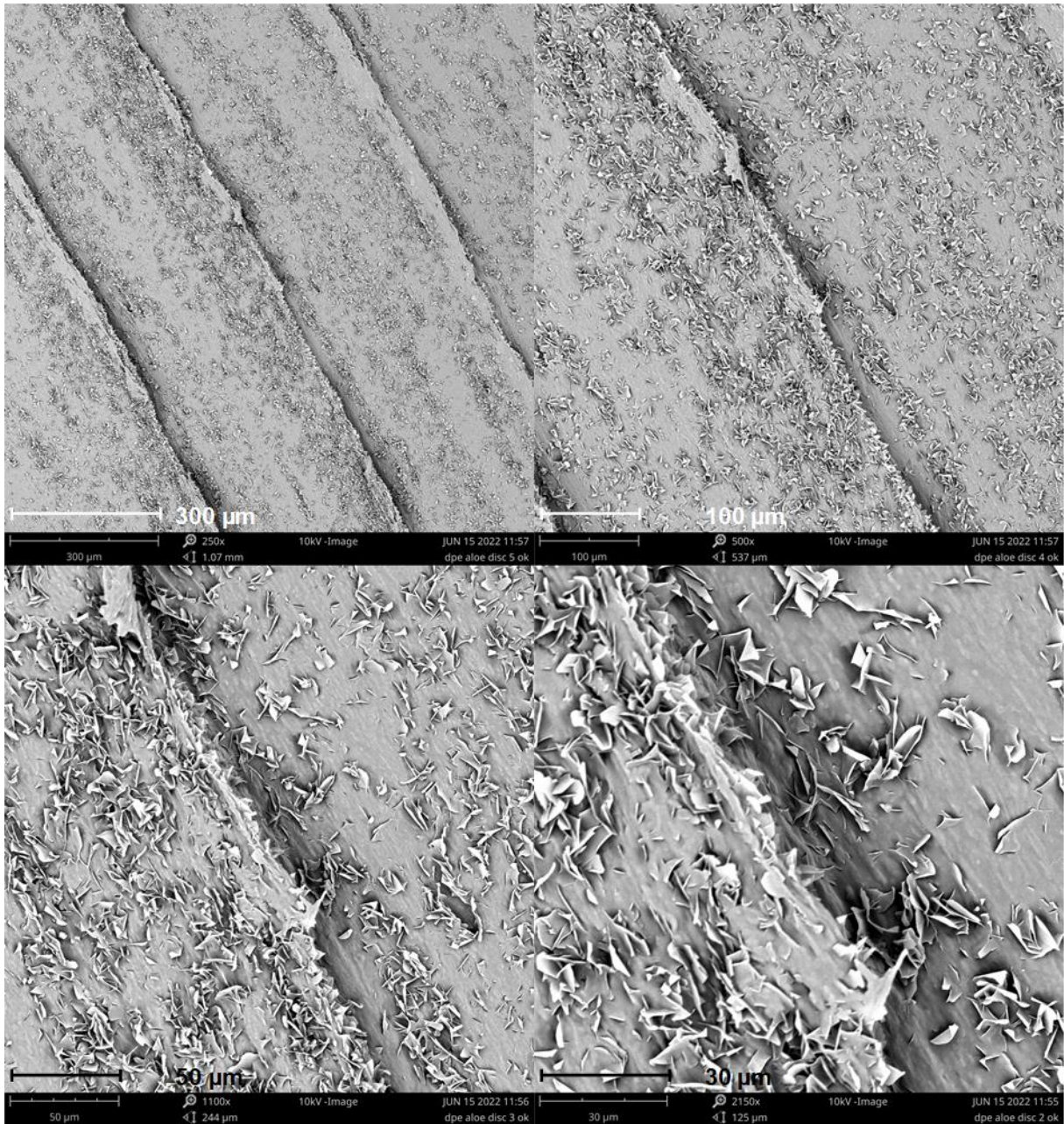


Figure 36 SEM images of the surface of the disc printed with DPE technology of aloe vera at different scales.

Using the same printing settings of aloe vera extract it was possible to print 6 discs and one capsule with reishi extract. Once again, the colour difference between the two printed objects is probably due to the exposition time to the heat. Although it was possible to print one capsule with reishi extract (Figure 37), the process was unreproducible and it was not possible to print other capsules. During the printing of the cap/body it was possible to print only the first few layers. After about 10 layers the filament started to extrude in an inconsistent way and the structure of the capsule started to collapse. The SEM pictures in Figure 38 (representing the capsules) and Figure 39 (representing the discs) clearly show the presence of big void spaces in the extrudate. The reason behind the inconsistency of the melted material could lie in the feeding phase of the process; before the printing, the powder blend is loaded into the hopper, the yellow section in Figure 24, during the printing, the powder is manually mixed and pushed through the screw with the help of a spatula. The manual mixing probably affects the density of powder present in the screw and therefore in the nozzle, consequently it affects the final object density and porosity.



Figure 37 picture of 3D printed object produced with DPE technology using the blend of reishi extract.

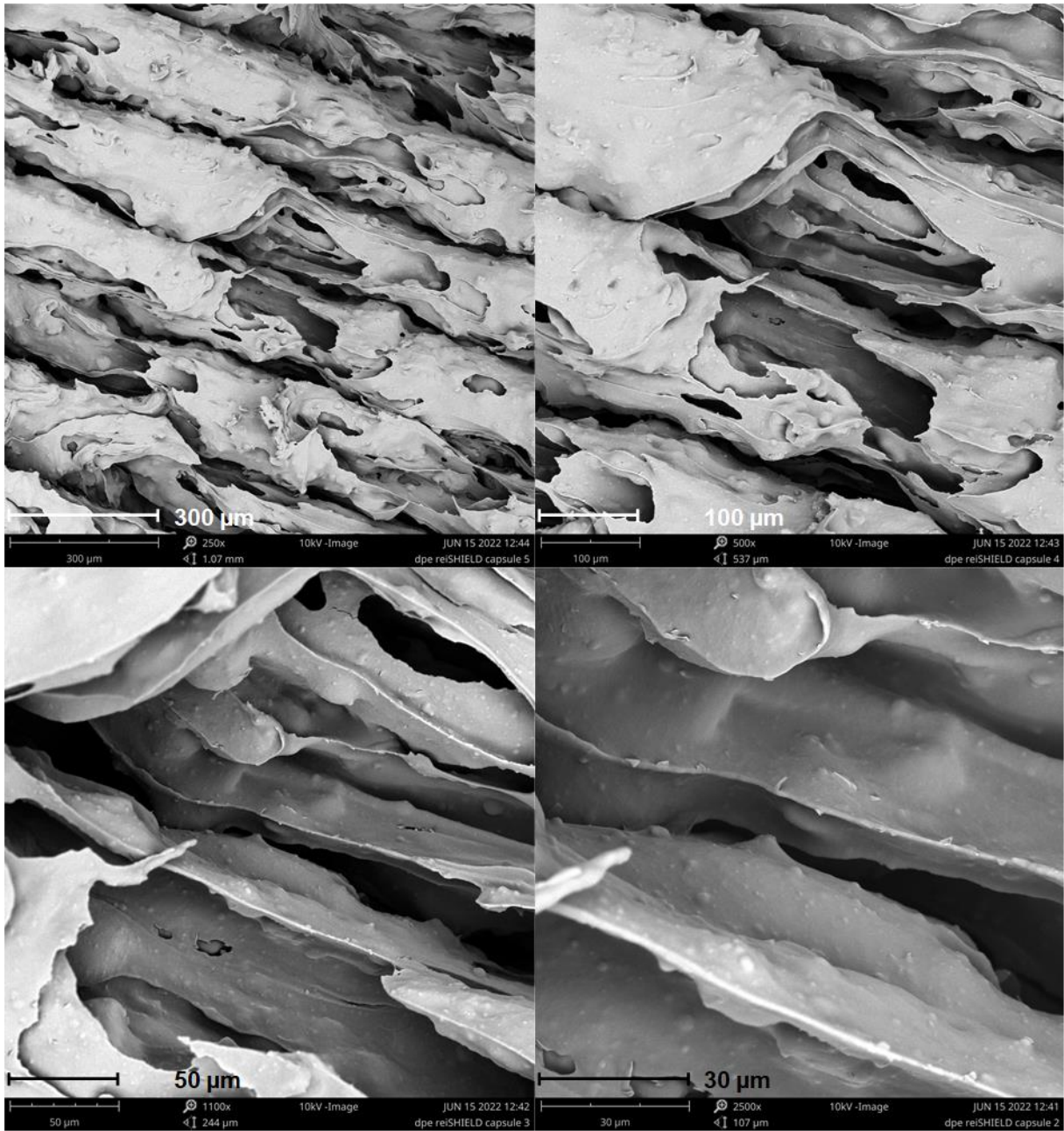


Figure 38 SEM images of the surface of the capsule printed with DPE technology of ReiSHIELD at different scales.

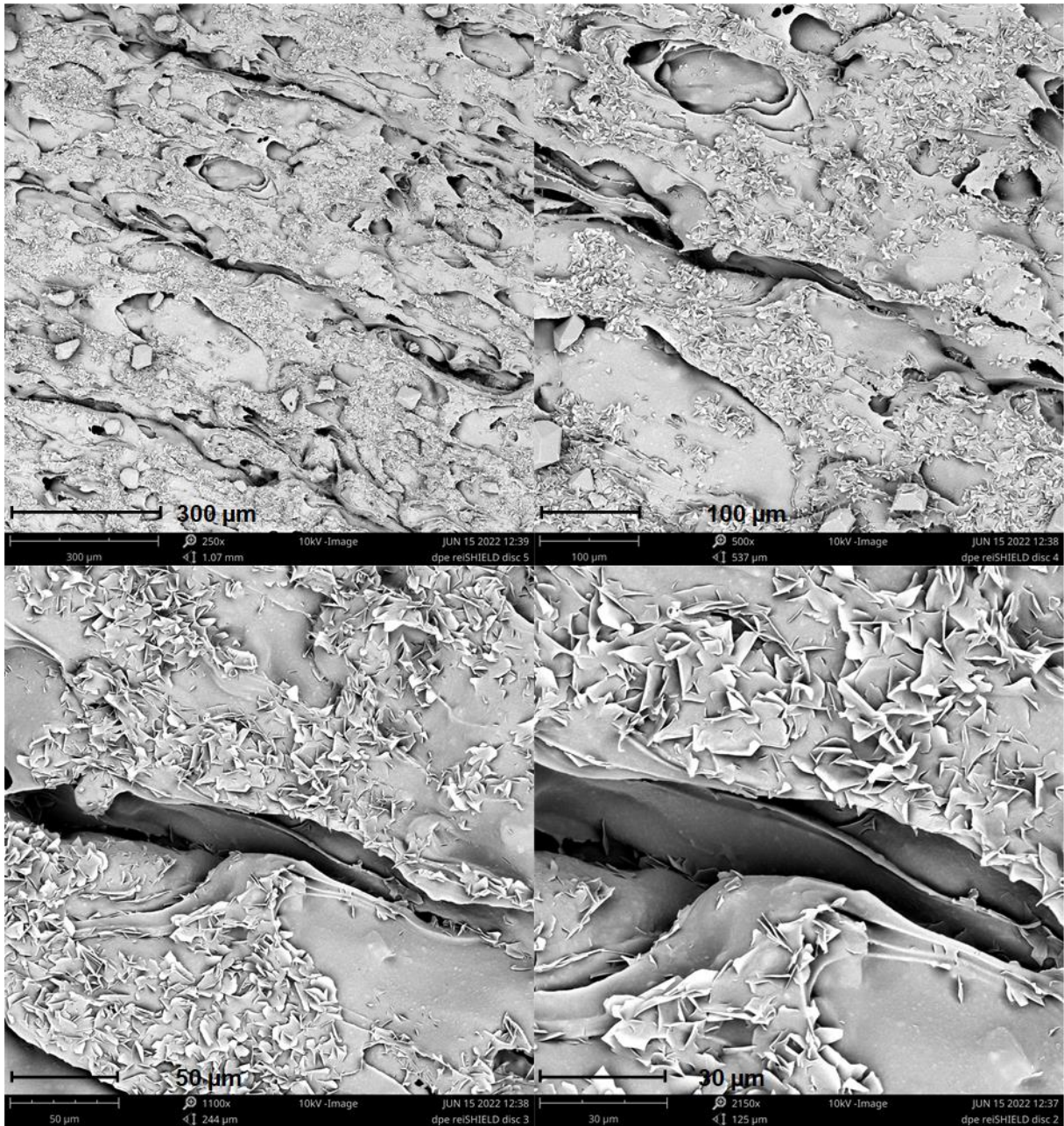


Figure 39 SEM images of the surface of the disc printed with DPE technology of reishi extract at different scales.

With xylan and starch it was possible to print only discs.

Xylan showed a unique behaviour compared to all the other polymers. During the printing it was possible to lowered the heating temperature of 30 °C and melt the material at 110 °C. In general, during the printing process, as soon as an object is completed the printer nozzle moves vertically up and then horizontally in order to reach the 0 position and start with a new object. What is interesting to notice is that while xylan was employed, an uncontrolled extrusion of material from the nozzle was observed once the printing of an object was completed. The melted material, following gravity, accumulates on the disc surface just printed Figure 40. The SEM picture of xylan printed disc (Figure 41) shows a cohesive structure and a good overlap of the printing layers. For this polymer it will be necessary to further optimize printing parameters such as temperature and speed in order to prevent the undesired material extrusion at the end of the printing process.

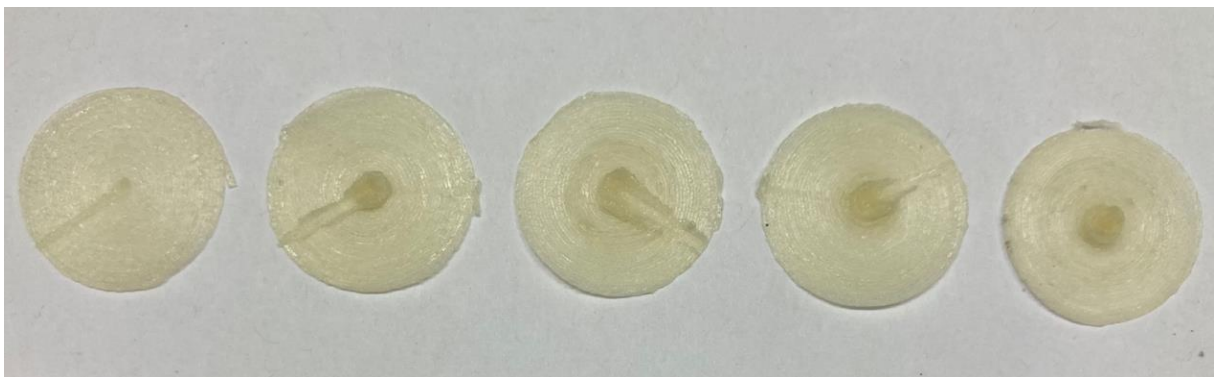


Figure 40 picture of discs produced with DPE technology using the blend of xylan.

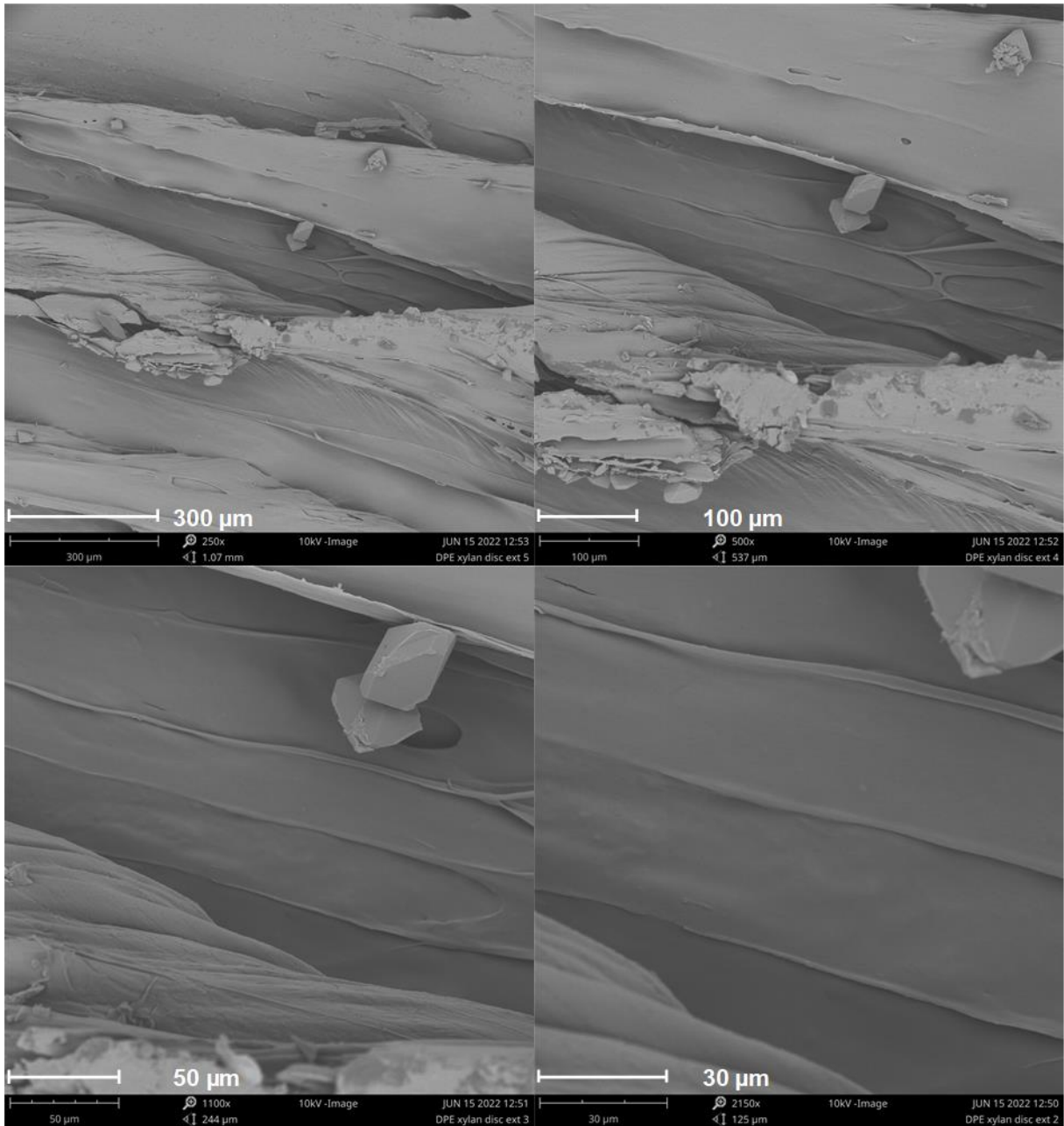


Figure 41 SEM images of the surface of the disc printed with DPE technology of xylan at different scales

Starch discs (Figure 42) were printed using the same parameters of polymers aloe and reishi extract. The SEM pictures of starch blend (Figure 43) shows a reduced presence of pores compared to the other polymers. In fact, it is harder to distinguish the different layers from one another.

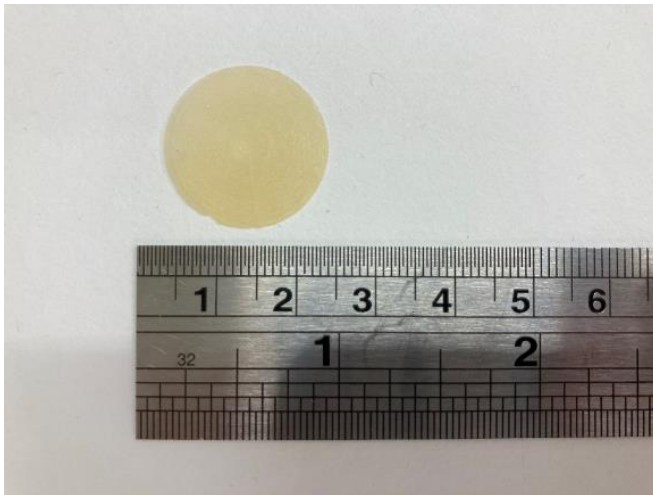


Figure 42 picture of 3D printed disc produced with DPE technology using the blend of starch.

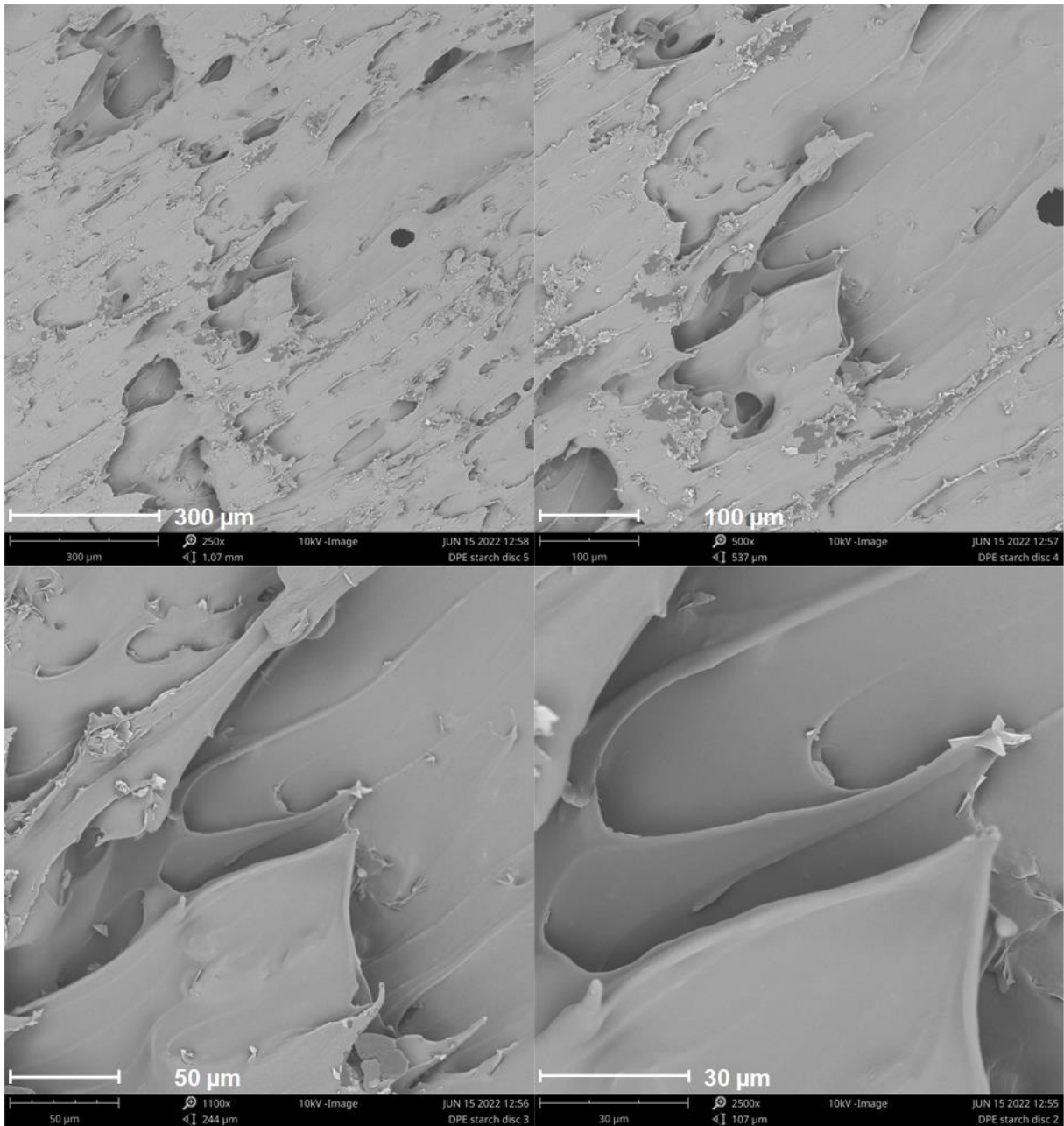


Figure 43 SEM images of the surface of the disc printed with DPE technology of starch at different scales

4.3.5. X-ray microtomography

The aim of the X-ray microtomography analysis was to evaluate the porosity of the 3D printed objects. This analysis confirmed what was observed in the SEM images: the capsule structure is porous and heterogeneous.

Between the six polysaccharides selected, it was possible to print multiple capsules only with aloe vera extract blended with ethylcellulose. For this reason, only aloe vera capsules were analysed.

Figures from 44 to 47 show the inner structure of one capsule at different crossing sections. It is important to remember that the capsules' bodies and the caps were printed separately and the association between one body and one cap was aleatory.

Figure X shows how at the beginning of the printing process the material extrudes from the nozzle in a more consistent and dense way. As the printing progressed the presence of pores increased and the structure became less and less dense. As anticipated previously, the reason behind this loss of density might be attributed to the manual mixing and feeding of the powder in the nozzle.

Furthermore, figure 47 shows the cross section of two different capsules and it is possible to see a big difference between the structures. The printing process needs to be further optimized in order to be reproducible.

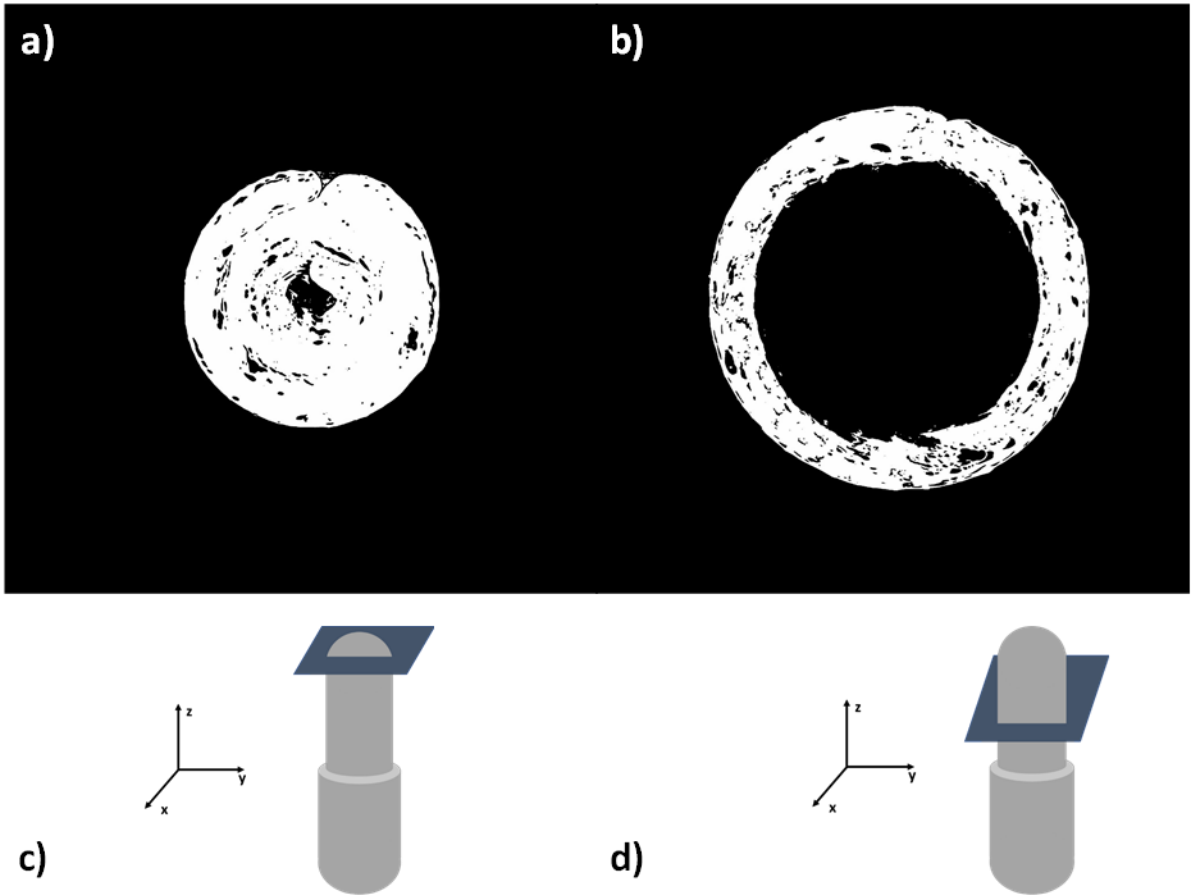


Figure 44 μ CT images of cross-sections of aloe vera blend capsule printed with DPE technology: a) base of the body b) intermediate portion of the body, c) and d) cartoons of the planes of the cross-sections. The capsule body external diameter was 0.5 m

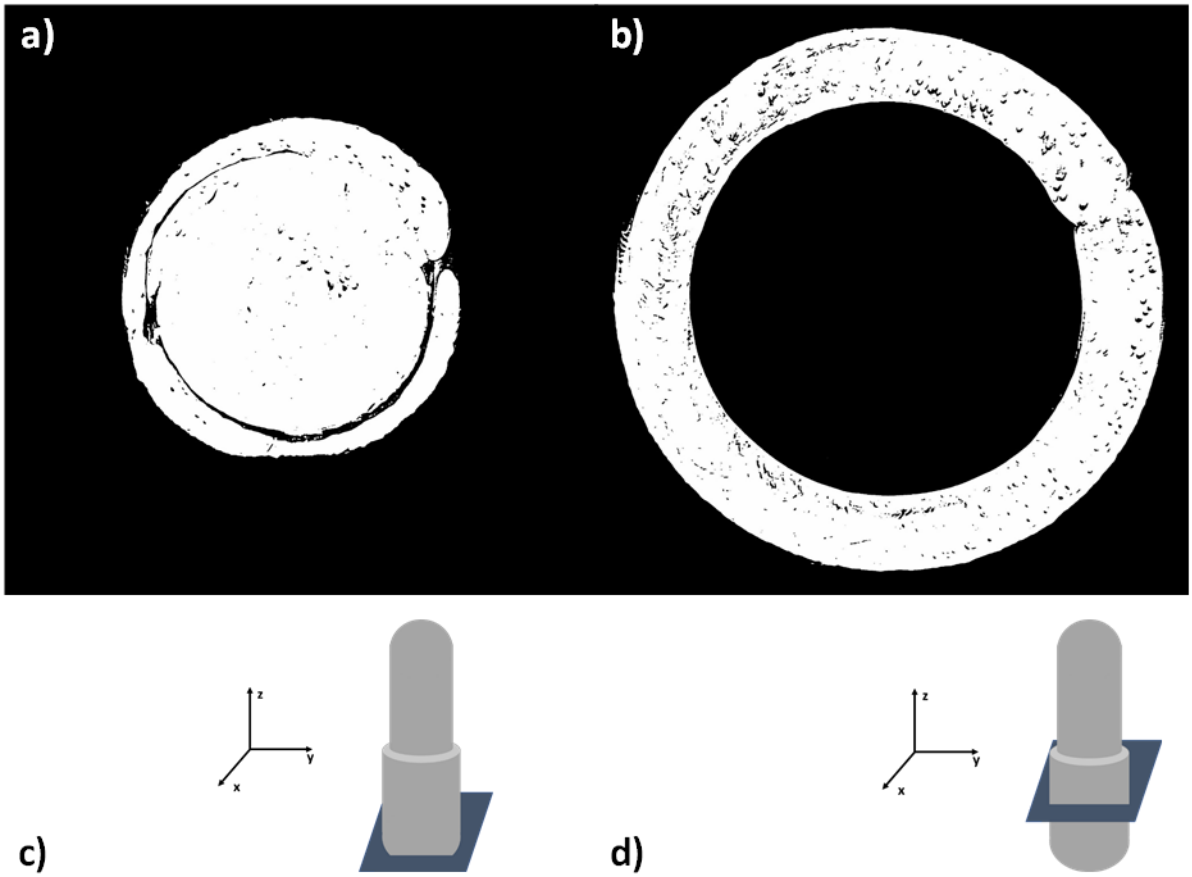


Figure 45 μ CT images of cross-sections of aloe vera blend capsule printed with DPE technology: a) base of the cap b) intermediate portion of the cap, c) and d) cartoons of the planes of the cross-sections of a) and b) respectively. The capsule cap external diameter was 0.5 mm.

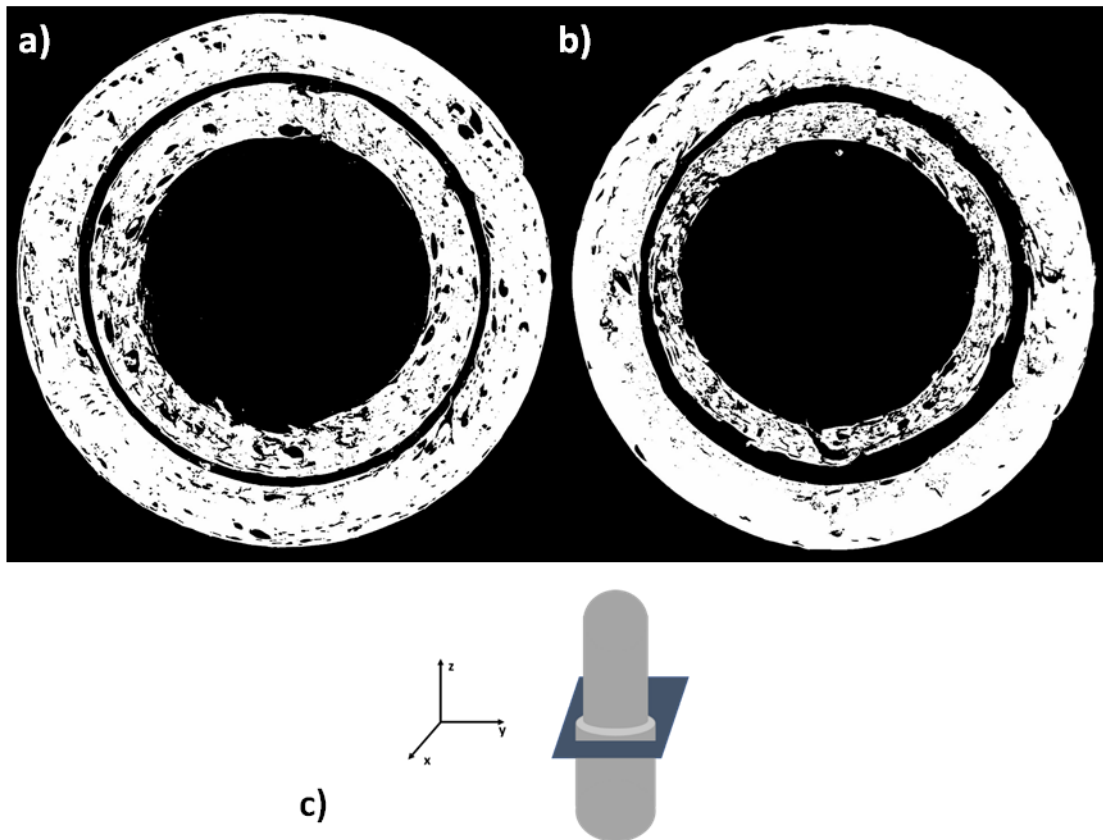


Figure 46 μ CT images of cross-sections of aloe vera blend capsule printed with DPE technology: a) intermediate portion of the capsule 1, b) intermediate portion of the capsule 2, c) cartoons of the plane of the cross-sections

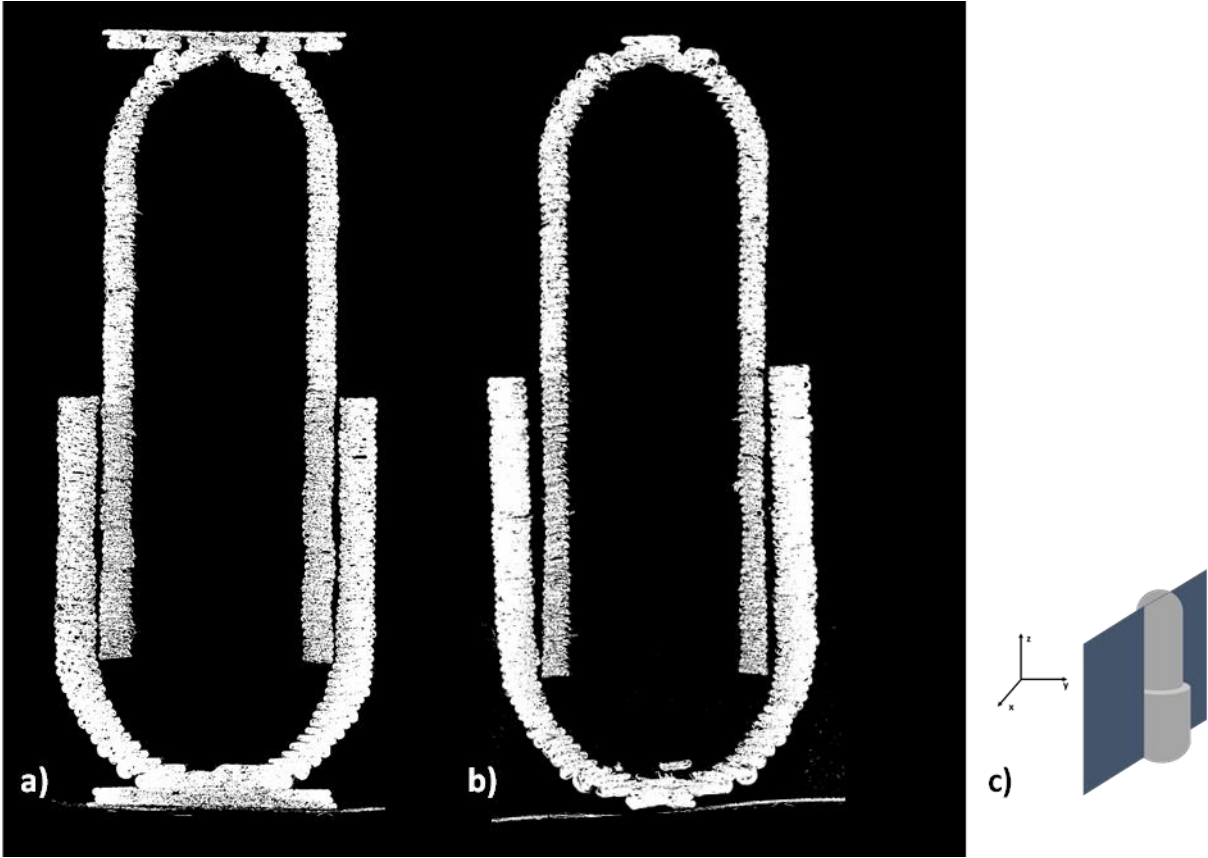


Figure 47 μ CT images of cross-sections of aloe vera blend capsule printed with DPE technology: a) intermediate portion of the capsule 1, b) intermediate portion of the capsule 2, c) cartoon of the plane of the cross-sections.

4.3.6. Development of a dissolution device

In order to study the mass transport properties of the 3D printed films/discs, a specific dissolution device was designed. It consists of three parts: the drug reservoir section, the film holder and the screws. The drug reservoir, lower portion in Figure 48 a) presents a circular cavity intended to contain the drug. Once the reservoir is filled with the drug, the 3D printed film is placed between the reservoir section and the holder section, (upper part in figure Figure 48)). By turning the screws, it is possible to close the device, keeping in place the 3D printed disc just above the drug reservoir cavity. In order to guarantee a hermetic tie-off, some grease is added around the perimeter of the disc, between the 2 device's sections.

The hole present in the holder portion allows the exposition of the 3D printed disc to the release medium (Figure 48 c)). The *in vitro* drug release will be performed in conditions simulating the colonic environment as reported in chapter 2.

Ideally, the bacteria present in the release medium will produce enzymes able to degrade the 3D printed discs. Once the film is degraded, the drug underneath is released.

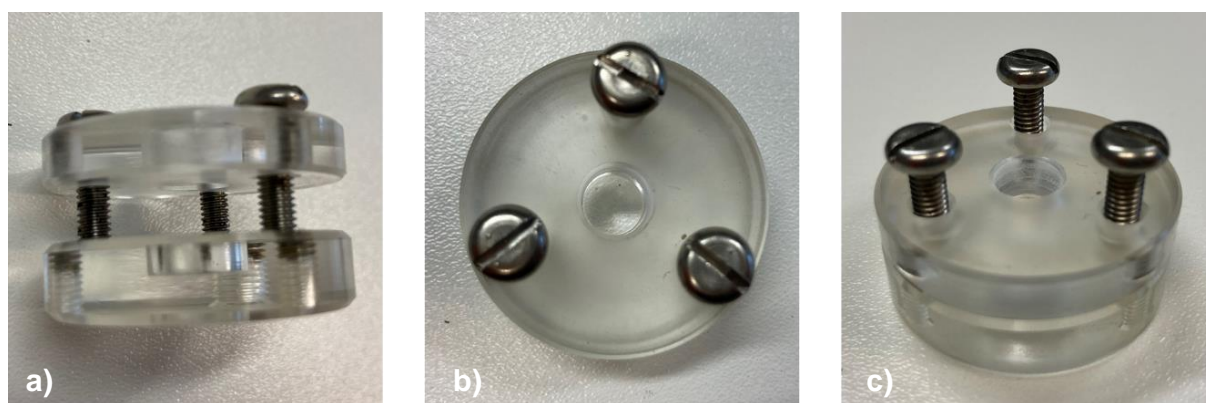


Figure 48 Pictures of the dissolution device designed for the study of 3D printed films release behaviours after exposure to conditions simulating the colonic environment.

4.4. Conclusion and further perspectives

Selective laser sintering technology presented some major limitations in the production of capsules for oral drug delivery systems for colon targeting using the selected polymer blends. Due to the high thermos-sensitivity, the exposition at high temperature for the whole production time (about 1 h) might lead to the complete polysaccharide degradation. With the parameters tested, this technology did not show promising results and will not be further investigated.

Direct powder extrusion technology allowed the production of 3D printed capsules and discs with an acceptable resolution. During the printing with DPE technology, the polymers are exposed to high temperature for a shorter period of time compared to the SLS technology. However, the polymer degradation has to be evaluated.

The SEM and X-ray analysis revealed the high degree of porosity of the structures, suggesting that parameters such the feeding and printing time need to be optimized in order to obtain a denser capsule wall and more reproducible objects.

Although the high porous structure 3D printed objects, no drug release was observed after 24 h exposure to the media inoculated with IBD patients' faecal slurries.

Alternative production techniques are under evaluation for the production of capsules; such as melt prep extrusion or deeping.

5. Chapter: Colonic delivery of short chain fatty acid

Part of the results reported in this chapter were performed by CNRS, INSERM, CHU Lille, Institut Pasteur de Lille, U1019 - UMR 9017 - CIIL - Center for Infection and Immunity

5.1. Overview

The microbiota is also called the second brain (228) not only because it has an equivalent mass (1.5 kg) but especially because it uses the same chemicals as the brain to regulate the digestion process and alert the immune systems in case of pathogenic threats (229). The brain-gut axis is lately considered one of the most important and complex mechanisms involved in the protection of the human body (230). Short chain fatty acids (SCFAs) such as acetate, butyrate and propionate play one of the key roles in this communication. SCFAs are the metabolic results of the dietary fibers fermentation and they contribute to the regulation of several functions such as appetite regulation, gut barrier function, glucose homeostasis and immunomodulation (231).

The positive effect of fibers and SCFAs in the moderation of chronic inflammatory disorders has gained more and more attention, and it opens to the possibility to use these molecules as co-treatment in clinical studies (232,233). The gut-brain, involved in the regulation of chronic inflammation, is also related to the control of influenza infections. A recent study demonstrates the beneficial effects of the administration of SCFAs to mice in the control influenza infection (234).

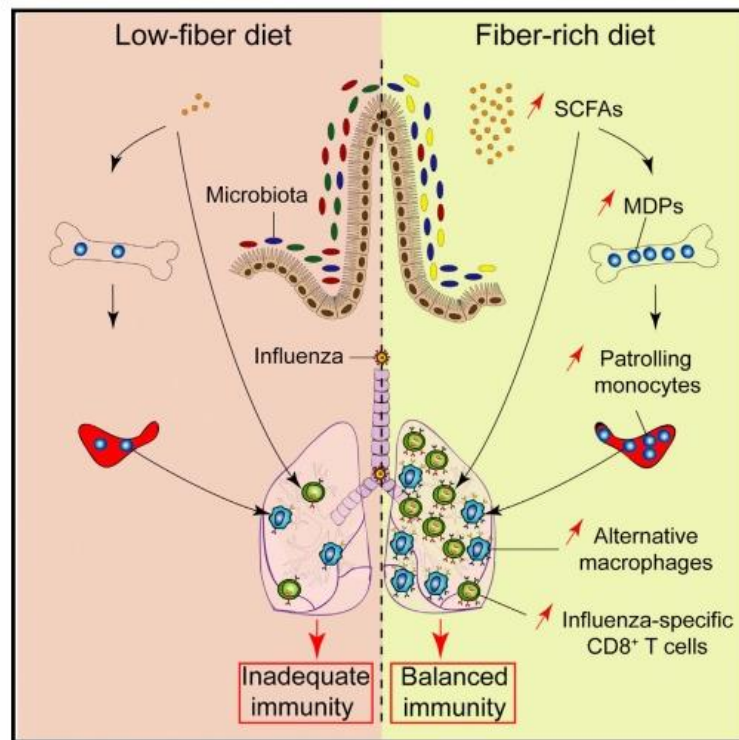


Figure 49 Dietary fiber protection effects against Flu mechanisms (234)

As mentioned previously, the colon hosts the higher concentration of bacteria in the human body. Since the SCFAs production is the result of the bacterial fermentation activities, the highest concentration of these metabolites resides in the colon. Interindividual differences in the microbiome composition can result in different types and production rates of SCFAs.

The colonic administration of SCFAs may provide health advantages while eliminating the complication of bacterial "singularity" (235).

As an example, butyrate is currently studied for its anti-cancer properties in the colon, where it promotes the cancerogenic cells' apoptosis and inhibits the oncogenic signalling (236,237). Although butyrate potential as a promising chemotherapeutic agent (237,238) its low bioavailability prevents its clinical translation (239). In order to improve butyrate bioavailability, tributyrin was formulated for the specific delivery to

the small intestine as a source of the metabolites (240) the results are encouraging but the concentrations delivered remains very low.

Another example is represented by inulin-propionate ester (IPE), where the covalent bound with inulin improves the molecule bioavailability. The bond is hydrolysed in the colon by the microbiome and the propionate is released (241,242). IPE showed promising results in the treatment of fatty liver disease (242), reducing further weight gain, intrahepatocellular lipid content, abdominal adipose tissue distribution and insulin sensitivity (241).

5.2. Materials and methods

5.2.1. Materials

Sodium acetate (Sigma-Aldrich Co., Steinheim, Germany); Eudragit® L100 (methacrylic acid-methyl methacrylate copolymer (1:1)), (Evonik Industries AG, Essen Germany); ethylcellulose (Ethocel™, Colorcon, Kent, England); potassium dihydrogen phosphate (VWR, Leuven, Belgium); Hydrochloric acid S.G. (FisherScientific, Loughborough, UK); Sodium hydroxide White Pellets (FisherScientific, Loughborough, UK).

5.2.2. Preparation of the spray dried formulation

Ethylcellulose (7 %) and Eudragit L (10 %) were dissolved in ethanol. Different amounts of sodium acetate were added (as indicated). The obtained dispersions were spray dried in a Mini Buchi Spray Dryer B-290, using the following conditions: inlet temperature = 90 °C, feed rate = 3 ml/min, nozzle diameter = 0.7 mm, drying gas flow = 414 L/h, aspirator flow rate 35 m³/h.

5.2.3. *In vitro* drug release measurements

40 mg microparticles were placed into 15 mL falcon tubes, filled with: (i) 10.0 mL HCl (pH=1.2); or (ii) 10.0 mL phosphate buffer (pH=6.8). The tubes were incubated at 37 °C under horizontal agitation (80 rpm). At predetermined time points, 1 mL samples were withdrawn using filter syringes and replaced with fresh medium. The drug content was determined by HPLC-IR analysis using a Waters Alliance e2695 (Coregel ORH-801 column, mobile phase: 10 mM H₂SO₄; flow rate: 0.6 mL/min; column temperature: 35 °C; injection volume: 50 uL). All experiments were performed in triplicate. Mean values +/- standard deviations are reported.

5.2.4. Impact of acetate loaded microparticle against IAV infection *in vivo*

Six 8-9 weeks old C57BL male mice received daily 45 mg microparticles (loaded with 30 % sodium acetate) suspended in 300 uL phosphate buffer (pH=6.8) (intra-gastric administration). Control groups received a phosphate buffer (pH=6.8) free of microparticles. The treatment started 5 days before the infection and until the end of the procedure. Infection was performed by a sub-lethal dose of influenza virus H3N2 (clinically isolated, 50 PFU/50 uL, given intranasally under anaesthesia), and animals were sacrificed 7 days post infection).

Experimental groups:

- 1: non-infected mice treated with buffer only (MOCK): n=5
- 2: infected mice treated with buffer only (IAV/ v_h) n=10
- 3: infected mice treated with Na-acetate suspension (IAV/Acetate) n=4.

Analysed parameters

Day -5: Acetate administration

Day 0: Animals are weighted and infected with IAV

From day 1 to day 7: Daily weighing of animals: measurement of body weight loss, clinical observation (spiky hair, consistency of faeces): morbidity/survival

Day 7: Sacrifice

Sampling of peripheral blood (ELISA)

Systemic inflammatory status. The quantification of inflammatory cytokines (examples: IL-6, IFN- γ) in the serum.

Lung recovery

Viral load: qRT-PCR (or plaque assay)

Histological analysis of the lungs (inflammation, congestion, haemorrhage, thrombosis, hyperplasia, edema, necrosis)

Inflammatory state and antiviral response: Expression of 15 genes (*IL-6*, *Ifng*, *Tnfa*, *Mx1*, *Ace2/Ace*, *Isg15*, etc.) by quantitative RT-PCR.

Colonic recovery

Inflammatory state of the colon: expression of 15 genes (examples: *IL-6*, *Ifng*, *Tnfa*, *Mx1*, *Ace2/Ace*, *Isg15*, etc.) by quantitative RT-PCR

Impact on the intestinal barrier: expression of *Zo-1*, *occludin* by quantitative RT-PCR

5.3. Results and discussion

5.3.1. *In vitro* drug release

Na-acetate is one of the main short chain fatty acids produced by the colonic microbiome through the anaerobic fermentation of indigestible polysaccharides. Multiple effects are associated with high concentration of this metabolite in the colon, including the increase of diversity and abundance of beneficial bacteria in the GIT (243) and the reduction of intestinal inflammation, by suppressing MAPK and NF- κ B signaling pathways (244).

Therefore, the colonic administration of Na-acetate could have a direct impact on the inflammation, regulating the chemical signalling of the immune response, and benefit to the microbiome population, promoting its growth and so reinforcing its protective action.

Na-acetate was vectorized to the colon encapsulating the molecule in a polymer blend. Ethylcellulose was selected as water insoluble polymer in order to prevent the Na-acetate release in the upper GIT and Eudragit[®] L100 is a pH sensitive polymer (pH threshold higher than 5.5).

The spray dried microparticles were loaded with different percentages (from 5 to 40 %) of drug (Na-acetate) in order to evaluate what was the maximum drug loading achievable and how the drug loading influences the drug release through the matrix. A fixed percentage of Eudragit[®] L100 and the amount ethylcellulose varied following the Na-acetate loading. *In vitro* drug release was performed in HCl pH=1.2 to evaluate the drug release in acidic condition and phosphate buffer pH=6.8 to evaluate the release in pH simulating the colonic environment. Figure 50 shows the drug release profiles of the formulations loaded with different percentages of Na-acetate. Between 5 % and 30 % drug loading, the higher is the concentration of drug in the formulation and the higher is the drug released during time. When the particles are loaded with 40 % of drug, the release is slower. During the preparation of the drug dispersion, prior spray drying, a precipitation phenomenon was observed when Na-acetate was added to the alcoholic

solution of ethylcellulose and methacrylic acid-methyl methacrylate copolymer. This phenomenon is currently under evaluation and might be the reason why different drug releases are observed at higher drug loading. Particular attention is paid to the possible protection of the drug prior dispersion in the alcoholic polymer solution. The hypothesis is that complexation phenomena take place between the drug and the polymeric matrix.

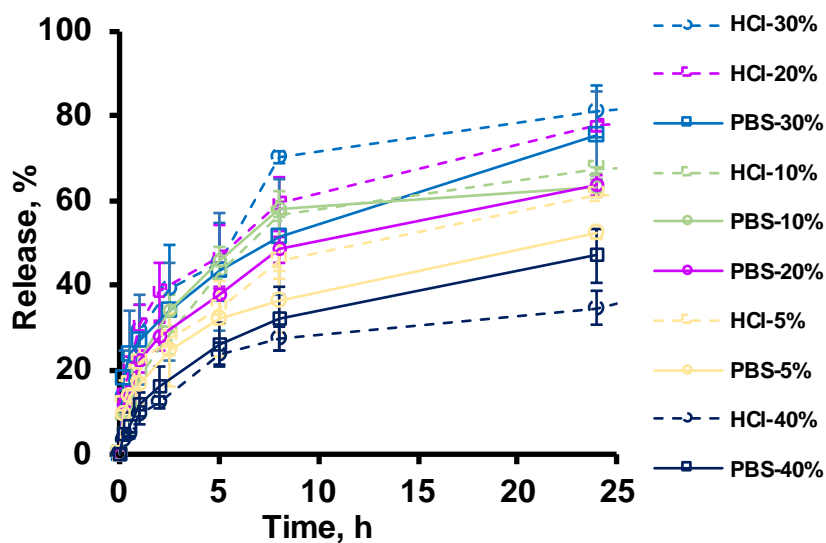


Figure 50 Na-acetate release from the investigated microparticles in HCl pH=1.2 (dashed curves) or phosphate buffer pH=6.8 (solid curves). The drug loading was varied as indicated.

5.3.2. *In vivo* study in mice model

Considering the *in vitro* drug release profiles of the different formulations, the microparticles loaded with 30 % of Na-acetate were selected for the *in vivo* study. This formulation shows the higher drug release with the higher drug loading. Although no difference is observed between the drug release in HCl (pH=1.2) or PB (pH=6.8), the drug release is controlled over time and almost 80% of drug is released within 24 h.

It is important to note that 2 mice out of 6 died in the group treated with acetate, one before infection and the second on D+1 post infection. As a result, only 4 mice remained in the experimental group. This mortality can be explained by the fact that the acetate solution was very thick and hardened in the gastric tube and may have obstructed the oesophagus.

The weight loss induced by the infection in comparison to control mice (MOCK), starting at 6DPI, was significantly attenuated ($p=0.053$) by acetate supplementation (Figure 51 A, B). Acetate was also able to limit the decreased length of the colon (Figure 51 C) and to reduce the viral load, measured at 7 DPI by specific TaqMan qRT-PCR (Figure 51 D).

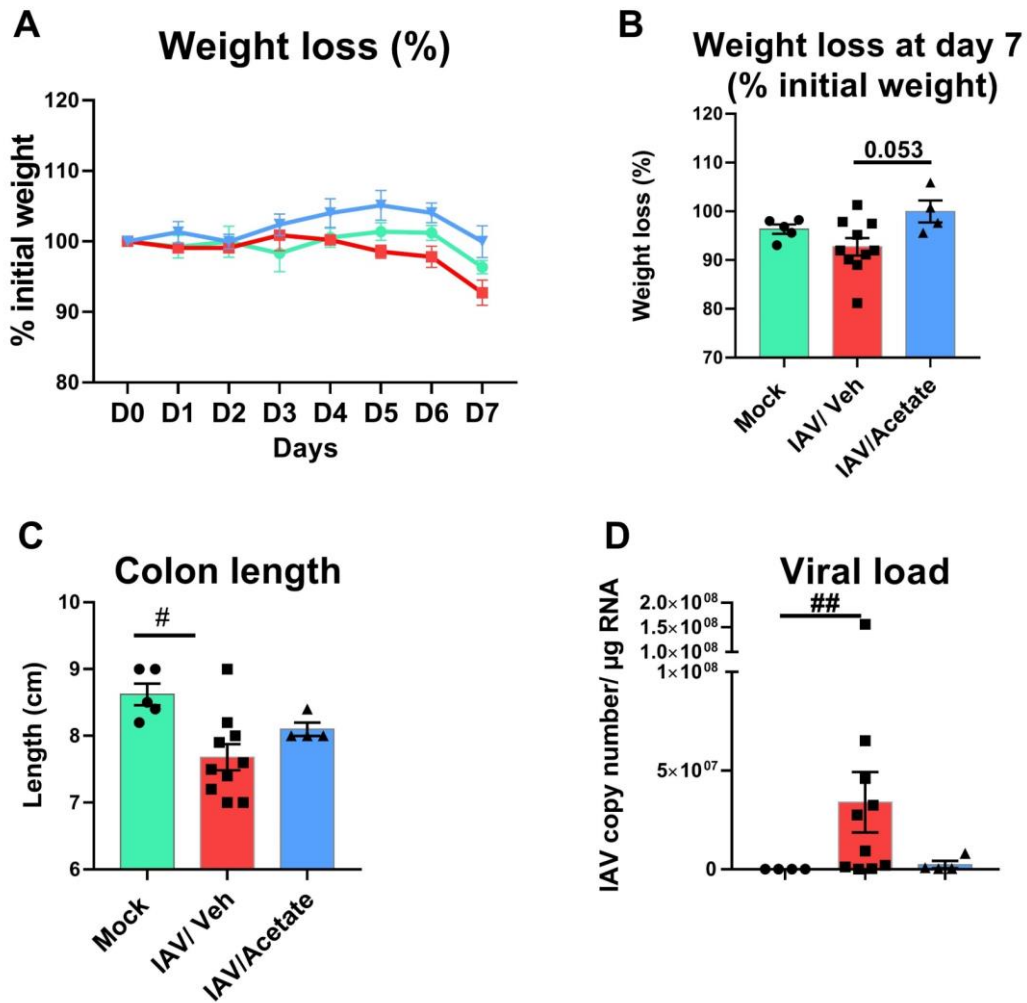


Figure 51 Protective effect of acetate against IAV infection. Weight loss A) during infection and B) at 7DPI and C) impact on colon length and D) viral load measured in the lung by specific qRT-PCR (Taq man). Results are expressed as mean \pm SEM. # corresponds to impact of IAV infection (IAV/Veh vs MOCK), * corresponds to treatment effect (IAV/Acetate vs IAV/ Veh); # $p < 0.05$; ## $p < 0.01$.

The reduction of the viral load induced by acetate supplementation was associated with a strong reduction of genes encoding type I (Ifnb), II (Ifng) and type III (Ifnl2, Ifnl3; $p < 0.05$) interferons (Figure 52 A), as well as interferon-stimulated genes (Mx1, Isg15, $p < 0.05$; Stat1; $p < 0.05$) (Figure 52 B). The protection was also associated with a reduction of inflammatory genes in the lung (Figure 52 C).

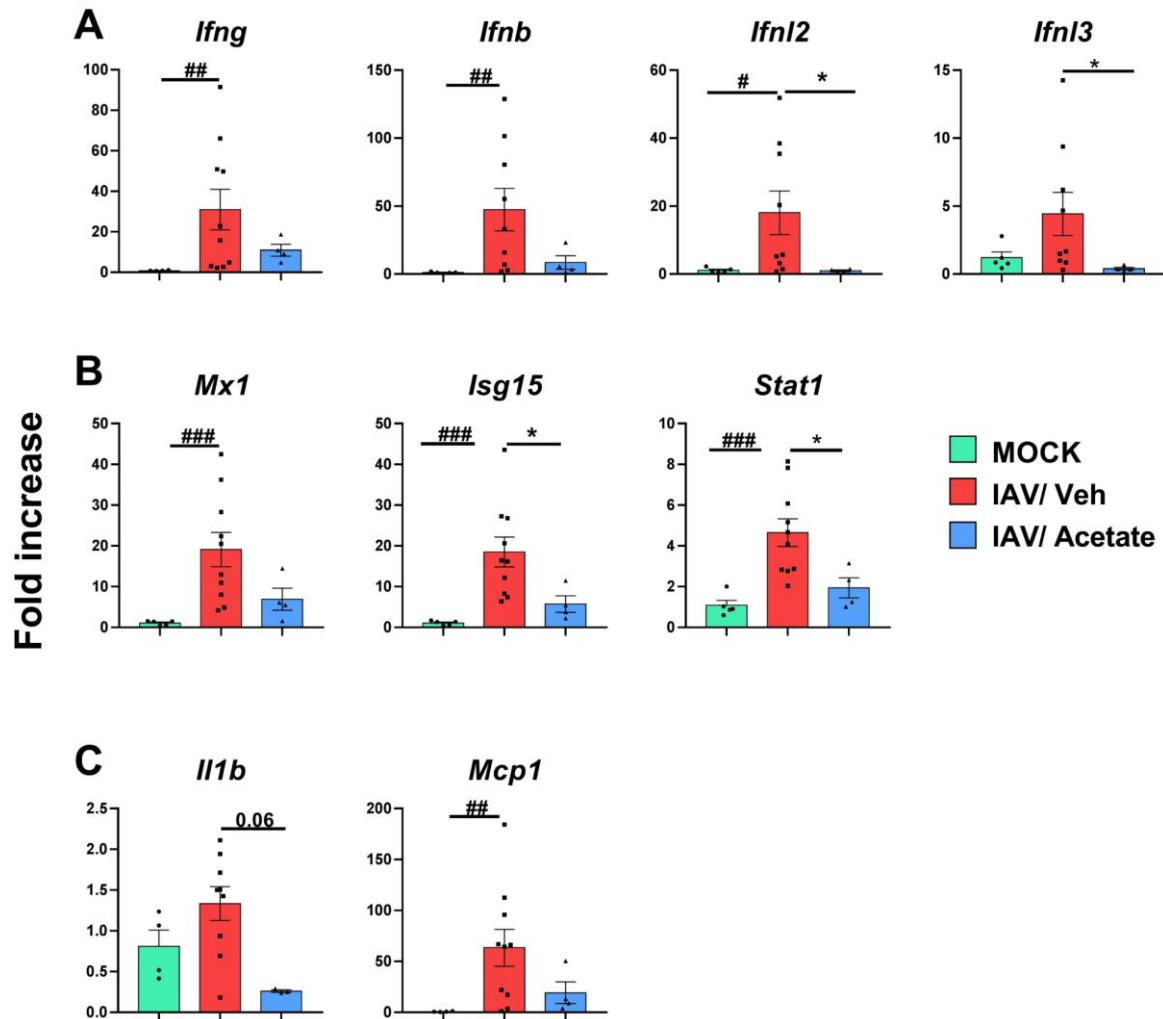


Figure 52 Impact of acetate supplementation on the expression of A) genes encoding interferons, B) interferon-stimulated genes and C) pro-inflammatory genes in the lung. Results are expressed as mean \pm SEM. # corresponds to impact of IAV infection (IAV/Veh vs MOCK), * corresponds to treatment effect (IAV/Acetate4 vs IAV/ Veh); # or * $p < 0.05$; ## $p < 0.01$, ### $p < 0.001$.

Even though the gut and lungs are anatomically distant from each other, a dynamic interaction of the gut and lung microbiota plays crucial roles to maintain immune homeostasis and prevent pulmonary diseases. Several reports have already shown that influenza infection is associated with gut dysbiosis and injuries, including reduction in the length of the colon, decreased mucosal integrity, increased gut permeability and mild diarrhea. In parallel, IAV infection also upregulated genes known as type I IFN-induced

genes in the gastrointestinal tract (GIT), however at a lower level than observed in the lung. It was indeed observed that IAV infection was associated with increased inflammatory and anti-viral responses in the colon which tend to be decreased in mice supplemented with acetate (Figure 53).

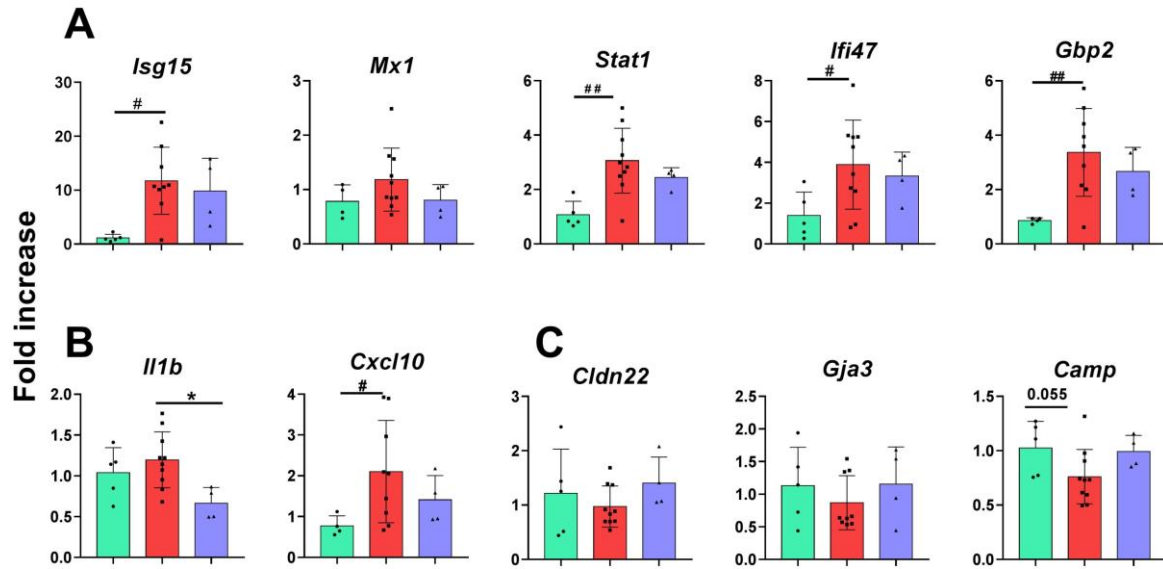


Figure 53 Impact of acetate supplementation on the expression of A) interferon-stimulated genes, B) inflammatory genes and C) genes encoding Cldn22 (Tight junction); GJA3 (gap junction) and Camp (cathelicidin antimicrobial peptide) in the colon. Results are expressed as mean \pm SEM. # corresponds to impact of IAV infection (IAV/Veh vs MOCK), # or * p < 0.05; ## p < 0.01.

5.4. Conclusion

Preliminary results suggest that controlled oral release of acetate has a positive impact on IAV infection, limiting weight loss and viral load, and a fairly significant impact on the anti-viral and inflammatory response markers in the lung, which correlates with the decreased viral load. Interestingly, this was linked to a decrease in the expression of ISG and inflammatory genes in the colon and slight restoration of genes involved in epithelium integrity.

6. Chapter: Conclusions and future perspectives

Outstanding progresses are constantly made by researchers in multiple fields. Patients' quality of life improves and the knowledge acquired by the healthcare industry has allowed targeted therapeutic treatments, improved patients' compliance and most of all increased life expectancy. Despite this, much still remains to be discovered and understood and the scientific effort, together with the technological advancement, are driving into a more specific and personalized medicine.

The rate of inflammatory bowel diseases worldwide increase of about 50 % in the last 20 years shifting from 3.32 million cases registered in 1990 to 4.9 million cases in 1990 (245). The purpose of this thesis is above all to provide technological alternatives to the oral treatment of inflammatory bowel disease, to improve the therapeutic effects and reduce the side effects of commercialized solutions.

The first part of the study focused on a polymer screening to identify the most promising polysaccharides able to deliver the drug directly to the colon. The site-specific delivery exploits the enzymatic degradation carried out by the colonic microbiota and several studies conducted *in vitro* showed the potential of six polymers. Aloe vera extract, reishi extract, pregelatinized starch, maize maltodextrin, xylan and inulin blended with ethylcellulose were able to prevent the drug release in the early hours of exposition to the release media and allowed the drug to be release in the presence of colonic bacteria from IBD patients after about 6 hours. Interestingly, two of the selected polymers: aloe vera and reishi extract, provided a similar drug release profile after exposition to human, dogs and rats' colonic bacteria. The ability to release the drug similarly in different species (animal models and human) is of major interest because this can prevent erroneous conclusions during the preclinical development phase.

The second part of the study focused on the development of 5-ASA loaded formulations coated with a blend of ethylcellulose and alternatively one of the six promising candidates selected in phase 1. *In vitro* drug release was performed using two different techniques: (i) in the laboratory, simulating the different section of the gastrointestinal

tract in a static way and (ii) using the m-SHIME[®], a semi-dynamic gastrointestinal release model for colon-targeting (developed by ProDigest). The results highlighted aloe vera extract powder ability to prevent the drug release in acidic conditions and partially in the small intestine simulated environment allowing the drug to be released mostly in the colon, thanks to the enzymatic degradation by the colonic microbiome.

The third phase of the study focused on pharmaceutical 3D Printing of capsule made with the blend of the selected polymers. Selective laser sintering (SLS) presented a limitation in the resolution of the 3D printed objects. It was possible to print only simple and flat shape and the object were too fragile and brittle to be manipulated. Direct powder extrusion was then employed for the production of more complex shapes such as capsules. This technique presented higher resolution; the objects' shape was more defined compare to the SLS technology. Although it was possible to print simple shapes with most of the polymer blends, only aloe vera allowed the 3D printing of capsules. X-ray microCT analysis showed the high porosity of the internal structure and underlined the fact the melted material disposition is not homogeneous during the printing process. An important density difference is observed in the object between the beginning and the end of the printing, furthermore the process is time consuming and not reproducible. Great caution must be paid to the selection of the printing settings to develop a robust technique and prevent the polymer degradation.

The last part of the project focused on the importance of the microbiome activity, in particular on the production of metabolites after the fermentation of non-digestible polysaccharides. These metabolites, mainly short chain fatty acids, play an important role in the regulation of the immune system response against infections and inflammation. The direct administration of such molecules to the colon, increased the in-site concentration of these mediators and improved the body defense both *in-site* (in the colon) and systemically (in the lungs).

Future studies should address the *in vivo* efficacy of these functional coatings in animal models of inflammatory bowel disease. Furthermore, a combination of enzyme-sensitive and pH-sensitive polymers should be studied to prevent the risk of therapeutic failure.

References

1. Awad A, Madla CM, McCoubrey LE, Ferraro F, Gavins FKH, Buanz A, et al. Clinical translation of advanced colonic drug delivery technologies. *Adv Drug Deliv Rev.* 2022 Feb;181:114076.
2. Crouwel F, Buijter HJC, de Boer NK. Gut microbiota-driven drug metabolism in inflammatory bowel disease. *J Crohns Colitis.* 2020 Jul 11;15(2):307–15.
3. Enright EF, Gahan CGM, Joyce SA, Griffin BT. The Impact of the Gut Microbiota on Drug Metabolism and Clinical Outcome. *Yale J Biol Med.* 2016 Sep 30;89(3):375–82.
4. Flowers SA, Evans SJ, Ward KM, McInnis MG, Ellingrod VL. Interaction Between Atypical Antipsychotics and the Gut Microbiome in a Bipolar Disease Cohort. *Pharmacotherapy.* 2017 Mar;37(3):261–7.
5. The Human Microbiome Project Consortium. Structure, function and diversity of the healthy human microbiome. *Nature.* 2012 Jun;486(7402):207–14.
6. Hatton GB, Madla CM, Rabbie SC, Basit AW. Gut reaction: impact of systemic diseases on gastrointestinal physiology and drug absorption. *Drug Discov Today.* 2019 Feb 1;24(2):417–27.
7. Haiser HJ, Seim KL, Balskus EP, Turnbaugh PJ. Mechanistic insight into digoxin inactivation by *Eggerthella lenta* augments our understanding of its pharmacokinetics. *Gut Microbes.* 2014;5(2):233–8.
8. van Kessel SP, Frye AK, El-Gendy AO, Castejon M, Keshavarzian A, van Dijk G, et al. Gut bacterial tyrosine decarboxylases restrict levels of levodopa in the treatment of Parkinson's disease. *Nat Commun.* 2019 Jan 18;10(1):310.
9. Wu H, Esteve E, Tremaroli V, Khan MT, Caesar R, Mannerås-Holm L, et al. Metformin alters the gut microbiome of individuals with treatment-naive type 2 diabetes, contributing to the therapeutic effects of the drug. *Nat Med.* 2017 Jul;23(7):850–8.
10. Hakoziaki T, Richard C, Elkrief A, Hosomi Y, Benlaïfaoui M, Mimpfen I, et al. The Gut Microbiome Associates with Immune Checkpoint Inhibition Outcomes in Patients with Advanced Non-Small Cell Lung Cancer. *Cancer Immunol Res.* 2020 Oct;8(10):1243–50.
11. Mager LF, Burkhard R, Pett N, Cooke NCA, Brown K, Ramay H, et al. Microbiome-derived inosine modulates response to checkpoint inhibitor immunotherapy. *Science.* 2020 Sep 18;369(6510):1481–9.

12. Routy B, Le Chatelier E, Derosa L, Duong CPM, Alou MT, Daillère R, et al. Gut microbiome influences efficacy of PD-1-based immunotherapy against epithelial tumors. *Science*. 2018 Jan 5;359(6371):91–7.
13. Wang J, Yadav V, Smart AL, Tajiri S, Basit AW. Stability of peptide drugs in the colon. *Eur J Pharm Sci*. 2015 Oct;78:31–6.
14. McConnell EL, Liu F, Basit AW. Colonic treatments and targets: issues and opportunities. Vol. 17, *J Drug Target*. 2009. p. 335–63.
15. Muller J, Keiser M, Drozdik M, Oswald S. Expression, regulation and function of intestinal drug transporters: an update. Vol. 398, *Biol Chem*. 2017. p. 175–92.
16. Tubic-Grozdanis M, Hilfinger JM, Amidon GL, Kim JS, Kijek P, Staubach P, et al. Pharmacokinetics of the CYP 3A substrate simvastatin following administration of delayed versus immediate release oral dosage forms. *Pharm Res*. 2008 Jul;25(7):1591–600.
17. Yadav V, Varum F, Bravo R, Furrer E, Basit AW. Gastrointestinal stability of therapeutic anti-TNF α IgG1 monoclonal antibodies. *Int J Pharm*. 2016 Apr 11;502(1–2):181–7.
18. Wang J, Yadav V, Smart AL, Tajiri S, Basit AW. Toward oral delivery of biopharmaceuticals: an assessment of the gastrointestinal stability of 17 peptide drugs. *Mol Pharm*. 2015 Mar 2;12(3):966–73.
19. Nugent SG, Kumar D, Rampton DS, Evans DF. Intestinal luminal pH in inflammatory bowel disease: possible determinants and implications for therapy with aminosalicylates and other drugs. *Gut*. 2001 Apr;48(4):571–7.
20. Stillhart C, Vučićević K, Augustijns P, Basit AW, Batchelor H, Flanagan TR, et al. Impact of gastrointestinal physiology on drug absorption in special populations--An UNGAP review. *Eur J Pharm Sci Off J Eur Fed Pharm Sci*. 2020 Apr 30;147:105280.
21. Effinger A, O’Driscoll C, McAllister M, Fotaki N. Gastrointestinal diseases and their impact on drug solubility: Ulcerative Colitis. *Eur J Pharm Sci Off J Eur Fed Pharm Sci*. 2020 Sep 1;152:105458.
22. Effinger A, O’Driscoll CM, McAllister M, Fotaki N. Predicting budesonide performance in healthy subjects and patients with Crohn’s disease using biorelevant in vitro dissolution testing and PBPK modeling. *Eur J Pharm Sci Off J Eur Fed Pharm Sci*. 2021 Feb 1;157:105617.
23. Effinger A, O’Driscoll CM, McAllister M, Fotaki N. Gastrointestinal diseases and their impact on drug solubility: Crohn’s disease. *Eur J Pharm Sci Off J Eur Fed Pharm Sci*. 2020 Sep 1;152:105459.

24. Effinger A, O'Driscoll CM, McAllister M, Fotaki N. Gastrointestinal diseases and their impact on drug solubility: Celiac disease. *Eur J Pharm Sci Off J Eur Fed Pharm Sci*. 2020 Sep 1;152:105460.
25. Litou C, Effinger A, Kostewicz ES, Box KJ, Fotaki N, Dressman JB. Effects of medicines used to treat gastrointestinal diseases on the pharmacokinetics of coadministered drugs: a PEARRL Review. *J Pharm Pharmacol*. 2019 Apr;71(4):643–73.
26. Press AG, Hauptmann IA, Hauptmann L, Fuchs B, Fuchs M, Ewe K, et al. Gastrointestinal pH profiles in patients with inflammatory bowel disease. *Aliment Pharmacol Ther*. 1998 Jul;12(7):673–8.
27. Fischer M, Siva S, Wo JM, Fadda HM. Assessment of Small Intestinal Transit Times in Ulcerative Colitis and Crohn's Disease Patients with Different Disease Activity Using Video Capsule Endoscopy. *AAPS PharmSciTech*. 2017 Feb;18(2):404–9.
28. Martini E, Krug SM, Siegmund B, Neurath MF, Becker C. Mend Your Fences: The Epithelial Barrier and its Relationship With Mucosal Immunity in Inflammatory Bowel Disease. *Cell Mol Gastroenterol Hepatol*. 2017 Jul;4(1):33–46.
29. El-Salhy M. Recent developments in the pathophysiology of irritable bowel syndrome. *World J Gastroenterol*. 2015;21(25):7621.
30. Walsh J, Griffin BT, Clarke G, Hyland NP. Drug-gut microbiota interactions: implications for neuropharmacology. *Br J Pharmacol*. 2018 Dec;175(24):4415–29.
31. Yadav V, Varum F, Bravo R, Furrer E, Bojic D, Basit AW. Inflammatory bowel disease: exploring gut pathophysiology for novel therapeutic targets. Vol. 176, *Transl Res*. 2016. p. 38–68.
32. Svartz N. Sulfasalazine: II. Some notes on the discovery and development of salazopyrin. *Am J Gastroenterol*. 1988 May;83(5):497–503.
33. Azad Khan AK, Piris J, Truelove SC. An experiment to determine the active therapeutic moiety of sulphasalazine. *Lancet Lond Engl*. 1977 Oct 29;2(8044):892–5.
34. RILEY S. What dose of 5-aminosalicylic acid (mesalazine) in ulcerative colitis? *Gut*. 1998 Jun;42(6):761–3.
35. Klotz U. Clinical pharmacokinetics of sulphasalazine, its metabolites and other prodrugs of 5-aminosalicylic acid. *Clin Pharmacokinet*. 1985;10(4):285–302.
36. Wadworth AN, Fitton A. Olsalazine. A review of its pharmacodynamic and pharmacokinetic properties, and therapeutic potential in inflammatory bowel disease. *Drugs*. 1991 Apr;41(4):647–64.

37. Chan RP, Pope DJ, Gilbert AP, Sacra PJ, Baron JH, Lennard-Jones JE. Studies of two novel sulfasalazine analogs, ipsalazide and balsalazide. *Dig Dis Sci*. 1983 Jul;28(7):609–15.
38. Rasmussen SN, Binder V, Maier K, Bondesen S, Fischer C, Klotz U, et al. Treatment of Crohn's disease with peroral 5-aminosalicylic acid. *Gastroenterology*. 1983 Dec;85(6):1350–3.
39. McConnell EL, Fadda HM, Basit AW. Gut instincts: explorations in intestinal physiology and drug delivery. Vol. 364, *Int J Pharm*. 2008. p. 213–26.
40. Wiley.com [Internet]. [cited 2021 Dec 8]. Textbook of Gastroenterology, 5th Edition | Wiley. Available from: <https://www.wiley.com/en-us/Textbook+of+Gastroenterology%2C+5th+Edition-p-9781444359411>
41. Helander HF, Fändriks L. Surface area of the digestive tract – revisited. *Scand J Gastroenterol*. 2014 Jun 1;49(6):681–9.
42. Lemmens G, Van Camp A, Kourula S, Vanuytsel T, Augustijns P. Drug Disposition in the Lower Gastrointestinal Tract: Targeting and Monitoring. *Pharmaceutics*. 2021 Jan 26;13(2):161.
43. Major G, Murray K, Singh G, Nowak A, Hoad CL, Marciani L, et al. Demonstration of differences in colonic volumes, transit, chyme consistency, and response to psyllium between healthy and constipated subjects using magnetic resonance imaging. *Neurogastroenterol Motil*. 2018 Sep;30(9):e13400.
44. Murray K, Hoad CL, Mudie DM, Wright J, Heissam K, Abrehart N, et al. Magnetic Resonance Imaging Quantification of Fasted State Colonic Liquid Pockets in Healthy Humans. *Mol Pharm*. 2017 Aug 7;14(8):2629–38.
45. Schiller C, Frohlich CP, Giessmann T, Siegmund W, Monnikes H, Hosten N, et al. Intestinal fluid volumes and transit of dosage forms as assessed by magnetic resonance imaging. Vol. 22, *Aliment Pharmacol Ther*. 2005. p. 971–9.
46. Tannergren C, Bergendal A, Lennernäs H, Abrahamsson B. Toward an Increased Understanding of the Barriers to Colonic Drug Absorption in Humans: Implications for Early Controlled Release Candidate Assessment. *Mol Pharm*. 2009 Feb 2;6(1):60–73.
47. Taherali F, Varum F, Basit AW. A slippery slope: On the origin, role and physiology of mucus. *Adv Drug Deliv Rev*. 2018 Jan;124:16–33.
48. Mahar KM, Portelli S, Coatney R, Chen EP. Gastric pH and Gastric Residence Time in Fasted and Fed Conscious Beagle Dogs using the Bravo® pH System. *J Pharm Sci*. 2012 Jul;101(7):2439–48.

49. Chen EP, Mahar Doan KM, Portelli S, Coatney R, Vaden V, Shi W. Gastric pH and Gastric Residence Time in Fasted and Fed Conscious Cynomolgus Monkeys Using the Bravo® pH System. *Pharm Res.* 2008 Jan;25(1):123–34.
50. Kararli TT. Comparison of the gastrointestinal anatomy, physiology, and biochemistry of humans and commonly used laboratory animals. *Biopharm Drug Dispos.* 1995 Jul;16(5):351–80.
51. Evans DF, Pye G, Bramley R, Clark AG, Dyson TJ, Hardcastle JD. Measurement of gastrointestinal pH profiles in normal ambulant human subjects. Vol. 29, *Gut.* 1988. p. 1035–41.
52. Dressman JB, Amidon GL, Reppas C, Shah VP. Dissolution testing as a prognostic tool for oral drug absorption: immediate release dosage forms. *Pharm Res.* 1998 Jan;15(1):11–22.
53. Ibekwe DF VC, Fadda, HM, McConnell, EL, Khela, MK, Evans, Basit AW. Interplay Between Intestinal pH, Transit Time and Feed Status on the In Vivo Performance of pH Responsive Ileo-Colonic Release Systems. Vol. 25, *Pharmaceutical Research.* 2008. p. 1828–35.
54. Bansal V, Malviya R, Malaviya T, Sharma PK. Novel prospective in colon specific drug delivery system. *Polim Med.* 2014 Jun;44(2):109–18.
55. Maderuelo C, Lanao JM, Zarzuelo A. Enteric coating of oral solid dosage forms as a tool to improve drug bioavailability. *Eur J Pharm Sci.* 2019 Oct;138:105019.
56. Maroni A, Moutaharrik S, Zema L, Gazzaniga A. Enteric coatings for colonic drug delivery: state of the art. *Expert Opin Drug Deliv.* 2017 Sep 2;14(9):1027–9.
57. Liu F, Lizio R, Meier C, Petereit HU, Blakey P, Basit AW. A novel concept in enteric coating: a double-coating system providing rapid drug release in the proximal small intestine. *J Control Release Off J Control Release Soc.* 2009 Jan 19;133(2):119–24.
58. Routledge & CRC Press [Internet]. [cited 2021 Dec 9]. *Pharmaceutical Dosage Forms - Tablets.* Available from: <https://www.routledge.com/Pharmaceutical-Dosage-Forms---Tablets/Augsburger-Hoag/p/book/9781420063455>
59. Yoshida T, Lai TC, Kwon GS, Sako K. pH- and ion-sensitive polymers for drug delivery. *Expert Opin Drug Deliv.* 2013 Nov;10(11):1497–513.
60. Limmatvapirat S, Limmatvapirat C, Luangtana-anan M, Nunthanid J, Oguchi T, Tozuka Y, et al. Modification of physicochemical and mechanical properties of shellac by partial hydrolysis. *Int J Pharm.* 2004 Jun;278(1):41–9.
61. Davis M, Ichikawa I, Williams EJ, Banker GS. Comparison and evaluation of enteric polymer properties in aqueous solutions. *Int J Pharm.* 1986 Feb;28(2–3):157–66.

62. Dew M, Hughes P, Lee M, Evans B, Rhodes J. An oral preparation to release drugs in the human colon. *Br J Clin Pharmacol*. 1982 Sep;14(3):405–8.
63. Dew M, Ryder R, Evans N, Evans B, Rhodes J. Colonic release of 5-amino salicylic acid from an oral preparation in active ulcerative colitis. *Br J Clin Pharmacol*. 1983 Aug;16(2):185–7.
64. Fadda HM, Basit AW. Dissolution of pH responsive formulations in media resembling intestinal fluids: bicarbonate versus phosphate buffers. *J Drug Deliv Sci Technol*. 2005;15(4):273–9.
65. Varum FJO, Hatton GB, Freire AC, Basit AW. A novel coating concept for ileo-colonic drug targeting: Proof of concept in humans using scintigraphy. *Eur J Pharm Biopharm*. 2013 Aug;84(3):573–7.
66. Merchant HA, Goyanes A, Parashar N, Basit AW. Predicting the gastrointestinal behaviour of modified-release products: Utility of a novel dynamic dissolution test apparatus involving the use of bicarbonate buffers. *Int J Pharm*. 2014 Nov;475(1–2):585–91.
67. Schellekens RCA, Stellaard F, Mitrovic D, Stuurman FE, Kosterink JGW, Frijlink HW. Pulsatile drug delivery to ileo-colonic segments by structured incorporation of disintegrants in pH-responsive polymer coatings. *J Controlled Release*. 2008 Dec;132(2):91–8.
68. Schellekens RCA, Stellaard F, Olsder GG, Woerdenbag HJ, Frijlink HW, Kosterink JGW. Oral ileocolonic drug delivery by the colopulse-system: A bioavailability study in healthy volunteers. *J Controlled Release*. 2010 Sep 15;146(3):334–40.
69. Safdi AV. Determination of 5-ASA in Whole or Partial Mesalamine Delayed-Release Tablets Recovered from Fecal Samples of Healthy Volunteers: 412. *Am J Gastroenterol*. 2005 Sep;100:S159.
70. Schroeder KW, Tremaine WJ, Ilstrup DM. Coated Oral 5-Aminosalicylic Acid Therapy for Mildly to Moderately Active Ulcerative Colitis. *N Engl J Med*. 1987 Dec 24;317(26):1625–9.
71. McConnell EL, Short MD, Basit AW. An in vivo comparison of intestinal pH and bacteria as physiological trigger mechanisms for colonic targeting in man. *J Controlled Release*. 2008 Sep;130(2):154–60.
72. Goyanes A, Hatton GB, Merchant HA, Basit AW. Gastrointestinal release behaviour of modified-release drug products: Dynamic dissolution testing of mesalazine formulations. *Int J Pharm*. 2015 Apr;484(1–2):103–8.
73. Yoshimura N, Tadami T, Kawaguchi T, Sako M, Saniabadi A, Takazoe M. Long-Term Efficacy of a pH-Dependent Release Mesalamine Formulation, Asacol in Patients With Ulcerative Colitis Who Showed Inadequate Response to a Time-

Dependent Release Mesalamine Formulation, Pentasa: A Prospective Study. *Gastroenterology*. 2011 May 1;140.

74. John V, Shotton P, Moppert J, Theobald W. Gastrointestinal transit of Oros drug delivery systems in healthy volunteers: a short report. *Br J Clin Pharmacol*. 1985 Apr;19(S2):203S-206S.
75. Nandhra GK, Mark EB, Di Tanna GL, Haase A, Poulsen J, Christodoulides S, et al. Normative values for region-specific colonic and gastrointestinal transit times in 111 healthy volunteers using the 3D-Transit electromagnet tracking system: Influence of age, gender, and body mass index. *Neurogastroenterol Motil* [Internet]. 2020 Feb [cited 2021 Dec 10];32(2). Available from: <https://onlinelibrary.wiley.com/doi/10.1111/nmo.13734>
76. Metcalf AM, Phillips SF, Zinsmeister AR, MacCarty RL, Beart RW, Wolff BG. Simplified assessment of segmental colonic transit. *Gastroenterology*. 1987 Jan;92(1):40–7.
77. Graff J, Brinch K, Madsen JL. Gastrointestinal mean transit times in young and middle-aged healthy subjects: Gastrointestinal mean transit times. *Clin Physiol*. 2001 Mar;21(2):253–9.
78. Mahony D, Leary P, Quigley EMM. Aging and Intestinal Motility: A Review of Factors that Affect Intestinal Motility in the Aged. *Drugs Aging*. 2002;19(7):515–27.
79. Wang YT, Mohammed SD, Farmer AD, Wang D, Zarate N, Hobson AR, et al. Regional gastrointestinal transit and pH studied in 215 healthy volunteers using the wireless motility capsule: influence of age, gender, study country and testing protocol. *Aliment Pharmacol Ther*. 2015 Sep;42(6):761–72.
80. Madla CM, Gavins FKH, Merchant HA, Orlu M, Murdan S, Basit AW. Let's talk about sex: Differences in drug therapy in males and females. *Adv Drug Deliv Rev*. 2021 Aug;175:113804.
81. Kumar D. In vitro inhibitory effect of progesterone on extrauterine human smooth muscle. *Am J Obstet Gynecol*. 1962 Nov;84(10):1300–4.
82. Gazzaniga A, Maroni A, Sangalli ME, Zema L. Time-controlled oral delivery systems for colon targeting. *Expert Opin Drug Deliv*. 2006 Sep;3(5):583–97.
83. Chacko A, Szaz KF, Howard J, Cummings JH. Non-invasive method for delivery of tracer substances or small quantities of other materials to the colon. *Gut*. 1990 Jan;31(1):106–10.
84. Chourasia MK, Jain SK. Pharmaceutical approaches to colon targeted drug delivery systems. *J Pharm Pharm Sci Publ Can Soc Pharm Sci Soc Can Sci Pharm*. 2003 Apr;6(1):33–66.

85. Kao CC, Chen SC, Sheu MT. Lag time method to delay drug release to various sites in the gastrointestinal tract. *J Controlled Release*. 1997 Feb 17;44(2):263–70.
86. Narisawa S, Nagata M, Danyoshi C, Yoshino H, Murata K, Hirakawa Y, et al. An Organic Acid-Induced Sigmoidal Release System for Oral Controlled-Release Preparations. *Pharm Res*. 1994 Jan 1;11(1):111–6.
87. Narisawa S, Nagata M, Ito T, Yoshino H, Hirakawa Y, Noda K. Drug release behavior in gastrointestinal tract of beagle dogs from multiple unit type rate-controlled or time-controlled release preparations coated with insoluble polymer-based film. *J Controlled Release*. 1995 Feb 1;33(2):253–60.
88. González-Rodríguez ML, Fernández-Hervás MJ, Caraballo I, Rabasco AM. Design and evaluation of a new central core matrix tablet. *Int J Pharm*. 1997 Jan 15;146(2):175–80.
89. González-Rodríguez ML, Maestrelli F, Mura P, Rabasco AM. In vitro release of sodium diclofenac from a central core matrix tablet aimed for colonic drug delivery. *Eur J Pharm Sci*. 2003 Sep 1;20(1):125–31.
90. Amidon S, Brown JE, Dave VS. Colon-Targeted Oral Drug Delivery Systems: Design Trends and Approaches. *AAPS PharmSciTech*. 2015 Aug;16(4):731–41.
91. Foppoli A, Maroni A, Moutaharrik S, Melocchi A, Zema L, Palugan L, et al. In vitro and human pharmacoscintigraphic evaluation of an oral 5-ASA delivery system for colonic release. *Int J Pharm*. 2019 Dec;572:118723.
92. HarperCollins Canada [Internet]. [cited 2021 Dec 9]. 10% Human - Alanna Collen - eBook. Available from: <https://www.harpercollins.ca/9780062346001/10-human/>
93. Dieterich W, Schink M, Zopf Y. Microbiota in the Gastrointestinal Tract. *Med Sci*. 2018 Dec 14;6(4):116.
94. MetaHIT Consortium, Qin J, Li R, Raes J, Arumugam M, Burgdorf KS, et al. A human gut microbial gene catalogue established by metagenomic sequencing. *Nature*. 2010 Mar;464(7285):59–65.
95. Myers B, Evans DN, Rhodes J, Evans BK, Hughes BR, Lee MG, et al. Metabolism and urinary excretion of 5-amino salicylic acid in healthy volunteers when given intravenously or released for absorption at different sites in the gastrointestinal tract. *Gut*. 1987 Feb 1;28(2):196–200.
96. Moens F, Van den Abbeele P, Basit AW, Dodoo C, Chatterjee R, Smith B, et al. A four-strain probiotic exerts positive immunomodulatory effects by enhancing colonic butyrate production in vitro. *Int J Pharm*. 2019 Jan 30;555:1–10.
97. Tian L, Wang XW, Wu AK, Fan Y, Friedman J, Dahlin A, et al. Deciphering functional redundancy in the human microbiome. *Nat Commun*. 2020 Dec;11(1):6217.

98. Zimmermann M, Zimmermann-Kogadeeva M, Wegmann R, Goodman AL. Mapping human microbiome drug metabolism by gut bacteria and their genes. *Nature*. 2019 Jun;570(7762):462–7.
99. Zimmermann M, Zimmermann-Kogadeeva M, Wegmann R, Goodman AL. Separating host and microbiome contributions to drug pharmacokinetics and toxicity. *Science*. 2019 Feb 8;363(6427):eaat9931.
100. Basit A. Advances in colonic delivery. Vol. 65, *Drugs*. 2005.
101. Bak A, Ashford M, Brayden DJ. Local delivery of macromolecules to treat diseases associated with the colon. *Adv Drug Deliv Rev*. 2018 Nov;136–137:2–27.
102. Pachuau L, Mazumder B. Colonic Drug Delivery Systems Based on Natural Polysaccharides and their Evaluation. *Mini-Rev Med Chem*. 2013 Oct 1;13(13):1982–91.
103. Kotla NG, Rana S, Sivaraman G, Sunnapu O, Vemula PK, Pandit A, et al. Bioresponsive drug delivery systems in intestinal inflammation: State-of-the-art and future perspectives. *Adv Drug Deliv Rev*. 2019 Jun 1;146:248–66.
104. Van Den Mooter G, Maris B, Samyn C, Augustijns P, Kinget R. Use of Azo Polymers for Colon-Specific Drug Delivery. *J Pharm Sci*. 1997 Dec;86(12):1321–7.
105. Leong CW, Newton JM, Basit AW, Podczeczek F, Cummings JH, Ring SG. The formation of colonic digestible films of amylose and ethylcellulose from aqueous dispersions at temperatures below 37 degrees C. *Eur J Pharm Biopharm Off J Arbeitsgemeinschaft Pharm Verfahrenstechnik EV*. 2002 Nov;54(3):291–7.
106. Siew LF, Basit AW, Newton JM. The properties of amylose–ethylcellulose films cast from organic-based solvents as potential coatings for colonic drug delivery. *Eur J Pharm Sci*. 2000 Aug;11(2):133–9.
107. Milojevic S, Newton JM, Cummings JH, Gibson GR, Louise Botham R, Ring SG, et al. Amylose as a coating for drug delivery to the colon: Preparation and in vitro evaluation using glucose pellets. *J Controlled Release*. 1996 Jan;38(1):85–94.
108. McCoubrey LE, Elbadawi M, Orlu M, Gaisford S, Basit AW. Harnessing machine learning for development of microbiome therapeutics. *Gut Microbes*. 2021 Jan 1;13(1):1872323.
109. Coombes Z, Yadav V, McCoubrey L, Freire C, Basit A, Conlan R, et al. Progestogens Are Metabolized by the Gut Microbiota: Implications for Colonic Drug Delivery. *Pharmaceutics*. 2020 Aug 12;12(8):760.
110. Carding S, Verbeke K, Vipond DT, Corfe BM, Owen LJ. Dysbiosis of the gut microbiota in disease. *Microb Ecol Health Dis* [Internet]. 2015 Feb 2 [cited 2021

111. Seifert A, Kashi Y, Livney YD. Delivery to the gut microbiota: A rapidly proliferating research field. *Adv Colloid Interface Sci.* 2019 Dec;274:102038.
112. Mulder M, Radjabzadeh D, Kiefte-de Jong JC, Uitterlinden AG, Kraaij R, Stricker BH, et al. Long-term effects of antimicrobial drugs on the composition of the human gut microbiota. *Gut Microbes.* 2020 Nov 9;12(1):1791677.
113. Maroni A, Del Curto MD, Zema L, Foppoli A, Gazzaniga A. Film coatings for oral colon delivery. *Int J Pharm.* 2013 Dec;457(2):372–94.
114. Joseph SK, Sabitha M, Nair SC. Stimuli-Responsive Polymeric Nanosystem for Colon Specific Drug Delivery. *Adv Pharm Bull.* 2020 Jan;10(1):1–12.
115. Hu Z, Kimura G, Mawatari S, Shimokawa T, Yoshikawa Y, Takada K. New preparation method of intestinal pressure-controlled colon delivery capsules by coating machine and evaluation in beagle dogs. *J Controlled Release.* 1998 Dec 4;56(1):293–302.
116. Takaya T, Ikeda C, Imagawa N, Niwa K, Takada K. Development of a Colon Delivery Capsule and the Pharmacological Activity of Recombinant Human Granulocyte Colony-stimulating Factor (rhG-CSF) in Beagle Dogs. *J Pharm Pharmacol.* 1995 Jun;47(6):474–8.
117. Matsuda KI, Takaya T, Shimoji F, Muraoka M, Yoshikawa Y, Takada K. Effect of food intake on the delivery of fluorescein as a model drug in colon delivery capsule after oral administration to beagle dogs. *J Drug Target.* 1996 Jan;4(2):59–67.
118. Barakat NS, Al-Suwayeh SA, Taha EI, Bakry Yassin AE. A new pressure-controlled colon delivery capsule for chronotherapeutic treatment of nocturnal asthma. *J Drug Target.* 2011 Jun;19(5):365–72.
119. Kamm MA, Sandborn WJ, Gassull M, Schreiber S, Jackowski L, Butler T, et al. Once-daily, high-concentration MMX mesalamine in active ulcerative colitis. *Gastroenterology.* 2007 Jan;132(1):66–75; quiz 432–3.
120. Merchant H, Fadda HM, Arafat BT, Basit AW. Physiological Bicarbonate Buffers: Stabilisation and Use as Dissolution Media for Modified Release Systems. *Int J Pharm.* 2009 Dec 1;382(1–2):56–60.
121. Wray H, Joseph R, Palmen M, Pierce D. P-0030: Combined pharmacokinetic and scintigraphic analyses for the comparison of 5-ASA release profiles from MMXTM mesalamine and another delayed-release mesalamine formulation. *Inflamm Bowel Dis.* 2008 Dec 1;14(suppl_3):S19–20.

122. Edsbäcker S, Bengtsson B, Larsson P, Lundin P, Nilsson A, Ulmius J, et al. A pharmacoscintigraphic evaluation of oral budesonide given as controlled-release (Entocort) capsules. *Aliment Pharmacol Ther.* 2003 Feb 15;17(4):525–36.
123. Travis SPL, Danese S, Kupcinkas L, Alexeeva O, D’Haens G, Gibson PR, et al. Once-daily budesonide MMX in active, mild-to-moderate ulcerative colitis: results from the randomised CORE II study. *Gut.* 2014 Mar;63(3):433–41.
124. Edsbäcker S, Andersson T. Pharmacokinetics of budesonide (Entocort EC) capsules for Crohn’s disease. *Clin Pharmacokinet.* 2004;43(12):803–21.
125. Bott C, Rudolph MW, Schneider ARJ, Schirrmacher S, Skalsky B, Petereit HU, et al. In vivo evaluation of a novel pH- and time-based multiunit colonic drug delivery system. *Aliment Pharmacol Ther.* 2004;20(3):347–53.
126. Casati F, Melocchi A, Moutaharrik S, Uboldi M, Foppoli A, Maroni A, et al. Injection Molded Capsules for Colon Delivery Combining Time-Controlled and Enzyme-Triggered Approaches. *Int J Mol Sci.* 2020 Mar 11;21(6):1917.
127. Yang L, Watanabe S, Li J, Chu JS, Katsuma M, Yokohama S, et al. Effect of Colonic Lactulose Availability on the Timing of Drug Release Onset in Vivo from a Unique Colon-Specific Drug Delivery System (CODES™). *Pharm Res Off J Am Assoc Pharm Sci.* 2003;20(3):429.
128. Katsuma M, Watanabe S, Takemura S, Sako K, Sawada T, Masuda Y, et al. Scintigraphic evaluation of a novel colon-targeted delivery system (CODES) in healthy volunteers. *J Pharm Sci.* 2004 May;93(5):1287–99.
129. Katsuma M, Watanabe S, Kawai H, Takemura S, Masuda Y, Fukui M. Studies on lactulose formulations for colon-specific drug delivery. *Int J Pharm.* 2002 Dec 5;249(1–2):33–43.
130. Ibekwe VC, Khela MK, Evans DF, Basit AW. A new concept in colonic drug targeting: a combined pH-responsive and bacterially-triggered drug delivery technology. *Aliment Pharmacol Ther.* 2008 Oct;28(7):911–6.
131. Dodoo CC, Wang J, Basit AW, Stapleton P, Gaisford S. Targeted delivery of probiotics to enhance gastrointestinal stability and intestinal colonisation. *Int J Pharm.* 2017 Sep 15;530(1):224–9.
132. Varum F, Freire AC, Fadda HM, Bravo R, Basit AW. A dual pH and microbiota-triggered coating (Phloral™) for fail-safe colonic drug release. *Int J Pharm.* 2020 Jun;583:119379.
133. Varum F, Freire AC, Bravo R, Basit AW. OPTICORE™, an innovative and accurate colonic targeting technology. *Int J Pharm.* 2020 Jun 15;583:119372.
134. Varum FJO, Veiga F, Sousa JS, Basit AW. Mucoadhesive platforms for targeted delivery to the colon. *Int J Pharm.* 2011 Nov 25;420(1):11–9.

135. Kararli TT, Kirchoff CF, Truelove JE. Ionic strength dependence of dissolution for Eudragit S-100 coated pellets. *Pharm Res.* 1995 Nov;12(11):1813–6.
136. Preisig D, Varum F, Bravo R, Hartig C, Spleiss J, Abbes S, et al. Colonic delivery of metronidazole-loaded capsules for local treatment of bacterial infections: A clinical pharmacoscintigraphy study. *Eur J Pharm Biopharm.* 2021 Aug 1;165:22–30.
137. D’Haens GR, Sandborn WJ, Zou G, Stitt LW, Rutgeerts PJ, Gilgen D, et al. Randomised non-inferiority trial: 1600 mg versus 400 mg tablets of mesalazine for the treatment of mild-to-moderate ulcerative colitis. *Aliment Pharmacol Ther.* 2017 Aug;46(3):292–302.
138. McCoubrey LE, Elbadawi M, Basit AW. Current clinical translation of microbiome medicines. *Trends Pharmacol Sci.* 2022 Apr;43(4):281–92.
139. Su Q, Liu Q, Lau RI, Zhang J, Xu Z, Yeoh YK, et al. Faecal microbiome-based machine learning for multi-class disease diagnosis. *Nat Commun.* 2022 Nov 10;13(1):6818.
140. Martinez-Guryn K, Leone V, Chang EB. Regional Diversity of the Gastrointestinal Microbiome. *Cell Host Microbe.* 2019 Sep 11;26(3):314–24.
141. McCoubrey LE, Basit AWB author AW. *The Pharmaceutical Journal.* 2022 [cited 2022 Dec 5]. Addressing drug–microbiome interactions: the role of healthcare professionals. Available from: <https://pharmaceutical-journal.com/article/research/addressing-emerging-drug-microbiome-interactions-the-role-of-healthcare-professionals-new>
142. James KR, Gomes T, Elmentaite R, Kumar N, Gulliver EL, King HW, et al. Distinct microbial and immune niches of the human colon. *Nat Immunol.* 2020 Mar;21(3):343–53.
143. Hua S. Physiological and Pharmaceutical Considerations for Rectal Drug Formulations. *Front Pharmacol.* 2019 Oct 16;10:1196.
144. Glassner KL, Abraham BP, Quigley EMM. The microbiome and inflammatory bowel disease. *J Allergy Clin Immunol.* 2020 Jan;145(1):16–27.
145. Kigerl KA, Mostacada K, Popovich PG. Gut Microbiota Are Disease-Modifying Factors After Traumatic Spinal Cord Injury. *Neurother J Am Soc Exp Neurother.* 2018 Jan;15(1):60–7.
146. Jin J, Cheng R, Ren Y, Shen X, Wang J, Xue Y, et al. Distinctive Gut Microbiota in Patients with Overweight and Obesity with Dyslipidemia and its Responses to Long-term Orlistat and Ezetimibe Intervention: A Randomized Controlled Open-label Trial. *Front Pharmacol.* 2021;12:732541.

147. Worby CJ, Schreiber HL, Straub TJ, van Dijk LR, Bronson RA, Olson BS, et al. Longitudinal multi-omics analyses link gut microbiome dysbiosis with recurrent urinary tract infections in women. *Nat Microbiol.* 2022 May;7(5):630–9.
148. Yan Y, Ren S, Duan Y, Lu C, Niu Y, Wang Z, et al. Gut microbiota and metabolites of α -synuclein transgenic monkey models with early stage of Parkinson's disease. *Npj Biofilms Microbiomes.* 2021 Sep 2;7(1):1–9.
149. Kaiyrylkyzy A, Kozhakhmetov S, Babenko D, Zholdasbekova G, Alzhanova D, Olzhayev F, et al. Study of gut microbiota alterations in Alzheimer's dementia patients from Kazakhstan. *Sci Rep.* 2022 Sep 6;12(1):15115.
150. McCoubrey LE, Gaisford S, Orlu M, Basit AW. Predicting drug-microbiome interactions with machine learning. *Biotechnol Adv.* 2022;54:107797.
151. Vinarov Z, Abdallah M, Agundez JAG, Allegaert K, Basit AW, Braeckmans M, et al. Impact of gastrointestinal tract variability on oral drug absorption and pharmacokinetics: An UNGAP review. *Eur J Pharm Sci.* 2021 Jul;162:105812.
152. Klünemann M, Andrejev S, Blasche S, Mateus A, Phapale P, Devendran S, et al. Bioaccumulation of therapeutic drugs by human gut bacteria. *Nature.* 2021 Sep;597(7877):533–8.
153. McCoubrey LE, Elbadawi M, Orlu M, Gaisford S, Basit AW. Machine Learning Uncovers Adverse Drug Effects on Intestinal Bacteria. *Pharmaceutics.* 2021 Jul 6;13(7):1026.
154. Hagan T, Cortese M, Rouphael N, Boudreau C, Linde C, Maddur MS, et al. Antibiotics-Driven Gut Microbiome Perturbation Alters Immunity to Vaccines in Humans. *Cell.* 2019 Sep 5;178(6):1313-1328.e13.
155. Maier L, Goemans CV, Wirbel J, Kuhn M, Eberl C, Pruteanu M, et al. Unravelling the collateral damage of antibiotics on gut bacteria. *Nature.* 2021 Nov;599(7883):120–4.
156. Vich Vila A, Collij V, Sanna S, Sinha T, Imhann F, Bourgonje AR, et al. Impact of commonly used drugs on the composition and metabolic function of the gut microbiota. *Nat Commun.* 2020 Jan 17;11(1):362.
157. Maier L, Pruteanu M, Kuhn M, Zeller G, Telzerow A, Anderson EE, et al. Extensive impact of non-antibiotic drugs on human gut bacteria. *Nature.* 2018 Mar;555(7698):623–8.
158. Graham H, Aman P. The pig as a model in dietary fibre digestion studies. *Scand J Gastroenterol Suppl.* 1987;129:55–61.
159. Hatton GB, Yadav V, Basit AW, Merchant HA. Animal Farm: Considerations in Animal Gastrointestinal Physiology and Relevance to Drug Delivery in Humans. Vol. 104, *J Pharm Sci.* 2015. p. 2747–76.

160. Hawksworth G, Drasar BS, Hill MJ. Intestinal bacteria and the hydrolysis of glycosidic bonds. *J Med Microbiol*. 1971 Nov;4(4):451–9.
161. Yadav V, Mai Y, McCoubrey LE, Wada Y, Tomioka M, Kawata S, et al. 5-Aminolevulinic Acid as a Novel Therapeutic for Inflammatory Bowel Disease. *Biomedicines*. 2021 May;9(5):578.
162. Karatza E, Vertzoni M, Muenster U, Reppas C. The Impact of Handling and Storage of Human Fecal Material on Bacterial Activity. *J Pharm Sci*. 2016 Nov;105(11):3458–61.
163. The Characterization of Feces and Urine: A Review of the Literature to Inform Advanced Treatment Technology - PMC [Internet]. [cited 2022 Dec 7]. Available from: <https://www.ncbi.nlm.nih.gov/pmc/articles/PMC4500995/>
164. de Sousa TJT. An assessment of the role of stability on the behaviour of drugs in the colonic environment [Internet] [Doctoral]. Doctoral thesis, UCL (University College London). UCL (University College London); 2009 [cited 2022 Dec 7]. Available from: <https://discovery.ucl.ac.uk/id/eprint/10106113/>
165. Ghyselinck J, Verstrepen L, Moens F, Van den Abbeele P, Said J, Smith B, et al. A 4-strain probiotic supplement influences gut microbiota composition and gut wall function in patients with ulcerative colitis. *Int J Pharm*. 2020 Sep 25;587:119648.
166. Gill PA, van Zelm MC, Muir JG, Gibson PR. Review article: short chain fatty acids as potential therapeutic agents in human gastrointestinal and inflammatory disorders. *Aliment Pharmacol Ther*. 2018 Jul;48(1):15–34.
167. Ilhan ZE, Marcus AK, Kang DW, Rittmann BE, Krajmalnik-Brown R. pH-Mediated Microbial and Metabolic Interactions in Fecal Enrichment Cultures. *mSphere*. 2017 May 3;2(3):e00047-17.
168. Feria-Gervasio D, Tottey W, Gaci N, Alric M, Cardot JM, Peyret P, et al. Three-stage continuous culture system with a self-generated anaerobiosis to study the regionalized metabolism of the human gut microbiota. *J Microbiol Methods*. 2014 Jan 1;96:111–8.
169. García MA, Varum F, Al-Gousous J, Hofmann M, Page S, Langguth P. In Vitro Methodologies for Evaluating Colon-Targeted Pharmaceutical Products and Industry Perspectives for Their Applications. *Pharmaceutics*. 2022 Jan 26;14(2):291.
170. Venema K, van den Abbeele P. Experimental models of the gut microbiome. *Best Pract Res Clin Gastroenterol*. 2013 Feb 1;27(1):115–26.
171. Van de Wiele T, Van den Abbeele P, Ossieur W, Possemiers S, Marzorati M. The Simulator of the Human Intestinal Microbial Ecosystem (SHIME®). In: Verhoeckx K, Cotter P, López-Expósito I, Kleiveland C, Lea T, Mackie A, et al., editors. *The Impact of Food Bioactives on Health: in vitro and ex vivo models*

[Internet]. Cham (CH): Springer; 2015 [cited 2022 Dec 7]. Available from: <http://www.ncbi.nlm.nih.gov/books/NBK500150/>

172. Ghyselinck J, Verstrepen L, Moens F, Van Den Abbeele P, Bruggeman A, Said J, et al. Influence of probiotic bacteria on gut microbiota composition and gut wall function in an in-vitro model in patients with Parkinson's disease. *Int J Pharm X*. 2021 Dec;3:100087.
173. Tannergren C, Borde A, Boreström C, Abrahamsson B, Lindahl A. Evaluation of an in vitro faecal degradation method for early assessment of the impact of colonic degradation on colonic absorption in humans. *Eur J Pharm Sci Off J Eur Fed Pharm Sci*. 2014 Jun 16;57:200–6.
174. Jones J, Reinke SN, Ali A, Palmer DJ, Christophersen CT. Fecal sample collection methods and time of day impact microbiome composition and short chain fatty acid concentrations. *Sci Rep*. 2021 Jul 7;11(1):13964.
175. Morrison DJ, Preston T. Formation of short chain fatty acids by the gut microbiota and their impact on human metabolism. *Gut Microbes*. 2016 May 3;7(3):189–200.
176. McCoubrey LE, Seegobin N, Elbadawi M, Hu Y, Orlu M, Gaisford S, et al. Active Machine learning for formulation of precision probiotics. *Int J Pharm*. 2022 Mar;616:121568.
177. U.S. Consumer Product Safety Commission [Internet]. [cited 2023 May 1]. CPSC Staff Statement on University of Cincinnati Report “Toxicity Review for Dibutyl Sebacate (DBS)”. Available from: <https://www.cpsc.gov/content/CPSC-Staff-Statement-on-University-of-Cincinnati-Report-%E2%80%9CToxicity-Review-for-Dibutyl-Sebacate-DBS%E2%80%9D>
178. Lear G, Kingsbury JM, Franchini S, Gambarini V, Maday SDM, Wallbank JA, et al. Plastics and the microbiome: impacts and solutions. *Environ Microbiome*. 2021 Dec;16(1):2.
179. De Weirdt R, Possemiers S, Vermeulen G, Moerdijk-Poortvliet TCW, Boschker HTS, Verstraete W, et al. Human faecal microbiota display variable patterns of glycerol metabolism: Glycerol metabolism in the human colon. *FEMS Microbiol Ecol*. 2010 Dec;74(3):601–11.
180. Trenfield SJ, Awad A, Madla CM, Hatton GB, Firth J, Goyanes A, et al. Shaping the future: recent advances of 3D printing in drug delivery and healthcare. *Expert Opin Drug Deliv*. 2019 Oct 3;16(10):1081–94.
181. Trenfield SJ, Awad A, Goyanes A, Gaisford S, Basit AW. 3D Printing Pharmaceuticals: Drug Development to Frontline Care. *Trends Pharmacol Sci*. 2018 May;39(5):440–51.

182. Ventola CL. Medical Applications for 3D Printing: Current and Projected Uses. *Pharm Ther.* 2014 Oct;39(10):704–11.
183. Chowdhry A. Forbes. [cited 2023 May 29]. What Can 3D Printing Do? Here Are 6 Creative Examples. Available from: <https://www.forbes.com/sites/amitchowdhry/2013/10/08/what-can-3d-printing-do-here-are-6-creative-examples/>
184. Muwaffak Z, Goyanes A, Clark V, Basit AW, Hilton ST, Gaisford S. Patient-specific 3D scanned and 3D printed antimicrobial polycaprolactone wound dressings. *Int J Pharm.* 2017 Jul 15;527(1–2):161–70.
185. Boetker J, Water JJ, Aho J, Arnfast L, Bohr A, Rantanen J. Modifying release characteristics from 3D printed drug-eluting products. *Eur J Pharm Sci Off J Eur Fed Pharm Sci.* 2016 Jul 30;90:47–52.
186. Trenfield SJ, Goyanes A, Telford R, Wilsdon D, Rowland M, Gaisford S, et al. 3D printed drug products: Non-destructive dose verification using a rapid point-and-shoot approach. *Int J Pharm.* 2018 Oct 5;549(1):283–92.
187. Khaled SA, Alexander MR, Wildman RD, Wallace MJ, Sharpe S, Yoo J, et al. 3D extrusion printing of high drug loading immediate release paracetamol tablets. *Int J Pharm.* 2018 Mar 1;538(1–2):223–30.
188. Genina N, Boetker JP, Colombo S, Harmankaya N, Rantanen J, Bohr A. Anti-tuberculosis drug combination for controlled oral delivery using 3D printed compartmental dosage forms: From drug product design to in vivo testing. *J Control Release Off J Control Release Soc.* 2017 Dec 28;268:40–8.
189. Awad A, Trenfield SJ, Gaisford S, Basit AW. 3D printed medicines: A new branch of digital healthcare. *Int J Pharm.* 2018 Sep 5;548(1):586–96.
190. Vuddanda PR, Alomari M, Dodoo C, Trenfield S, Velaga S, Basit A, et al. Personalisation of warfarin therapy using thermal ink-jet printing. *Eur J Pharm Sci.* 2018 Feb 1;117.
191. Awad A, Trenfield SJ, Goyanes A, Gaisford S, Basit AW. Reshaping drug development using 3D printing. *Drug Discov Today.* 2018 Aug;23(8):1547–55.
192. Goyanes A, Scarpa M, Kamlow M, Gaisford S, Basit AW, Orlu M. Patient acceptability of 3D printed medicines. *Int J Pharm.* 2017 Sep 15;530(1–2):71–8.
193. Fina F, Goyanes A, Madla CM, Awad A, Trenfield SJ, Kuek JM, et al. 3D printing of drug-loaded gyroid lattices using selective laser sintering. *Int J Pharm.* 2018 Aug 25;547(1–2):44–52.
194. Kruth JP, Mercelis P, Van Vaerenbergh J, Froyen L, Rombouts M. Advances in Selective Laser Sintering, Invited keynote paper. *Proc 1st Int Conf Adv Res Virtual Rapid Prototyp VRAP2003 Leir 1-4 Oct 2003.* 2003;59–70.

195. Alhnan MA, Okwuosa TC, Sadia M, Wan KW, Ahmed W, Arafat B. Emergence of 3D Printed Dosage Forms: Opportunities and Challenges. *Pharm Res.* 2016 Aug 1;33(8):1817–32.
196. Cheah CM, Leong KF, Chua CK, Low KH, Quek HS. Characterization of microfeatures in selective laser sintered drug delivery devices. *Proc Inst Mech Eng [H].* 2002;216(6):369–83.
197. Leong KF, Chua CK, Gui WS, Verani. Building Porous Biopolymeric Microstructures for Controlled Drug Delivery Devices Using Selective Laser Sintering. *Int J Adv Manuf Technol.* 2006 Dec 1;31(5):483–9.
198. Fina F, Goyanes A, Gaisford S, Basit AW. Selective laser sintering (SLS) 3D printing of medicines. *Int J Pharm.* 2017 Aug 30;529(1):285–93.
199. Awad A, Fina F, Goyanes A, Gaisford S, Basit AW. Advances in powder bed fusion 3D printing in drug delivery and healthcare. *Adv Drug Deliv Rev.* 2021 Jul;174:406–24.
200. Goyanes A, Robles Martinez P, Buanz A, Basit AW, Gaisford S. Effect of geometry on drug release from 3D printed tablets. *Int J Pharm.* 2015 Oct 30;494(2):657–63.
201. Arafat B, Qinna N, Cieszynska M, Forbes RT, Alhnan MA. Tailored on demand anti-coagulant dosing: An in vitro and in vivo evaluation of 3D printed purpose-designed oral dosage forms. *Eur J Pharm Biopharm.* 2018 Jul 1;128:282–9.
202. Goyanes A, Fernández-Ferreiro A, Majeed A, Gomez-Lado N, Awad A, Luaces-Rodríguez A, et al. PET/CT imaging of 3D printed devices in the gastrointestinal tract of rodents. *Int J Pharm.* 2018 Jan 30;536(1):158–64.
203. Liang K, Carmone S, Brambilla D, Leroux JC. 3D printing of a wearable personalized oral delivery device: A first-in-human study. *Sci Adv.* 2018 May;4(5):eaat2544.
204. Vithani K, Goyanes A, Jannin V, Basit AW, Gaisford S, Boyd BJ. An Overview of 3D Printing Technologies for Soft Materials and Potential Opportunities for Lipid-based Drug Delivery Systems. *Pharm Res.* 2018 Nov 7;36(1):4.
205. Alhijaj M, Belton P, Qi S. An investigation into the use of polymer blends to improve the printability of and regulate drug release from pharmaceutical solid dispersions prepared via fused deposition modeling (FDM) 3D printing. *Eur J Pharm Biopharm.* 2016 Nov 1;108:111–25.
206. Melocchi A, Parietti F, Maroni A, Foppoli A, Gazzaniga A, Zema L. Hot-melt extruded filaments based on pharmaceutical grade polymers for 3D printing by fused deposition modeling. *Int J Pharm.* 2016 Jul 25;509(1):255–63.

207. Arafat B, Wojsz M, Isreb A, Forbes RT, Isreb M, Ahmed W, et al. Tablet fragmentation without a disintegrant: A novel design approach for accelerating disintegration and drug release from 3D printed cellulosic tablets. *Eur J Pharm Sci.* 2018 Jun 15;118:191–9.
208. Pietrzak K, Isreb A, Alhnan MA. A flexible-dose dispenser for immediate and extended release 3D printed tablets. *Eur J Pharm Biopharm.* 2015 Oct 1;96:380–7.
209. Goyanes A, Fina F, Martorana A, Sedough D, Gaisford S, Basit AW. Development of modified release 3D printed tablets (printlets) with pharmaceutical excipients using additive manufacturing. *Int J Pharm.* 2017 Jul 15;527(1):21–30.
210. Goyanes A, Det-Amornrat U, Wang J, Basit AW, Gaisford S. 3D scanning and 3D printing as innovative technologies for fabricating personalized topical drug delivery systems. *J Controlled Release.* 2016 Jul 28;234:41–8.
211. Goyanes A, Buanz ABM, Hatton GB, Gaisford S, Basit AW. 3D printing of modified-release aminosalicylate (4-ASA and 5-ASA) tablets. *Eur J Pharm Biopharm.* 2015 Jan 1;89:157–62.
212. Fuenmayor E, Forde M, Healy AV, Devine DM, Lyons JG, McConville C, et al. Material Considerations for Fused-Filament Fabrication of Solid Dosage Forms. *Pharmaceutics.* 2018 Jun;10(2):44.
213. Liu X, Chi B, Jiao Z, Tan J, Liu F, Yang W. A large-scale double-stage-screw 3D printer for fused deposition of plastic pellets. *J Appl Polym Sci.* 2017;134(31):45147.
214. Withers PJ, Bouman C, Carmignato S, Cnudde V, Grimaldi D, Hagen CK, et al. X-ray computed tomography. *Nat Rev Methods Primer.* 2021 Dec;1(1):18.
215. Starborg T, O’Sullivan JDB, Carneiro CM, Behnsen J, Else KJ, Grecis RK, et al. Experimental steering of electron microscopy studies using prior X-ray computed tomography. *Ultramicroscopy.* 2019 Jun 1;201:58–67.
216. Routledge & CRC Press [Internet]. [cited 2022 Jul 22]. *MicroComputed Tomography: Methodology and Applications, Second Edition.* Available from: <https://www.routledge.com/MicroComputed-Tomography-Methodology-and-Applications-Second-Edition/Stock/p/book/9781032337388>
217. Withers PJ. X-ray nanotomography. *Mater Today.* 2007 Dec 1;10(12):26–34.
218. Bravin A, Coan P, Suortti P. X-ray phase-contrast imaging: from pre-clinical applications towards clinics. *Phys Med Biol.* 2013 Jan 7;58(1):R1-35.
219. Shefer E, Altman A, Behling R, Goshen R, Gregorian L, Roterman Y, et al. State of the Art of CT Detectors and Sources: A Literature Review. *Curr Radiol Rep.* 2013 Mar 1;1(1):76–91.

220. Villarraga-Gómez H, Herazo E, Smith S. X-ray computed tomography: from medical imaging to dimensional metrology. *Precis Eng.* 2019 Nov 2;60:544–69.
221. Leonard F, Stein J, Soutis C, Withers P. The quantification of impact damage distribution in composite laminates by analysis of X-ray computed tomograms. *Compos Sci Technol.* 2017 Sep 1;152.
222. Schoeman L, Williams P, Du Plessis A, Manley M. X-ray micro-computed tomography (μ CT) for non-destructive characterisation of food. *Trends Food Sci Technol.* 2015 Oct 1;47.
223. Obata Y, Bale H, Barnard H, Parkinson D, Alliston T, Acevedo C. Quantitative and qualitative bone imaging: A review of synchrotron radiation microtomography analysis in bone research. *J Mech Behav Biomed Mater.* 2020 Jun 1;110:103887.
224. Lombardi CM, Zambelli V, Botta G, Moltrasio F, Cattoretti G, Lucchini V, et al. Postmortem microcomputed tomography (micro-CT) of small fetuses and hearts. *Ultrasound Obstet Gynecol Off J Int Soc Ultrasound Obstet Gynecol.* 2014 Nov;44(5):600–9.
225. Yap CY, Chua CK, Dong ZL, Liu ZH, Zhang DQ, Loh LE, et al. Review of selective laser melting: Materials and applications. *Appl Phys Rev.* 2015 Dec;2(4):041101.
226. Awad A, Fina F, Goyanes A, Gaisford S, Basit AW. 3D printing: Principles and pharmaceutical applications of selective laser sintering. *Int J Pharm.* 2020 Aug;586:119594.
227. Goyanes A, Allahham N, Trenfield SJ, Stoyanov E, Gaisford S, Basit AW. Direct powder extrusion 3D printing: Fabrication of drug products using a novel single-step process. *Int J Pharm.* 2019 Aug;567:118471.
228. Cleveland Clinic [Internet]. [cited 2023 Jun 10]. Gut-Brain Connection: What It is, Behavioral Treatments. Available from: <https://my.clevelandclinic.org/health/treatments/16358-gut-brain-connection>
229. Eckburg PB, Bik EM, Bernstein CN, Purdom E, Dethlefsen L, Sargent M, et al. Diversity of the human intestinal microbial flora. *Science.* 2005 Jun 10;308(5728):1635–8.
230. Barrea L, Muscogiuri G, Annunziata G, Laudisio D, Pugliese G, Salzano C, et al. From gut microbiota dysfunction to obesity: could short-chain fatty acids stop this dangerous course? *Horm Athens Greece.* 2019 Sep;18(3):245–50.
231. Gibson GR, Roberfroid MB. Dietary modulation of the human colonic microbiota: introducing the concept of prebiotics. *J Nutr.* 1995 Jun;125(6):1401–12.

232. Trompette A, Gollwitzer ES, Yadava K, Sichelstiel AK, Sprenger N, Ngom-Bru C, et al. Gut microbiota metabolism of dietary fiber influences allergic airway disease and hematopoiesis. *Nat Med*. 2014 Feb;20(2):159–66.
233. Maslowski KM, Vieira AT, Ng A, Kranich J, Sierro F, Yu D, et al. Regulation of inflammatory responses by gut microbiota and chemoattractant receptor GPR43. *Nature*. 2009 Oct 29;461(7268):1282–6.
234. Trompette A, Gollwitzer ES, Pattaroni C, Lopez-Mejia IC, Riva E, Pernot J, et al. Dietary Fiber Confers Protection against Flu by Shaping Ly6c- Patrolling Monocyte Hematopoiesis and CD8+ T Cell Metabolism. *Immunity*. 2018 May 15;48(5):992-1005.e8.
235. Topping DL. Targeted delivery of short-chain fatty acids to the human large bowel. *Am J Clin Nutr*. 2016 Jul 1;104(1):1–2.
236. Donohoe DR, Collins LB, Wali A, Bigler R, Sun W, Bultman SJ. The Warburg effect dictates the mechanism of butyrate-mediated histone acetylation and cell proliferation. *Mol Cell*. 2012 Nov 30;48(4):612–26.
237. Chen J, Zhao KN, Vitetta L. Effects of Intestinal Microbial–Elaborated Butyrate on Oncogenic Signaling Pathways. *Nutrients*. 2019 May 7;11(5):1026.
238. Ma X, Zhou Z, Zhang X, Fan M, Hong Y, Feng Y, et al. Sodium butyrate modulates gut microbiota and immune response in colorectal cancer liver metastatic mice. *Cell Biol Toxicol*. 2020 Oct;36(5):509–15.
239. Foglietta F, Serpe L, Canaparo R, Vivenza N, Riccio G, Imbalzano E, et al. Modulation of butyrate anticancer activity by solid lipid nanoparticle delivery: an in vitro investigation on human breast cancer and leukemia cell lines. *J Pharm Pharm Sci Publ Can Soc Pharm Sci Soc Can Sci Pharm*. 2014;17(2):231–47.
240. Donovan JD, Bauer L, Fahey GC, Lee Y. In Vitro Digestion and Fermentation of Microencapsulated Tributyrin for the Delivery of Butyrate. *J Food Sci*. 2017 Jun;82(6):1491–9.
241. Chambers ES, Viardot A, Psichas A, Morrison DJ, Murphy KG, Zac-Varghese SEK, et al. Effects of targeted delivery of propionate to the human colon on appetite regulation, body weight maintenance and adiposity in overweight adults. *Gut*. 2015 Nov;64(11):1744–54.
242. Chambers ES, Byrne CS, Ruyendo A, Morrison DJ, Preston T, Tedford C, et al. The effects of dietary supplementation with inulin and inulin-propionate ester on hepatic steatosis in adults with non-alcoholic fatty liver disease. *Diabetes Obes Metab*. 2019 Feb 1;21(2):372–6.
243. Xun P, Zhou C, Huang X, Huang Z, Yu W, Yang Y, et al. Effects of dietary sodium acetate on intestinal health of juvenile *Trachinotus ovatus* based on multi-omics approach. *Aquaculture*. 2023 Jan;562:738776.

244. Li M, Hu FC, Qiao F, Du ZY, Zhang ML. Sodium acetate alleviated high-carbohydrate induced intestinal inflammation by suppressing MAPK and NF- κ B signaling pathways in Nile tilapia (*Oreochromis niloticus*). *Fish Shellfish Immunol.* 2020 Mar;98:758–65.
245. Wang R, Li Z, Liu S, Zhang D. Global, regional and national burden of inflammatory bowel disease in 204 countries and territories from 1990 to 2019: a systematic analysis based on the Global Burden of Disease Study 2019. *BMJ Open.* 2023 Mar 1;13(3):e065186.

Résumé en Français

Le but de cette thèse est de préparer et caractériser de nouvelles formes galéniques permettant une libération ciblée du côlon.

Ce projet s'inscrit dans le cadre du projet Interreg des 2 mers "Site-specific Drug Delivery" (<https://www.interreg2seas.eu/fr/Site-Drug>).

La libération ciblée d'un principe actif au côlon peut présenter des avantages majeurs pour une thérapie médicamenteuse, par exemple si des maladies inflammatoires du côlon doivent être traitées localement. Des formes galéniques conventionnelles mènent à une libération rapide et complète du principe actif dans l'estomac et l'intestin grêle et –généralement- une absorption rapide dans la circulation sanguine. Par conséquent, les concentrations systémiques en principe actif et les effets indésirables associés peuvent être considérables. Par ailleurs, les concentrations résultantes en principe actif au site d'action (le côlon enflammé) sont faibles, résultant en une faible efficacité thérapeutique. Une forme galénique idéale pour traiter localement les maladies coliques devrait empêcher de manière efficace la libération de la substance active dans l'estomac et l'intestin grêle. En revanche, une fois le côlon atteint, la libération doit débiter et être contrôlée dans le temps (incluant -si désiré- une libération rapide et complète). Dans le cas de traitement des maladies inflammatoires du côlon (ex : maladie de Crohn et recto colique hémorragique), le principe actif est, ainsi, libéré à son site d'action, offrant des effets thérapeutiques optimaux et des effets secondaires minimisés.

Différents types de systèmes de délivrance de principe actif ont été décrits dans la littérature visant à libérer de manière site-spécifique le principe actif au côlon. Souvent, le principe actif est piégé dans une matrice polymérique, ou un réservoir de principe actif (ex : des minigranules, gélules ou comprimés chargés en principe actif) est enrobé d'un film polymérique. Les polymères idéaux utilisés à cette fin sont peu perméables pour le principe actif dans la partie haute du tube digestif, mais deviennent perméables dès que le côlon est atteint. Afin de permettre une telle augmentation en principe actif, différents systèmes ont été proposés, basés notamment sur : (i) des changements de pH

le long du tractus gastro-intestinal, (ii) une dégradation du polymère par des enzymes préférentiellement localisés dans le côlon, ou (iii) des changements structuraux dans les réseaux polymériques après un certain délai, tels que la formation de fissures dans des pelliculages peu perméables. Néanmoins, une attention particulière doit être payée car les conditions pathophysiologiques dans le côlon de patients souffrant de maladies inflammatoires du côlon peuvent être significativement différentes de celles chez des sujets sains

- (i) le pH du contenu du tractus gastro-intestinal,
- (ii) la qualité et la quantité de la microflore (secrétant les enzymes),
- (iii) les temps de transit dans les différentes sections du tractus gastro-intestinal.

Ainsi, une forme galénique qui libère avec succès un principe actif dans le côlon d'un sujet sain peut échouer chez un patient. De même, la variabilité inter et intra-individuelle des effets thérapeutiques peut être considérable, si la forme galénique n'est pas adaptée de manière appropriée à l'état pathologique.

L'objectif de ce projet de thèse est de développer de nouvelles formes galéniques ciblant la libération du principe actif au côlon et qui soient adaptés à l'état pathologique. La libération du principe actif sera déclenchée par des enzymes localisés au niveau du côlon, indépendamment de l'état pathologique.

2. Méthodologie

Les systèmes ont été préparés par pelliculage fonctionnel de micro granules chargés en principe actif.

Ces systèmes ont été caractérisés physico-chimiquement dans différents milieux simulant le tractus gastro-intestinal, cela inclut notamment l'exposition à des milieux contenant des selles de patients atteints de maladies inflammatoires du côlon ainsi que des selles de modèles animal de ces maladies (TNBS rats) et des selles de chien (sain) en condition d'anaérobiose, en collaboration avec l'INSERM U995 (Dr. Christel Neut).

La principale technique de caractérisation utilisées concerne l'étude des cinétiques de libération des systèmes exposés à ces différents milieux de libération. Les formulations

qui ont montré les résultats les plus prometteurs pendant les études *in vitro* effectuées à l'université de Lille ont été envoyées à Frederic Moens, directeur du département de recherche et développement de Prodigest, partenaire industriel du projet Interreg. Prodigest est une entreprise spin-off leader dans le développement d'un modèle unique de laboratoire pour la simulation du tract gastrointestinal de l'homme ainsi que des animaux (Simulator of the Human Intestinal Microbial Ecosystem – SHIME).

Un court séjour dans le laboratoire du Pr. Abul Basit (UCL, Londres) également partenaire du projet Interreg a permis de réaliser une étude de faisabilité sur la production des systèmes 3D pour la libération contrôlée des médicaments dans le côlon. Les techniques utilisées dans ce projet sont : « Selective laser sintering » et « direct powder extrusion ». Les systèmes 3D imprimés en collaboration avec l'université de Londres ont ensuite été caractérisée par X-ray microCT dans le laboratoire du Pr. Axel Zeitler (University of Cambridge). Les systèmes les plus prometteurs sont actuellement testés *in vivo* en collaboration avec le Dr. Laurent Dubuquoy (INSERM U995, également partenaire du projet INTERREG Site Drug) sur un modèle expérimental colique de rat transgénique afin d'évaluer cliniquement leur efficacité.

3. Résultats

Entre les différentes formulations étudiées, deux ont été brevetés grâce à leurs capacités de délivrer le médicament spécifiquement dans le côlon, indépendamment de l'espèce (humane ou animal) étudié. Le mélange des polymères utilisé pour l'enrobage des formulations oral solide (pellets) a permis la prévention de la libération du principe active dans la portion supérieur du tract gastrointestinal. Une fois dans le côlon, le film est partiellement dégradé par les enzymes produits par les bactéries coliques, permettant une libération ciblée dans le côlon. Les résultats obtenus *in vitro* dans le laboratoire de l'université ont été confirmés par l'étude effectué par l'entreprise Prodigest. Les systèmes 3D imprimés et caractérisés en Angleterre nécessitent d'être optimisées afin de pouvoir contrôler la cinétique de libération du principe actif.

4. Conclusions

Certains polymères étudiés montrent un potentiel prometteur pour le ciblage du côlon chez les patients atteints de MICI et présentant des schémas de libération similaires chez les rats et les chiens en bonne santé.

Summary in English

The aim of this thesis is to produce and characterize novel drug delivery systems for colon targeting.

This project is part of the Interreg des 2 mers “Site-specific Drug Delivery” (<https://www.interreg2seas.eu/fr/Site-Drug>).

The site-specific delivery of drugs to the colon presents major therapeutical advantages, for example in the treatment of inflammatory bowel diseases which required a local action. Conventional oral dosage forms lead to a fast and complete drug release in the stomach and small intestine and, generally, a systemic absorption into the bloodstream. Therefore, systemic concentrations of drugs and associated adverse effects can be considerable. Furthermore, the resulting concentrations of drug at the site of action (the inflamed colon) are low, resulting in low therapeutic efficacy. An ideal dosage form for the local treatment of colonic diseases should effectively prevent the release of the active substance in the stomach and small intestine. On the other hand, once the colon is reached, the release must begin and be controlled over time (including -if desired- a rapid and complete release).

In the case of treatment of inflammatory diseases of the colon (e.g. Crohn's disease and haemorrhagic ulcerative colitis), the active ingredient is thus released at its site of action, offering optimal therapeutic effects and minimized side effects.

Different types of drug delivery systems have been described in the literature aiming at site-specific release to the colon. Often, the drug is trapped in a polymeric matrix, or a drug reservoir (e.g. minigranules, capsules or tablets loaded with active ingredient) is coated with a polymeric film. The ideal polymers used for this purpose have low permeability for the drug in the upper part of the gastrointestinal tract, but become permeable as soon as the colon is reached. In order to allow such control delivery, various systems have been proposed, based in particular on: (i) changes in pH along the gastrointestinal tract, (ii) degradation of the polymer by enzymes preferentially located

in the colon, or (iii) structural changes in the polymeric networks after a certain delay, such as the formation of cracks in low permeability films.

Nevertheless, special attention should be paid because the pathophysiological conditions in the colon of patients with inflammatory bowel diseases may be significantly different from those in healthy subjects.

- (i) the pH of the contents of the gastrointestinal tract,
- (ii) the quality and quantity of microflora (secreting enzymes),
- (iii) transit times in different sections of the gastrointestinal tract.

Thus, a galenic formulation which successfully releases an active ingredient in the colon of a healthy subject may fail in a patient. Similarly, the inter- and intra-individual variability of therapeutic effects can be considerable, if the dosage form is not appropriately adapted to the pathological state.

The objective of this thesis project is to develop new galenic forms targeting the release of the active ingredient in the colon and which are adapted to the pathological state. The release of the drug will be triggered by enzymes located in the colon, regardless of the pathological state.

1. Methods

The systems were prepared by functional coating of microgranules loaded with 5-ASA as drug.

These systems have been characterized physico-chemically in different media simulating the gastrointestinal tract, this includes in particular exposure to media containing stools from patients with inflammatory bowel diseases as well as stools from animal models of these diseases (TNBS rats) and dog stools (healthy) under anaerobic conditions, in collaboration with INSERM U995 (Dr. Christel Neut).

The main characterization technique used concerns the study of the release kinetics of systems exposed to these different release media. The formulations that showed the most promising results during the *in vitro* studies carried out at the University of Lille were

sent to Frederic Moens, director of the research and development department of Prodigest, industrial partner of the Interreg project. Prodigest is a leading spin-off company in the development of a unique laboratory model for the simulation of the human and animal gastrointestinal tract (Simulator of the Human Intestinal Microbial Ecosystem – SHIME).

A short stay in the laboratory of Professor Abul Basit (UCL, London), also a partner in the Interreg project, made it possible to carry out a feasibility study on the production of 3D printed systems for the controlled release of drugs to the colon. The techniques used in this project are: “selective laser sintering” and “direct powder extrusion”. The 3D systems printed in collaboration with the University of London were then characterized by X-ray microCT in the laboratory of Professor Axel Zeitler (University of Cambridge). The most promising systems are currently being tested *in vivo* in collaboration with Dr. Laurent Dubuquoy (INSERM U995, also a partner in the INTERREG Site Drug project) on an experimental transgenic rat colon model in order to clinically assess their effectiveness.

2. Results

Among the different formulations studied, two have been patented thanks to their ability to deliver the drug specifically in the colon, regardless of the species (human or animal) studied. The mixture of polymers used for the coating of solid oral formulations (pellets) allowed the prevention of the release of the active ingredient in the upper portion of the gastrointestinal tract. Once in the colon, the film is partially degraded by enzymes produced by colonic bacteria, allowing targeted release in the colon. The results obtained *in vitro* in the university laboratory were confirmed by the study carried out by the company Prodigest. The 3D printed systems characterized in England need to be optimized in order to be able to control the release kinetics of the active ingredient.

4. Conclusions

Some investigated polymers show promising potential for targeting the colon in patients with IBD and show similar release patterns in rats disease model and healthy dogs.

Publications

- Clinical translation of advanced colonic drug delivery technologies (1).